國立臺灣大學獸醫專業學院臨床動物醫學研究所

碩士論文

Graduate Institute of Veterinary Clinical Science

School of Veterinary Medicine

National Taiwan University

Master Thesis

臺灣五種瀕危龜類之白血球型態學及超微結構研究

Morphologic and Ultrastructural Study on Leukocytes
of Five Endangered Turtle Species in Taiwan

王奕凡

Yi-Fan Wang

指導教授：季昭華　教授

Advisor: Chao-Hua Chi, Ph.D.

中華民國 108 年 2 月

February 2019

誌　　謝

由衷感謝臺北市立動物園以及所有捐助動物認養保育研究計畫的民眾與企業，野生動物的研究成果得來不易，往往需要耗費大量的成本卻時常面臨經費上的困境，這些資源我們相當珍惜，期待今天的成果可以真正的對於這些物種的保育有所幫助。謝謝電顯室鄭穹翔老師和涵涵學姊的耐心指導，總是盡力的想辦法幫助學生，沒想到我會有這樣的機緣學會電子顯微鏡的樣本製備和操作，真的是一輩子受用的經驗和技術！感謝孫瑞學長投入那麼多的時間幫我處理樣本和一起找血球，還記得一開始怎麼切都切不到血球只有一堆奇怪的 artifact，我們還在那邊苦中作樂幫它們想故事，走了這麼遠卻好像昨天的事一樣！謝謝海大海洋生態暨保育研究室的程一駿老師，以及各位學長姊、助理、學弟妹，對於研究需要幫忙的地方總是無條件的協助我，很開心很榮幸和你們一起照顧了好多海龜讓他們可以回家。謝謝海生館還有最感謝的李宗賢獸醫師，一開始我對於研究需要的種種申請流程一無所知，您不但毫不猶豫答應幫忙我、耐心協助我相關的申請作業，還為了配合我們送檢體時間一大早特地幫我們採樣，以及後續狀況的追蹤，謝謝您的幫助和鼓勵！謝謝每一隻龜龜，我知道可以在同一個時空與那麼神奇美好的你們（對你們來說我們大概是吵雜又恐怖）相遇不是理所當然的，好希望你們與你們的家可以一直安好，這是我們人類該負起的責任。

謝謝季老師給我機會讓我進入研究室這個大家庭，總是讓我們自由選擇、思考，又不時提點照顧我們。謝謝品奐學長幫我一起想出我喜歡的題目，我真的很不會寫論文和manuscript，真是辛苦你無比耐心地幫我細細修改，好希望投稿可以成功！謝謝這三年在研究室的大家，炎道學長、阿官學長、惠淳學姊、吊嘎學長、以琳學姊、傑凱學長、小咖、主霖、泡麵、文伶、白熊、立心、羿慈，在實驗室真的很需要你們，每個人都不知道拯救了我各種大小事多少次，數都數不完，謝謝你們！要謝謝我重要的物理治療師、家人、老朋友新朋友還有男朋友，對於我想辦法要做到的事情只有滿滿的支持和幫忙，你們是我溫暖的土壤。這些年那麼豐富，見到去到了從沒想過的地方、去做了沒想過自己會做的事，像一個新長出來的人生，但我知道會繼續長下去的！會常常回來！

摘　　要

研究背景：瀕危龜種的保育亟需其在醫學診斷及處置上的進展，然而過去針對海龜白血球分類之研究文獻存在不一致性且多有缺漏，而柴棺龜(*Mauremys mutica*)及食蛇龜(*Cuora flavomarginata*)更無已發表之相關資料可供參考。此外，異嗜球的毒性變化廣泛被臨床獸醫採用作為全身性炎症反應以及預後的重要指標，但在海龜仍缺乏相關文獻，因此目前對於此一變化的臨床意義了解非常有限。

研究目的：本研究目標為辨識 5 個台灣瀕危龜種血循中白血球的特徵並清楚分類，比較三種常用血片染色方法的效果，並且增進對於海龜異嗜球毒性變化臨床上應用及限制之了解。

研究方法：本研究中的血液樣本來自 2017 年一月至 2018 年九月的 30 隻救傷海龜(包含 21 隻綠蠵龜 *Chelonia mydas*、6 隻欖蠵龜 *Lepidochelys olivacea* 及 3 隻玳瑁 *Eretmochelys imbricata*)、8 隻柴棺龜及 7 隻食蛇龜。血球型態學檢驗及穿透式電子顯微鏡超微結構檢驗均依標準流程進行。

研究結果：在各研究物種，均可將白血球分類為異嗜球、嗜酸性球、嗜鹼性球、淋巴球以及單核球五種血球，其型態學特徵大致與文獻中相近物種類似。海龜具有兩種嗜酸性球(大嗜酸性球及小嗜酸性球)，且發現其嗜鹼性球型態與其他爬蟲及鳥類物種相似。在穿透式電子顯微鏡下，海龜的不同種異嗜球顆粒在細胞質當中分布不均，而在嗜酸性球當中，並沒有觀察到具有晶體結構之顆粒。柴棺龜及食蛇龜的顆粒球超微結構與黃腹彩龜（*Trachemys scripta scripta*）及廟龜（*Heosemys annandalii*）相似，但在食蛇龜嗜鹼性球顆粒中觀察到的多角形晶體並沒有在其他淡水龜有記錄。有毒性變化的海龜異嗜球之形態特徵包含細胞質顆粒染色不均、細胞質嗜鹼性增加、脫顆粒以及出現嗜鹼性顆粒，而在穿透式電子顯微鏡下則可發現毒性異嗜球具有平滑的細胞膜、細胞顆粒數量顯著減少、顆粒變小或大小不一、細胞質中膜性胞器及聚集的深色多聚核糖體數量顯著增加。Wright Giemsa 染劑、Diff-Quik 染劑以及劉氏染劑在白血球分類上之效果並無顯著差異，但 Wright Giemsa 染劑及劉氏染劑在用於判讀異嗜球

毒性變化上顯著的較 Diff-Quik 染劑可靠。在異嗜球毒性變化的檢測上，血片鏡檢與穿透式電子顯微鏡檢驗相當，但異嗜球毒性變化與臨床上炎症狀態及治療預後的相關性均弱且不顯著。

結論：本研究明確分類出 5 個瀕危龜種血循中之白血球，並提供詳細型態學特徵敘述及高品質的顯微照片，同時，首次描述了海龜異嗜球毒性變化之型態學特徵，亦為首次關於爬蟲類異嗜球毒性變化的超微結構研究。本研究提供了瀕危龜種的基礎血液學資訊，以及未來這些物種進一步在臨床病理及免疫學研究上的方向。
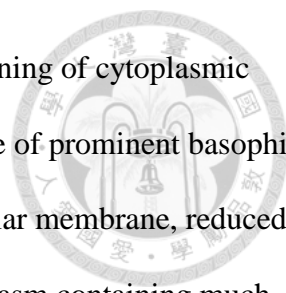
關鍵字：型態學，超微結構，白血球，毒性變化，海龜，染色方法

Abstract

Background: Advances in medical diagnosis and management is warranted for the conservation of endangered chelonian species. Disagreement and deficiency exist among past studies on sea turtles' leukocytes differentiation, and no published morphologic or ultrastructural study on *Mauremys mutica* and *Cuora flavomarginata* was available. Widely used as an important indication of systemic inflammation and prognosis in many species, heterophil toxic change is, however, poorly understood in sea turtles.

Objectives: This study aims to identify and characterize the circulating leukocytes in 5 endangered turtle species in Taiwan, compare the efficacy of accessible staining methods, and provide better understanding of the clinical applications and limitations of toxic change examination in sea turtles.

Methods: Blood samples were collected from 30 rescued sea turtles (21 *Chelonia mydas*, 6 *Lepidochelys olivacea* and 3 *Eretmochelys imbricata*), 8 captive *Mauremys mutica* and 7 captive *Cuora flavomarginata* from January 2017 to September 2018. Morphologic and ultrastructural examination were performed using standard methods.

Results: 5 types of leukocytes were identified in each species: heterophils, eosinophils, basophils, lymphocytes and monocytes. Morphologic features were generally comparable to similar species. Two types of eosinophils (large and small) were seen in sea turtles. Basophils of sea turtles were similar to those of other reptile and avian species. Ultrastructurally, heterophil granules were unevenly distributed. No crystalloid granulations were observed in eosinophils of sea turtles. The granulocytes ultrastructure of *Mauremys mutica* and *Cuora flavomarginata* were similar to those of *Trachemys scripta scripta* and *Hieremys annandalii*, but the polygonal crystalloid structures seen in the basophil granules of *Cuora flavomarginata* have not been reported in other species of freshwater

turtles. Toxic heterophils in sea turtles were characterized with uneven staining of cytoplasmic granules, increased cytoplasmic basophilia, degranulation, and the presence of prominent basophilic cytoplasmic granules. Ultrastructurally, toxic heterophils had smooth cellular membrane, reduced cytoplasmic granules that were smaller or more variable in size, and cytoplasm containing much greater amount of membranous organelles and clusters of dark polyribosomes. There was no significant difference among Wright Giemsa stain, Diff-Quik stain and Liu's stain on the efficacy of leukocyte differentiation, however Wright-Giemsa's stain and Liu's stain were significantly superior than Diff-Quik stain for assessing toxic change. Microscopic examination of toxic change is comparable to TEM examination, however the correlation of the presence toxic change with both clinical inflammatory state and the treatment outcome is both weak and insignificant in sea turtles.

Conclusions: The differentiation and characteristics of circulating leukocytes of 5 endangered chelonian species was clarified and described in details, each complemented with high quality micrographs. Toxic change morphology in sea turtles and toxic change ultrastructure in reptile species were described for the first time in this study. This study provided fundamental hematologic information for endangered turtle species and insights to further investigations on clinical pathology and immunity of these species.

Keywords: morphology, ultrastructure, leukocytes, toxic change, sea turtles, staining methods

Contents

Tables

Figures

Chapter 1. Introduction

Reptile hematology is heterogenous among species, however, current knowledge in this field is very much in a developing stage. Insufficient basic study caused limitation and difficulties of the interpretation of clinical information of these species. All five species included in this study: the green sea turtles (*Chelonia mydas*), the olive ridley sea turtles (*Lepidochelys olivacea)*, the hawksbill sea turtles (*Eretmochelys imbricate*), the yellow pond turtles (*Mauremys mutica)*, and the Chinese box turtles (*Cuora flavomarginata)* were all on the IUCN Red List of Threatened Species (IUCN, 2018), and diseased individuals presented in rescue facilities required more sophisticated medical care.

Most blood cells morphology were presented in Wright Giemsa stain. In veterinary facilities or circumstances where such stains are unavailable, veterinarians in Taiwan relied on quick stains such as Diff-Quik or Liu's stain for blood cells differentiation. However, without morphological descriptions and micrographs using these stains, the use of Diff-Quik and Liu's stain is greatly limited.

Heterophil toxic change was widely used as an indicator for systemic inflammation by veterinary clinicians, however toxic change is poorly understood in reptile species, especially sea turtles. No descriptions or micrographs of toxic heterophils morphology in sea turtles can be found in published literature, and there were no ultrastructural studies done on the toxic change of reptile heterophils. Therefore, it is unknown whether toxic change is a reliable indicator for clinical inflammation or prognosis in sea turtles, how often are they seen, what are the cellular changes to look for on a blood film, and what exactly changed on a cellular level.
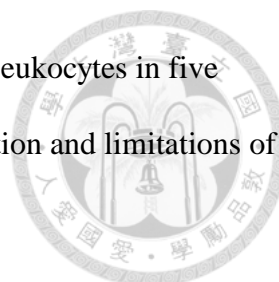
The aim of this study is to identify and characterize the circulating leukocytes in five endangered turtle species in Taiwan, and to understand the clinical application and limitations of heterophil toxic change in sea turtles.

In this thesis, principles in reptile hematology following species specific morphological and ultrastructural studies in the literature were used as the basis to identify and characterize leukocytes in the five studied turtle species. Morphologic characteristics of leukocytes stained with Wright Giemsa, Diff-Quik and Liu's stain were each described and presented in micrographs. Transmission electron microscopy (TEM) were used to identify and characterize leukocytes on the ultrastructural level, and to discover the cellular changes in toxic heterophils. The discoveries, and the similarities as well as differences between previous studies and the results of this study were discussed.

This study is expected to provide morphologic and ultrastructural details on circulating leukocytes of the studied turtle species for better cell differentiation and understanding, and to improve our knowledge on the clinical application and limitations of heterophil toxic change in sea turtle species.

Chapter 2. Literature Review

2.1 Differentials of leukocytes by morphologic characteristics

Reptile leukocytes classification is rather inconsistent comparing to birds and mammals. Variable criteria have been used for categorization, and cells are described according to appearance instead of cell function. (Claver & Quaglia, 2009) Chelonian leukocytes are generally divided into granulocytes (heterophils, eosinophils, basophils) and mononuclear cells (lymphocytes, monocytes). Circulating mononuclear cells are similar among reptiles, birds and mammals; while wide variation can present in granulocyte cell size and morphology between different species. (Montali, 1988; Nardini, Leopardi, & Bielli, 2013; Strik, Alleman, & Harr, 2007) In addition, the classification of reptilian azurophils is still inconclusive. Azurophils are less seen in reptile groups other than snakes, and some considered them immature forms of monocytes due to their consistency in both cytochemical and ultrastructural characteristics. Some authors also point out that there is little clinical advantage to separate azurophils from monocytes in WBC differential counts. (Nardini et al., 2013)

2.1.1 Heterophils

Heterophils of reptiles are the predominant cells elicited in experimentally induced inflammation, and their primary functions are phagocytosis and microbicidal activity. That is to say, they are functionally equivalent to neutrophils of mammals, although they rely mostly on oxygen-independent mechanisms to destroy phagocytized microorganisms, which is more similar to birds. (Campbell, 2012; Montali, 1988; Wilkinson, McArthur, & Meyer, 2004) Chelonian heterophils are large, round cells with irregular margin (pseudopodia sometimes present) and a

3

single round to oval shaped nucleus (often non-segmented) eccentrically located in the cell. With Romanowsky stains, the colorless cytoplasm contains abundant, bright eosinophilic refractile cytoplasmic granules, typically fusiform or rod shaped but can vary with the species. The nucleus is basophilic, and has a densely clumped chromatin pattern. (Campbell, 2012; Nardini et al., 2013; Orós, Casal, & Arencibia, 2010; B. Stacy & Pessier, 2007; Strik et al., 2007; Wilkinson et al., 2004)

2.1.2 Eosinophils

Eosinophils are the second type of chelonian acidophils that are derived from an independent cell line from hetereophils, despite the similar staining properties of their cytoplasmic granules under light microscope. (Montali, 1988) Study on the common snapping turtles (*Chelydra serpentina*) has demonstrated the chelonian eosinophils' participation in immune response, and their phagocytic properties. (Mead & Borysenko, 1984) Contains in reptilian eosinophils function as toxins for parasites, inactivate leukotrienes, or cause histamine release from mast cells. The significance of eosinophilia is still unclear but mostly associated with parasitism and nonspecific immune stimulation. (Campbell, 2012; Wilkinson et al., 2004) The description of chelonian eosinophil morphology in literature is diverse. Generally, they are described as large (similar to heterophils in size) and round cells, with a centrally or eccentrically located nucleus that can be single or bilobed, round or elongated in shape. (Cambell, 2006; Campbell, 2012; Nardini et al., 2013; Orós et al., 2010; N. I. Stacy & Raskin, 2015; Strik et al., 2007) The number and distribution of the spherical cytoplasmic granules are greatly variable. With Romanowsky stains, the clear or weakly basophilic cytoplasm contains well-defined, eosinophilic granules. The nucleus is strongly basophilic with a clumped chromatin pattern. (Nardini et al., 2013; Orós et al., 2010) In addition, two types of eosinophils have been described in green sea turtles. Despite the difference in size, the large eosinophils have a vacuolated cytoplasm and sparse, variably sized, metachromatic (bright

4

eosinophilic core surrounded by a slightly refractile halo) granules; while small eosinophils have a

blue cytoplasm and numerous round, dull eosinophilic or clear, well-defined granules. (Work,

Raskin, Balazs, & Whittaker, 1998)
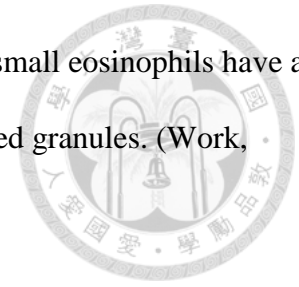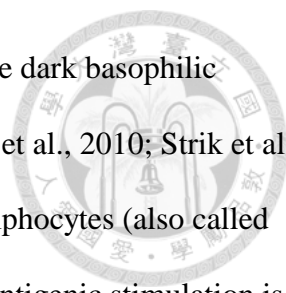
2.1.3 Basophils

Basophils of reptiles appears to function similarly to that of mammals. Reptile's basophils

are involved in surface immunoglobulins processing and also histamine release. Increased number

of reptile basophils seems to be associated with the presence blood parasites or viral infection. (Strik

et al., 2007) Chelonian basophils are described as small, round cells containing variable numbers of

round granules that often obscured the slightly eccentric, non-lobed nucleus. The granules of

basophils are prone to dissolve or degranulate, regardless of the type of stains being used, and lead

to a vacuolated appearance of the cytoplasm. (Cambell, 2006; Campbell, 2012; Nardini et al., 2013;

Strik et al., 2007; Wilkinson et al., 2004) With Romanowsky stains, the basophil cytoplasm is clear,

but may appear purplish when degranulation happens. The granules are darkly basophilic and can be

metachromatic, and the nucleus appears dark purple in color with a clumped chromatin pattern.

(Cambell, 2006; Campbell, 2012; Nardini et al., 2013; Orós et al., 2010; N. I. Stacy, Alleman, &

Sayler, 2011; Strik et al., 2007; Sykes & Klaphake, 2015)

2.1.4 Lymphocytes

Lymphocytes of reptiles resemble those of mammals and birds. Chelonian lymphocytes vary

in size, but are often small, irregularly round to oval cells with scant cytoplasm and a relatively large

(high nucleus to cytoplasm ratio), round, non-lobed (but sometimes indented), central or slightly

eccentric nucleus. The cytoplasm is generally homogenous, usually lack of cytoplasmic granules or

vacuoles, but occasionally phagocytized particles or erythrocytes can be seen. With Romanowsky

5

stains, the cytoplasm of chelonian lymphocytes is lightly basophilic, and the dark basophilic chromatin is heavily clumped. (Campbell, 2012; Nardini et al., 2013; Orós et al., 2010; Strik et al., 2007; Sykes & Klaphake, 2015; Wilkinson et al., 2004) When reactive lymphocytes (also called large lymphocytes, in contrast to the mature small lymphocytes) are seen, antigenic stimulation is indicated. Reactive lymphocytes are larger in size, may present cytoplasmic projections, and has a more abundant cytoplasm which contains small amount of discrete and punctuate vacuoles or sometimes a variable number of small azurophilic granules. The nucleus is also larger in size, and nucleoli is more evident. (Strik et al., 2007; Sykes & Klaphake, 2015) The differentiation of lymphocytes from thrombocytes is one of the most challenging task in reptilian leukocyte identification. Compared to thrombocytes, lymphocytes are usually larger in size, rounder in shape, have a more distinct cellular margin and a more basophilic cytoplasm. (Strik et al., 2007; Sykes & Klaphake, 2015)

2.1.5 Monocytes

Monocytes of reptiles are similar to their counterparts in mammals regarding both function and morphology. (Strik et al., 2007) Chelonian monocytes are large, round to ameboid cells with smooth outlines and an abundant, foamy cytoplasm that may contains vacuoles and fine granules, or sometimes phagocytized materials. The shape of the single, large nucleus varies from oval to indented or lobed. (Campbell, 2012; Nardini et al., 2013; Strik et al., 2007; Wilkinson et al., 2004) With Romanowsky stains, the cytoplasm of monocytes is grayish and pale basophilic, and the fine cytoplasmic granules may be eosinophilic or azurophilic. The nucleus is stained more lightly basophilic and the chromatin pattern is less condensed and finely clumped comparing to lymphocytes. (Campbell, 2012; Nardini et al., 2013; Orós et al., 2010; Strik et al., 2007)

2.2 Blood films staining methods

2.2.1 The appropriate stain for chelonian leukocytes differentiation

Romanowsky-type stains are preferred for reptile blood film staining. Romanowsky quick stains (ie. Diff-Quick) are considered adequate and have obvious advantages such as rapid results and minimal procedures, which are practical in most veterinary clinic settings; however, more time-consuming alternatives (ie. Wright, Giemsa, Wright-Giemsa, May-Grunwald Giemsa) may be superior in cell differentiation. For instance, Diff-Quick stain reportedly caused coalescence of heterophil granules in Hermann's tortoises (*Testudo hermanni*); lead to less eosinophilic and less distinct heterophils in Chinese water dragon (*Physignathus spp.*); may damage lymphocytes and may understain immature erythrocytes and lymphocytes. (Cambell, 2006; Nardini et al., 2013; Sykes & Klaphake, 2015) On the other hand, May-Grünwald Giemsa stain is preferred over rapid stains in differentiating thrombocytes and lymphocytes and staining basophils in marine turtles. Wright's stain facilitates lymphocytes and thrombocytes differentiation by giving a bluish color to the cytoplasm of lymphocytes while leaving the cytoplasm of thrombocytes translucent. (Wilkinson et al., 2004) Wright-Giemsa stains produced great staining properties as well, but may be less practical in some clinical laboratory settings. (Nardini et al., 2013; Strik et al., 2007)

2.2.2 Problems of current staining methods

The current recommended staining methods were mainly based on experts' opinions, or findings mentioned in a few hematology studies of one specific species, which subsequently were cited in textbook to represent all species under the reptile class. Very few experiment was done to evaluate and compare the results of different staining methods. Finally, while micrographs of stained cells were crucial in understanding morphology, the only stain presented in the majority of literature were Wright Giemsa stain, which when inaccessible, made interpretation of morphology

7

using other stains inconvenient and difficult. As a result, what is the stain of choice in many reptile species, as well as the staining properties of many staining methods remains poorly understood.

On a practical setting, we look at the most commonly used stains by veterinary laboratories in Taiwan: Wright Giemsa stain, Diff-Quik stain and Liu's stain. Wright Giemsa stain was considered one of the best blood film staining methods in reptiles, and most blood cells micrographs veterinarians can find in textbooks were stained with Wright Giemsa, which gave it a huge advantage. However, while the Wright Giemsa automatic slide stainer is convenient and produce consistent staining properties, it takes longer than 10 minutes to complete, and is unrealistic on field or in smaller clinical settings. Even in large teaching hospitals, in the off-hours veterinarians are in need of a manual staining method to evaluate blood films.

Diff-Quik stain was one of the most widely used manual quick stains for blood film staining. It takes less than a minute to produce a well-stained blood film, the staining procedure is straightforward, and the kit is portable. However, the stain kit is expensive, and produce less satisfying cytoplasmic result in some species in reptiles. On the other hand, Liu's stain was more widely equipped by veterinary clinics in Taiwan comparing to the costly Diff-Quik stain. Like Diff-Quik stain, Liu's stain quickly (2 minutes) produce a satisfying staining result, and the kit is very affordable. However, no studies on reptile leukocyte morphology have used Liu's stain and such micrographs cannot be found in textbook.

Therefore, it is necessary to establish an assessment on the staining properties of the aforementioned staining methods in the studied chelonian species.

8
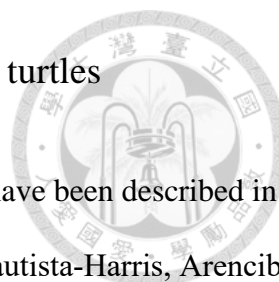
2.3 Morphologic and ultrastructural studies of leukocytes in sea turtles

2.3.1 A review of past studies

Microscopic morphologic characteristics of peripheral blood cells have been described in loggerhead sea turtles (Bradley, Norton, & Latimer, 1998; Casal, Freire, Bautista-Harris, Arencibia, & Orós, 2007; Casal & Orós, 2007; Di Santi et al., 2013; Orós et al., 2010), green sea turtles (Tristan, 2008; Wood & Ebanks, 1984; Work et al., 1998), juvenile olive ridley sea turtles (Zhang, Li, Gu, & Ye, 2011), and Kemp's ridley sea turtles (Cannon, 1992).

Leukocytes morphology of loggerhead sea turtles

The heterophils of loggerhead sea turtles stained with Diff-Quik stain appear large (diameter=11.75-21.06 μm) and round with a dense, oval or bilobed, strongly purple or medium blue, often eccentric nucleus containing clumped chromatin. More centrally located nucleus were round in shape. The abundant, clear to light blue or weak eosinophilic cytoplasm contained numerous eosinophilic or vivid orange, fusiform or oval to elongated granules that can obscure the nucleus or were difficult to see clearly. (Bradley et al., 1998; Casal & Orós, 2007; Orós et al., 2010) (See Appx. 1)

The eosinophils of juvenile loggerhead sea turtles stained with Diff-Quik stain were described as round, variably sized cells with a generally eccentric, round or oval to indented, strongly purple or eosinophilic nucleus with coarse, clumped chromatin. The abundant cytoplasm was weakly basophilic or colorless with a lacy appearance, and contained scarce or a moderate number of round, well-defined eosinophilic or dark red granules. (Bradley et al., 1998; Casal & Orós, 2007; Orós et al., 2010) (See Appx. 2)

The basophils of juvenile loggerhead sea turtles were difficult to find in blood smears. With Diff-Quik stain, they were described as round and smaller than heterophils, and contained a dense, violet–blue or eosinophilic, generally eccentric nucleus, with a condensed or clumped chromatin

9

pattern. The cytoplasm is pale blue and contained numerous, scattered basophilic or metachromatic granules that are occasionally partially degranulated or masked the nucleus. However, the only presented micrograph in the study by Casal & Orós seemed more likely a heterophil with artifact due to overstaining, thus the morphological descriptions were considered less reliable and the micrograph is not presented here. (Bradley et al., 1998; Casal & Orós, 2007; Orós et al., 2010)

Lymphocytes of juvenile loggerhead sea turtles stained with Diff-Quik stain were small and round with a well-defined, round to infrequently indented, purple–blue or eosinophilic nucleus that contained prominently clumped or coarsely aggregated chromatin. The scant cytoplasm is moderately granular, basophilic (medium blue), and sometimes exhibits blebs or broad pseudopods around the nucleus. The visual estimate nucleus/cytoplasm (N/C) ratio was typically 0.6. The micrograph in the study by Casal & Orós seemed more likely an immature monocyte and thus is not presented here. (Bradley et al., 1998; Casal & Orós, 2007; Orós et al., 2010) (See Appx. 3)

Monocytes of juvenile loggerhead sea turtles stained with Diff-Quik stain were round or amoeboid with a generally oval to bean-shaped, kidney-like form or fusiform, eccentrically located purple-blue or eosinophilic nucleus with a chromatin pattern slightly less clumped and condensed than lymphocytes, although not consistently. The cytoplasm was more abundant than other cells, and was weak (light blue) to moderately basophilic, sometimes contained intracytoplasmic vacuoles of variable size. Azurophilic granules were not seen. Pseudopodia may be present. (Bradley et al., 1998; Casal & Orós, 2007; Orós et al., 2010) (See Appx. 4)

Leukocytes morphology of green sea turtles

Heterophils of green sea turtles under Romanowsky-type stain were large (10-18μm in diameter), round cells with dense, round to oval, basophilic, often eccentrically located nucleus. The cytoplasm is completely filled with numerous round or fusiform, dull-red, red or strongly

10

eosinophilic granules. Heterophils of green sea turtles has been falsely identified as eosinophils and described in earlier research. (Tristan, 2008; Wood & Ebanks, 1984; Work et al., 1998) (See Appx. 5)

2 types of eosinophils were identified in green sea turtles. Under Romanowsky-type stain, the large eosinophils were slightly larger than heterophils (14-22μm in diemeter), has an eccentrically located amorohous or spherical to oval, strongly basophilic (purple-blue) nucleus. The abundant, pale blue or clear cytoplasm contains sparse, large, round, brightly eosinophilic (occasionally with a refractile "halo") granules which were less numerous and larger than that of heterophils. These cells were falsely identified as neutrophils or heterophils in earlier research. The small eosinophils were smaller (12-16μm in diameter) cells with a well-defined, round, dense and purple-blue nucleus. The blue cytoplasm contains numerous well-defined, round, dull orange or clear granules. The later type of granules can leave the cells with a vacuolated appearance. (Tristan, 2008; Wood & Ebanks, 1984; Work et al., 1998) (See Appx. 6)

Basophils are rare in green sea turtles. Under Romanowsky-type stain, these cells were small (approximately the size of the erythrocyte nucleus) and spherical, with a centrally located, strongly basophilic (purple-blue) and dense nucleus that occupies about one-half the cell. The well-defined cytoplasm contained numerous, small, spherical granules that are strongly basophilic, entirely filling the cell and usually completely obscured the nucleus. (Tristan, 2008; Wood & Ebanks, 1984; Work et al., 1998) (See Appx. 7)

Lymphocytes of green sea turtles range in size (6-14μm in diameter) and shape from small, spherical cells to large, spherical or oval cells. Under Romanowsky-type stain, the nucleus can be round and well-defined or irregularly shaped, purple-blue in color, with prominently clumped chromatin. The basophilic cytoplasm was often blebbed, sometimes contains vacuoles, with or without granules (previous observations were contradicted). N/C ratio is typically 2:1, but the

nucleus size range from virtually filling the cell to taking up one third of the cell. (Tristan, 2008; Wood & Ebanks, 1984; Work et al., 1998) (See Appx. 8)

Monocytes of green sea turtles with Romanowsky-type stain were large (11-26μm), round to amoeboid cells with a round, oval, or indented and purple-blue nucleus with a fine chromatin pattern. The mildly to moderately basophilic cytoplasm had either well-defined or irregular margins, and contained vacuoles with variable size, while azurophilic granules were not observed. (Tristan, 2008; Work et al., 1998) (See Appx. 9)

Leukocytes morphology of olive ridley sea turtles

Heterophils of juvenile olive ridley sea turtles under Wright-Giemsa stain were round cells with a generally eccentrically located, dense, blue nucleus. The cytoplasm was filled with generally spindle, rod, or oval shaped eosinophilic granules. (Zhang et al., 2011) (See Appx. 10)

Two types of eosinophils were observed in juvenile olive ridley sea turtles. With Wright-Giemsa stain, large eosinophils were round with an eccentrically located nucleus. The abundant cytoplasm was pale blue with numerous small, coalescing vacuoles. The cytoplasmic granules were well-defined, round and eosinophilic, with a bright orange core and a blue-orange, slightly refractile halo. The small eosinophils had a dense, purple-blue nucleus, and the cytoplasm was filled with numerous well-defined, round, eosinophilic granules. (Zhang et al., 2011) (See Appx. 11)

Basophils were rare in juvenile olive ridley sea turtles. With Wright-Giemsa stain, they were round with an eccentrically located oval nucleus, and the cytoplasm was filled with round or oval, dark basophilic granules that often obscured the nucleus. (Zhang et al., 2011) (See Appx. 12)
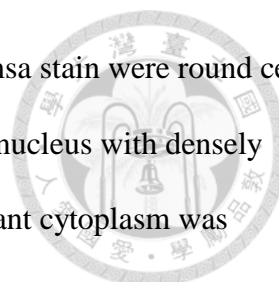
Lymphocytes of juvenile olive ridley sea turtles under Wright-Giemsa stain were round cells of variable size. The small lymphocytes had a round or notched, dark blue nucleus with densely clumped chromatin. The N/C ratio is the highest of all cell type, and the scant cytoplasm was basophilic and appeared as a thin rim around the nucleus or was located in the notched side of the nucleus. The large lymphocytes had a round or oval, blue nucleus with moderately condensed chromatin. The cytoplasmic volume was bigger than that of the small lymphocytes, and was stained blue. (Zhang et al., 2011) (See Appx. 13)

Monocytes of juvenile olive ridley sea turtles under Wright-Giemsa stain were round or occasionally amoeboid cells with an eccentrically to centrally located, oval or kidney shaped to rod shaped purple nucleus with a slightly less clumped chromatin pattern comparing to lymphocytes. The cytoplasm was abundant, weak to moderately basophilic, and occasionally contained extremely fine, light-purple granules and vacuoles of variable size. (Zhang et al., 2011) (See Appx. 14)

Leukocytes morphology of Kemp's ridley sea turtles

Heterophils of Kemp's ridley sea turtles were previously identified as large and small eosinophils in the work of early investigators. Heterophils ranged in size from 10-14μm in diameter, and had an eccentrically located, ovoid to round, dense nucleus. With Wright-Giemsa stain, numerous (70-85) round to ovoid, orange and refractile cytoplasmic granules were seen. A second type of smaller, less refractile granules were also identified. No detailed descriptions of other granulocytes were available, possibly due to smaller numbers found on blood films. Lymphocytes were small (7.2-8.5μm in diameter), round to slightly oval cells with a round, occasionally indented, dense nucleus that nearly fills the cell. The sky-blue cytoplasm sometimes contained a few azurophilic cytoplasmic granules. Morphological descriptions of monocytes were not available. (Cannon, 1992) (See Appx. 15)
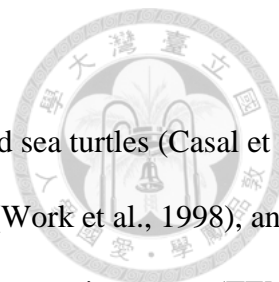
Leukocytes ultrastructure

Leukocytes ultrastructure has been studied in 15 juvenile loggerhead sea turtles (Casal et al., 2007), 9 loggerhead sea turtles (Di Santi et al., 2013); 26 green sea turtles (Work et al., 1998), and 5 juvenile olive ridley sea turtles (Zhang et al., 2011) using transmission electron microscope (TEM).

Heterophils of juvenile loggerhead sea turtles were round cells with an eccentrically located round nucleus that contained moderate amounts of heterochromatin. The cytoplasm was abundant and contained numerous round or elongated, electron-dense granules. Very small amount of pleomorphic granules of variable density, some mitochondria, and endoplasmic reticulum were also found within the cytoplasm. (Casal et al., 2007; Di Santi et al., 2013; Orós et al., 2010)

In green sea turtles, the heterophils nucleus contained moderate amount of heterochromatin, and numerous elongated to round, electron-dense cytoplasmic granules along with fewer pleomorphic, variably dense cytoplasmic granules were observed. Small number of mitochondria and some endoplasmic reticulum were also seen. (Work et al., 1998)

The heterophils of juvenile olive ridley sea turtles had an oval nucleus with moderate amount of heterochromatin. 2 types of cytoplasmic granules were also seen, including numerous elongated to round, moderately electron-dense granules and a small number of round granules with very strong electron density. Some mitochondria and endoplasmic reticulum were observed, as in other sea turtles. (Zhang et al., 2011)

Eosinophils of juvenile loggerhead sea turtles were homogeneous in size and shape (round), with a round or oval nucleus that contained variable amounts of heterochromatin. Well-defined cytoplasmic granules were round, electron-dense and homogeneous. No crystalline structures were seen within granules except for one study, in which the presented "paracrystalloid core" seemed more likely scratches caused by unsmooth knife edges. (Di Santi et al., 2013) Some cells contained numerous clear cytoplasmic vacuoles or one big vacuole. Mitochondria, golgi complexes and

14

endoplasmic reticulum were commonly seen. (Casal et al., 2007; Orós et al., 2010)

Green sea turtle had eosinophils with a round to oval nucleus that contained variable amount of heterochromatin. Large eosinophils had a few large, round to pleomorphic, variably electron-dense cytoplasmic granules on one end of the cell, and a few of these granules had an electron-dense core, which resembled the crystalloid granules that were found in other species, however no lamellar periodicity were seen. Numerous small, poorly defined and coalescing, clear vacuoles were also seen in the abundant cytoplasm. Cytoplasmic granules of small eosinophils were well-defined, round, homogenous and electron-dense, which contained elongated crystalline structures that caused deformity of the granules. A few small eosinophils contained numerous granules of variable electron density, which often contained multiple, small or a single, large, clear vacuole. (Work et al., 1998)

Large eosinophils of juvenile olive ridley sea turtles had an oval nucleus that contained moderate amount of heterochromatin. Few large, well-defined, round and homogeneously electron-dense granules were observed on one side of the cell. Small eosinophils electron micrographs were not available due to scarcity of this type of cell. (Zhang et al., 2011)

Ultrastructural features of basophils have never been described in sea turtles because this cell type is very rare in the studied species. (Casal et al., 2007; Di Santi et al., 2013; Orós et al., 2010; Work et al., 1998; Zhang et al., 2011)

Lymphocytes of juvenile loggerhead sea turtles were irregularly round in shape, with a round and often indented nucleus that contained abundant heterochromatin. The cytoplasm was scant, and had few mitochondria, endoplasmic reticulum, polyribosomes, and small, electron-dense cytoplasmic granules. (Casal et al., 2007; Orós et al., 2010)

In green sea turtles, lymphocytes had a round, often indented nucleus with a large amount of heterochromatin. The cytoplasm was scant, containing few mitochondria, small electron-dense

15

granules, and endoplasmic reticulum. (Work et al., 1998)

Ultrastructural characteristics of lymphocytes in juvenile olive ridley sea turtles were not described in details and were reportedly similar to aforementioned species. (Zhang et al., 2011)
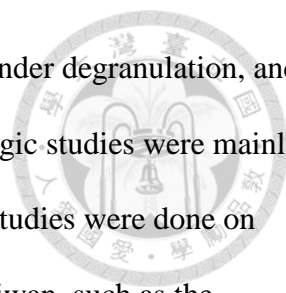
Monocytes of juvenile loggerhead sea turtles were round or fusiform with a round nucleus that contained scant heterochromatin. The cytoplasm had a large golgi complex, some small electron-dense granules, mitochondria and endoplasmic reticulum. (Casal et al., 2007)

In green sea turtles, the nucleus of monocytes had scant heterochromatin, and sometimes nucleoli were found. The cytoplasm was abundant, containing a large golgi zone, a few small electron-dense granules, mitochondria and endoplasmic reticulum. (Work et al., 1998)

Monocytes of juvenile olive ridley sea turtles were normally round, and sometimes pseudopods can be seen. The nucleus had very little heterochromatin. Cytoplasmic organelles including small electron-dense granules, mitochondria and endoplasmic reticula were easily observed. (Zhang et al., 2011)

2.3.2 Controversies and limitations of past studies

Due to the exceptional morphology features (especially granulocytes) of sea turtles and scarce research materials available, there has been confusions among investigators to date, and the descriptions of cell morphology of the same species in different publications can be diverse or even conflicted. Among a handful of existing studies, morphologic descriptions disagreed with one another, micrographs were sometimes presented in poor resolution and color contrast, and leukocytes were frequently falsely differentiated, as presented in the review. Rare cells such as basophils and small eosinophils were exceptionally poorly documented in sea turtles. For both, referable micrographs were only seen in two studies: one on green sea turtles and one on olive ridley sea turtles, with the former one presented in poor resolution and contrast, and also stained with a

16

stain not accessible to clinicians in Taiwan today; and the latter one were under degranulation, and for the basophil only remnants remained. Last but not least, such morphologic studies were mainly focused on loggerhead sea turtles, and green sea turtles at most. Very few studies were done on other species, and no information can be found at all in some species in Taiwan, such as the hawksbill sea turtles.

TEM was utilized in most studies to aid in or confirm cell differentiation by looking into the ultrastructure. However, the same problems arose as in the morphologic studies, and the information is even more problematic. Due to the costly and complex procedure, there are fewer research and smaller sample size available. Protocols were not standardized or specified in most literature, and the electron micrographs varied in quality. Falsely differentiated leukocytes, misinterpretation, and contradicted descriptions were as common as in the morphologic studies. Poor resolution and contrast, as well as artifact rendered the images less practical in use.

These contradicted and extremely insufficient information have created great confusions for veterinarians that work with sea turtles, and failure to accurately differentiate and interpret leukocytes on morphology easily lead to misdiagnosis. There is compelling evidence that more morphologic and ultrastructural studies on the leukocytes of sea turtles needs to be done to provide integrated information and clarification.

2.4 Morphologic and ultrastructural studies of leukocytes in yellow pond turtles and Chinese box turtles
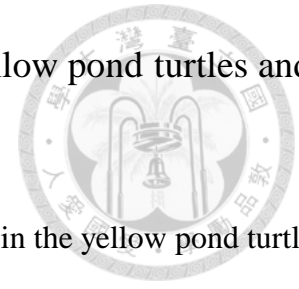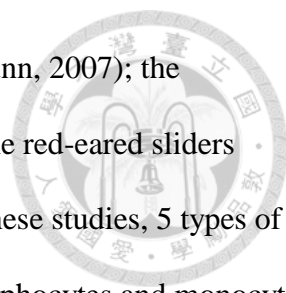
No published morphologic and ultrastructural study has been done in the yellow pond turtles (*Mauremys mutica*) and the Chinse box turtles (*Cuora flavomarginata*), which is crucial for leukocyte differentiation and subsequently more accurate diagnosis in these endangered species. A review of the morphologic and ultrastructural studies on the leukocytes of other freshwater turtle species is warranted for the morphology interpretation of newly studied species.

2.4.1 A review of studies on freshwater turtles

Leukocytes morphology

Microscopic morphologic characteristics of peripheral blood cells have been described in many species of freshwater turtles, including the yellow-bellied sliders (*Trachemys scripta scripta*) (J. Hernández, Castro, Saavedra, Ram írez, & Orós, 2017; J. D. Hernández, Orós, Artiles, Castro, & Blanco, 2016); the D'Orbigny's sliders (*Trachemys dorbigni*) (Azevedo & Lunardi, 2003); the Arrau turtles (*Podocnemis expansa*) (Oliveira-Júnior, Tavares-Dias, & Marcon, 2009); the hatchlings of the Arrau turtles, the yellow-spotted river turtles (*Podocnemis unifilis*) and the six-tubercled Amazon River turtles (*Podocnemis sextuberculata*) (Oliveira et al., 2011); the European pond turtles (*Emys orbicularis*) (Javanbakht, Vaissi, & Parto, 2013; Metin et al., 2006) ; the Caspian turtles (*Mauremys caspica*) (Javanbakht et al., 2013); the Sicilian pond turtles (*Emys trinacris*) (Arizza, Russo, Marrone, Sacco, & Arculeo, 2014); the Chinese stripe-necked turtles (*Ocadia sinensis*) (Chung, Cheng, Chin, Lee, & Chi, 2009); the Hilaire's side-necked turtles (*Phrynops hilarii*) (Pitol, Issa, Caetano, & Lunardi, 2007); the Geoffroy's side-necked turtles (*Phrynops geoffroanus*) (Zago et al., 2010); the yellow-headed temple turtles (*Hieremys annandalii*) (Chansue, Sailasuta, Tangtrongpiros, Wangnaitham, & Assawawongkasem, 2011); the juvenile head-started

18

northern red-bellied cooters (*Pseudemys rubriventris*) (Innis, Tlusty, & Wunn, 2007); the

Colombian sliders (*Trachemys callirostris*) (Velásquez et al., 2014); and the red-eared sliders

(*Trachemys scripta elegans*) (Taylor & Kaplan, 1961). In the majority of these studies, 5 types of

leukocytes were identified, namely heterophils, eosinophils, basophils, lymphocytes and monocytes.

A few authors adapted the term azurophils (recent investigations generally agreed that these cells

are immature form of monocytes in chelonian species, see 2.1.2) instead of monocytes (Chansue et

al., 2011; Oliveira-Júnior et al., 2009; Oliveira et al., 2011), and the study on the Geoffroy's

side-necked turtle found neutrophils as well as azurophils in addition to the commonly described 5

types of leukocytes. (Zago et al., 2010)

The two types of eosinophilic granulocytes present in the peripheral blood of freshwater

turtles had been clarified and confirmed as heterophils and eosinophils by the study on the

D'Orbigny's sliders using cytochemical methods, and the microscopic along with ultrstructural

characteristics had been described for each type of cells, respectively. (Azevedo & Lunardi, 2003)

The heterophils of the studied freshwater turtles were generally described as large, round (J.

Hernández et al., 2017; Oliveira-Júnior et al., 2009; Oliveira et al., 2011; Taylor & Kaplan, 1961) or

irregular (Chansue et al., 2011; Chung et al., 2009; Metin et al., 2006) cells with an eccentrically

located (Arizza et al., 2014; Azevedo & Lunardi, 2003; Chansue et al., 2011; J. Hernández et al.,

2017; Innis et al., 2007; Javanbakht et al., 2013; Metin et al., 2006; Oliveira-Júnior et al., 2009;

Oliveira et al., 2011; Zago et al., 2010), round (Pitol et al., 2007) to oval (Metin et al., 2006) or

irregular (Innis et al., 2007), sometimes lobulated (Arizza et al., 2014; Azevedo & Lunardi, 2003; J.

Hernández et al., 2017; Javanbakht et al., 2013; Oliveira-Júnior et al., 2009; Oliveira et al., 2011;

Zago et al., 2010), pale (Metin et al., 2006) or darkly (Azevedo & Lunardi, 2003; J. Hernández et al.,

2017) basophilic (Arizza et al., 2014; Javanbakht et al., 2013) nucleus containing clumped

(Azevedo & Lunardi, 2003; J. Hernández et al., 2017) or dense (Arizza et al., 2014; Javanbakht et

19
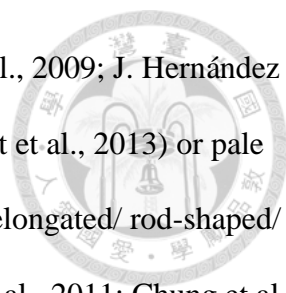
al., 2013) chromatin. The abundant (Azevedo & Lunardi, 2003; Chung et al., 2009; J. Hernández et al., 2017) cytoplasm was light blue or clear (Arizza et al., 2014; Javanbakht et al., 2013) or pale pink (Metin et al., 2006), and contained numerous eosinophilic, fusiform/ elongated/ rod-shaped/ spindle-shaped (Arizza et al., 2014; Azevedo & Lunardi, 2003; Chansue et al., 2011; Chung et al., 2009; Innis et al., 2007; Taylor & Kaplan, 1961; Zago et al., 2010) or pleomorphic (J. Hernández et al., 2017; Metin et al., 2006) or round (Javanbakht et al., 2013) cytoplasmic granules. (See Appx. 20)

The second type of eosinophilic granulocytes found in these freshwater turtles were the eosinophils. These cells were round with an eccentrically located, round to oval (Arizza et al., 2014; Chung et al., 2009; J. Hernández et al., 2017; Javanbakht et al., 2013; Metin et al., 2006) or irregular-shaped (Chung et al., 2009; Innis et al., 2007), single or bi-lobed (Arizza et al., 2014; Innis et al., 2007; Javanbakht et al., 2013; Metin et al., 2006; Zago et al., 2010) or rarely segmented (Oliveira-Júnior et al., 2009; Oliveira et al., 2011), basophilic nucleus containing clumped (Arizza et al., 2014; J. Hernández et al., 2017; Javanbakht et al., 2013) chromatin. The pale pink to weak purple (J. Hernández et al., 2017) or colorless (Javanbakht et al., 2013) cytoplasm was packed with (Arizza et al., 2014; Azevedo & Lunardi, 2003; Chansue et al., 2011; Chung et al., 2009; Javanbakht et al., 2013; Taylor & Kaplan, 1961) or contained moderate amount of (J. Hernández et al., 2017) eosinophilic and round (Arizza et al., 2014; Azevedo & Lunardi, 2003; Chansue et al., 2011; Chung et al., 2009; J. Hernández et al., 2017; Innis et al., 2007; Javanbakht et al., 2013; Metin et al., 2006; Taylor & Kaplan, 1961; Zago et al., 2010) or oval (Pitol et al., 2007), large (Azevedo & Lunardi, 2003) or small (J. Hernández et al., 2017) granules. (See Appx. 21)

The basophils of the studied freshwater turtles were generally described as smaller (Arizza et al., 2014; J. Hernández et al., 2017), round (J. Hernández et al., 2017; Oliveira-Júnior et al., 2009; Oliveira et al., 2011; Pitol et al., 2007; Taylor & Kaplan, 1961) or variably shaped (Chansue et al.,

20

2011) cells with a centrally (Arizza et al., 2014; Chung et al., 2009; Javanbakht et al., 2013; Metin et al., 2006) or centrally to eccentrically (J. Hernández et al., 2017; Innis et al., 2007) located, rounded (Arizza et al., 2014; J. Hernández et al., 2017; Oliveira-Júnior et al., 2009; Oliveira et al., 2011; Taylor & Kaplan, 1961) or segmented (Pitol et al., 2007; Zago et al., 2010), basophilic nucleus. The somewhat vacuolated or moth-eaten appearing, easily degranulated (Innis et al., 2007; Oliveira-Júnior et al., 2009) cytoplasm contained numerous, round, large (Javanbakht et al., 2013; Metin et al., 2006) or different sized (J. Hernández et al., 2017), deeply basophilic granules, which often obscured the nucleus. (Chansue et al., 2011; J. Hernández et al., 2017; Innis et al., 2007; Javanbakht et al., 2013; Oliveira-Júnior et al., 2009; Oliveira et al., 2011; Taylor & Kaplan, 1961) One study on the yellow-headed temple turtles observed that cell size can be varied and were possibly related to the size and number of cytoplasmic granules, and the granules were unstained under Wright-Giemsa stain and Diff-Quik stain; however, the same observation have not been stated in other studies on freshwater turtles using the same types of stains. (Chansue et al., 2011) (See Appx. 22)

The lymphocytes of the studied freshwater turtles were small to variably (small to medium–large) sized (Chansue et al., 2011; J. Hernández et al., 2017; Metin et al., 2006) cells, with a rounded shape and a centrally (Innis et al., 2007) or eccentrically (Chansue et al., 2011; Pitol et al., 2007) located, round, basophilic nucleus containing a clumped (Chansue et al., 2011; Chung et al., 2009; J. Hernández et al., 2017) or a fine reticular (Arizza et al., 2014; Javanbakht et al., 2013) chromatin pattern. The scant (Arizza et al., 2014; Chung et al., 2009; J. Hernández et al., 2017; Javanbakht et al., 2013; Metin et al., 2006) or scant to moderate (Innis et al., 2007) cytoplasm stained basophilic. N/C ratio was reportedly consistently high in all studies, ranging from 0.75 (J. Hernández et al., 2017) to greater than 1 (Arizza et al., 2014; Javanbakht et al., 2013), while bigger lymphocytes had more cytoplasm than smaller ones. (J. Hernández et al., 2017) Some authors have

observed few small, eosinophilic cytoplasmic granules within small number of lymphocytes, although most lymphocytes were agranular. (Chansue et al., 2011) Lymphocytes were easier to distinguish from thrombocytes in some species (ie. the Sicilian pond turtles) (Arizza et al., 2014), and some characterized features included a larger, lighter staining nucleus, rough cytoplasmic borders (Chung et al., 2009) and being more spheroid in cell shape. (Javanbakht et al., 2013) (See Appx. 23)

The monocytes of the studied freshwater turtles were large (but unlike mammals, not always the largest cell in peripheral blood), often round to irregular (Innis et al., 2007; Metin et al., 2006) cells with an eccentrically located (Pitol et al., 2007), basophilic nucleus that was kidney-like/ fusiform/ curved/ indented or oval (Arizza et al., 2014; Javanbakht et al., 2013; Metin et al., 2006; Pitol et al., 2007) in shape, unlobed or lobed to irregular (Innis et al., 2007; Metin et al., 2006), containing dense (Arizza et al., 2014; Javanbakht et al., 2013; Zago et al., 2010) or less clumped (J. Hernández et al., 2017) chromatin that stained less intense (Metin et al., 2006). The abundant cytoplasm was pale grayish blue (Arizza et al., 2014; Chung et al., 2009; J. Hernández et al., 2017; Innis et al., 2007; Javanbakht et al., 2013; Metin et al., 2006) or clear (Zago et al., 2010) in color, and sometimes contained fine, basophilic and eosinophilic granules (Arizza et al., 2014; J. Hernández et al., 2017) and/or clear cytoplasmic vacuoles (Arizza et al., 2014; Chung et al., 2009; Innis et al., 2007; Javanbakht et al., 2013). The N/C ratio was estimated to be approximately 0.5 in the yellow-bellied sliders. (J. Hernández et al., 2017). Monocytes were not identified in some freshwater turtle species, including the Arrau turtles, the yellow-headed temple turtles, and the hatchlings of the yellow-spotted river turtles and the six-tubercled Amazon River turtles (Chansue et al., 2011; Oliveira-Júnior et al., 2009; Oliveira et al., 2011). (See Appx. 24)

Leukocytes ultrastructure

Leukocytes ultrastructure has been studied in 10 yellow-bellied sliders (J. D. Hernández et al., 2016), the D'Orbigny's sliders (sample size not documented) (Azevedo & Lunardi, 2003), 6 Hilaire's side-necked turtles (Pitol et al., 2007), 4 yellow-headed temple turtles (Chansue et al., 2011) and 2 Geoffroy's side-necked turtle (Zago et al., 2010) using TEM.
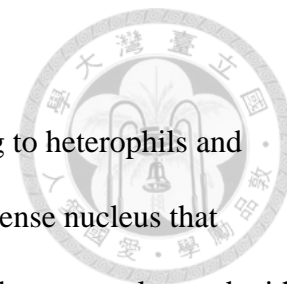
Heterophils of yellow-bellied sliders were similar to those described in sea turtles. These cells were round in shape, with an eccentrically located, oval to fusiform nucleus that contained variable but moderate amount of heterochromatin. The abundant cytoplasm contained numerous oval to elongated, homogeneous, usually moderately electron-dense granules. Fewer smaller, round, variably electron-dense granules were also found in some cells, suggesting different development stages. The most commonly observed organelles were the mitochondria and the smooth endoplasmic reticulum, and Golgi complex could also be seen, while β-granules (glycogen occurring in cells that average approximately 20-30nm in diameter) were scarce. (J. D. Hernández et al., 2016) In the D'Orbigny's sliders, the heterophils had an indented nucleus with heterochromatin that aggregated near the nuclear envelope. The cytoplasm contained a heterogeneous population of cytoplasmic granules, including round, elongated and dumbbell-shaped granules and some smaller granules that were surrounded by a membrane containing homogeneous, electron-dense materials. Within the cytoplasm, small, elongated and spherical mitochondria, sparse endoplasmic reticulum, an inconspicuous Golgi apparatus, and fine, electron-dense granulation that suggested glycogen deposits could be seen. (Azevedo & Lunardi, 2003) The heterophils of the Hilaire's side-necked turtles had an eccentrically located, segmented and heterophilic nucleus. Cytoplasmic granules were elongated in shape. (Pitol et al., 2007) Yellow-headed temple turtles had heterophils with a pleomorphic nucleus that contained euchromatin. The nonvacuolated cytoplasm had large, pleomorphic (mostly spindle-shaped) granules with distinct central cores of heterogeneous

23
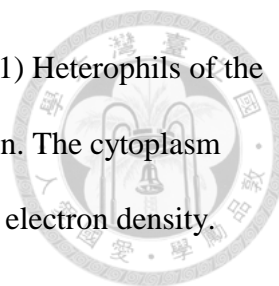
electron-dense matrix, and scattered, small ribosomes. (Chansue et al., 2011) Heterophils of the Geoffroy's side-necked turtle had a nucleus with peripheral heterochromatin. The cytoplasm contained rich granules of variable sizes, shaped (round and stick-like) and electron density. Secretion vesicles were also found. (Zago et al., 2010) (See Appx. 25)

Eosinophils of yellow-bellied sliders were similar in ultrastructural characteristics to eosinophils of loggerhead sea turtles and the small eosinophils of green sea turtles. These cells were homogeneously round in shape, similar to that of heterophils. The eccentrically located, oval to fusiform nucleus contained variable amount of heterochromatin. Within the cytoplasm, round to oval, highly electron-dense (comparing to that of heterophils) granules without crystalline structures were observed. Smaller granular inclusions and β-granules were also seen, as well as mitochondria, smooth endoplasmic reticulum and rough endoplasmic reticulum, while Golgi complex and vacuoles were relatively rare. (J. D. Hernández et al., 2016) In the D'Orbigny's sliders, the eosinophils had an indented nucleus with heterochromatin that aggregated near the nuclear envelope. The cytoplasm contained large and spherical granules that were surrounded by a membrane containing homogeneous, electron-dense materials; some smaller granules; a few oval or round mitochondria; large amount of granular endoplasmic reticulum; and a well-developed Golgi complex. (Azevedo & Lunardi, 2003) The spherical eosinophils of the Hilaire's side-necked turtles had an eccentrically located nucleus. The cytoplasm was filled with oval granules. (Pitol et al., 2007) Yellow-headed temple turtles had eosinophils with a nucleus that contained mainly heterochromatin. The cytoplasm had numerous, less tightly packed, large, round to elongated, homogeneously electron-dense (more electron-dense comparing to heterophils) granules. Few mitochondria and small ribosomes were seen, but cytoplasmic vacuoles were absent. (Chansue et al., 2011) Eosinophils of the Geoffroy's side-necked turtle had a large nucleus with slightly dense heterochromatin. Variably sized, round or oval shaped, electron-dense secretory granules were

24

observed in the cytoplasm. (Pitol et al., 2007) (See Appx. 26)

Basophils of yellow-bellied sliders were round, smaller (comparing to heterophils and eosinophils) cells with a large, round, eccentrically located, low electron-dense nucleus that contained moderate amounts of heterochromatin. The usually scarce cytoplasm was clumped with round, sometimes pleomorphic appearing granules, mostly well-defined and highly electron-dense, while some were undergoing a degeneration process. Fewer, less electron-dense granules that were rich in microtubules were also observed. Other cytoplasmic organelles included mitochondria, smooth and rough endoplasmic reticulum, Golgi complex, and abundant β-granules. (J. D. Hernández et al., 2016) Descriptions on basophil ultrastructure of the D'Orbigny's sliders were not available. The Hilaire's side-necked turtles had spherical basophils with a segmented nucleus. Round granules were seen in the cytoplasm. (Pitol et al., 2007) Yellow-headed temple turtles had basophils with a nucleus that contained mainly heterochromatin. The abundant cytoplasm contained fine, lamellar and electron-dense granules, large vacuoles (occasionally filled with dense granules), and numerous mitochondria. (Chansue et al., 2011) Basophils of the Geoffroy's side-necked turtle had an eccentrically located nucleus with heterochromatin that aggregated near the nuclear envelope. The cytoplasm contained homogeneous, electron-dense secretion granules and lipids. (Pitol et al., 2007) (See Appx. 27)

Lymphocytes of yellow-bellied sliders were usually round in cell shape, but frequently had irregular margins and cytoplasmic projections, with a round, often indented or segmented nucleus that contained abundant heterochromatin. The cytoplasm had abundant mitochondria, rough endoplasmic reticulum, and polyribosomes; while smooth endoplasmic reticulum, Golgi complex, and some, small electron-dense granules were also seen. These features were similar to those described in sea turtles. (J. D. Hernández et al., 2016) Detailed descriptions on lymphocyte ultrastructure of the D'Orbigny's sliders and the Hilaire's side-necked turtles were not available.

Yellow-headed temple turtles had lymphocytes with a round to indented nucleus that contained heterochromatin. The cytoplasm exhibited numerous pseudopodia, and contained large mitochondria, rough endoplasmic reticulum, and free ribosomes. (Chansue et al., 2011) In Geoffroy's side-necked turtles, lymphocytes had a large nucleus (almost occupied the whole cell) that contained dense chromatin that aggregated near the nuclear envelope. Nucleolus were not evident in these cells. Within the cytoplasm, few mitochondria, a well-developed endoplasmic reticulum, and ribosomes were observed. (Pitol et al., 2007) (See Appx. 28)

Monocytes of yellow-bellied sliders were generally large, round to fusiform or amoeboid in shape, that contained a proportionally small, fusiform, usually indented nucleus with less heterochromatin comparing to lymphocytes. The most frequently observed cytoplasmic organelles were mitochondria, rough and smooth endoplasmic reticulum, and some small vacuoles. Small, pleomorphic, heterogeneously electron-dense cytoplasmic granules were also found. These features were similar to those described in sea turtles. (J. D. Hernández et al., 2016) Detailed descriptions on monocyte ultrastructure in D'Orbigny's sliders, the Hilaire's side-necked turtles, or the yellow-headed temple turtle were not available. In Geoffroy's side-necked turtles, monocytes exhibited a U-shaped nucleus with heterochromatin that aggregated near the nuclear envelope. The cytoplasm contained mitochondria, endoplasmatic reticulum, secretion granules, and secretion vesicles. (Zago et al., 2010) (See Appx. 29)

26

2.5 Studies on heterophil toxic change

2.5.1 A review of past studies in reptiles

Abnormal heterophil morphology, in particular toxic change or left-shifting, indicates severe systemic disease such as inflammatory diseases, infections or necrosis. (T. Campbell, 2015; Campbell, 2012; Nardini et al., 2013; N. Stacy, Fredholm, Rodriguez, Castro, & Harvey, 2017; N. I. Stacy et al., 2011; Strik et al., 2007) Toxicity and left-shifting are frequently observed concurrently, and are believed to result from bone marrow alternation in response to inflammatory stimulus. The heterophil production is accelerated, and heterophils in a more primitive stage of development are released into the peripheral circulation, which may contain more ribosomes, primary granules, decreased number of definite granules, nucleus degeneration and so on. (T. Campbell, 2015; Nardini et al., 2013) Quantitative and qualitative assessment of heterophil toxicity provides vital clinical information of the patient, and is considered an important prognostic indicator. (N. Stacy et al., 2017; N. I. Stacy et al., 2011) Commonly described morphological alternations of reptile toxic heterophils include increased cytoplasm basophilia, degranulation, vacuolation, excessive nuclear lobation and abnormal granules (abnormal shapes and/ or staining). (Campbell, 2012; Nardini et al., 2013; N. I. Stacy et al., 2011; Strik et al., 2007) Degranulation can result from artifacts such as inappropriate sample handling or blood film preparation, prolonged storage in anticoagulant, and improper blood film fixation. Therefore, degranulation represents inflammatory disease only when it is seen together with other toxic changes (i.e. cytoplasm basophilia, vacuolation, excessive nuclear lobation or abnormal granules). Increased cytoplasm basophilia alone indicates mild disease, while the presence of cytoplasmic vacuolation, excessive nuclear lobation in species with non-lobed heterophils, or abnormal granules all indicate severe inflammation, which is usually caused by bacterial toxins and is therefore commonly associated with enteric diseases or Gram negative bacterial infection. (Campbell, 2012; N. I. Stacy et al., 2011; Strik et al., 2007) Some authors have

adopted the avian heterophil toxic change grading system and classified toxic heterophils from 1+ to 4+ on severity. (See Appendix 30) (Campbell, 2012; T. W. Campbell, 2015) However, a subjective grading system specifically applied to reptile species has yet to be established.
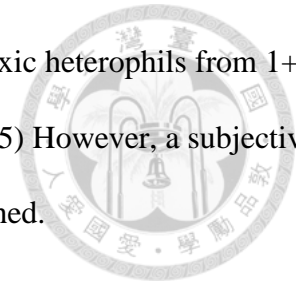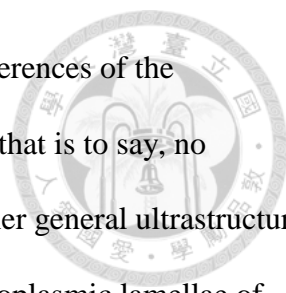
Microscopic morphology

There are very limited studies that specifically describe the morphologic criteria indicating immaturity and toxicity of heterophils in sea turtles or freshwater turtles. Sporadic cases in reptile species are available in literature and are presented in Appendix 31 and 32.

Ultrastructure

Currently, no studies have been conducted to investigate the ultrastructural changes in the reptilian heterophils with toxic changes. Until now, our knowledge on the exact ultrastructure which presented as the toxic change we see on blood film with light microscope were based on studies of avian heterophils and neutrophils of mammals.

Specifically, increased cytoplasmic basophilia in neutrophils and heterophils was well-recognized as the result of retention of polyribosomes. Döhle bodies in neutrophils were clearly identified as 3 or more rows of rough endoplasmic reticulum (RER) aggregated in lamellar form. Cytoplasmic vacuolation in neutrophils were seen as a membrane bound, electron-lucent areas of homogeneous matrix under electron microscope, and occasionally the vacuoles contained cytoplasmic constituents, which suggested autophagy. Toxic granulation has, however, remained a well-recognized but poorly understood phenomenon. Electron-cytochemical studies have demonstrated that the toxic granules seen on blood films were not phagocytized extraneous materials, newly formed abnormal granules, or autophagic bodies. Instead, toxic granules were found to resulted from altered affinity for Wright stain (alternations in the membrane or

28

composition of these granules were speculated reasons), but consistent differences of the ultrastructure comparing to normal neutrophil granules were undetectable; that is to say, no ultrastructure difference were seen between toxic and normal granules. Other general ultrastructural findings of toxic neutrophils comparing to normal neutrophils included cytoplasmic lamellae of RER, more cells with prominent Golgi complex, and more granules that exhibited a heterogeneous, stippled, or moth-eaten internal structure. These ultrastructural observations, combined with relative studies, have illustrated that the presence of toxic change under severe bacterial infection denoted cellular immaturity and/or stimulation or degeneration (Maxwell & Robertson, 1998; McCall, Katayama, Cotran, & Finland, 1969; Schofield, Stone, Beddall, & Stuart, 1983).

Studies on turpentine-induced acute inflammation in chicken found that toxic heterophils exhibited intracellular edema, cytoplasmic granule dissolution, ribosomes retention, nuclear membrane blebs, and decreased heterochromatin density ultrastructurally, while lamellar aggregates of rough endoplasmic reticulum (suggestive of Döhle bodies) were not observed. (Latimer, Tang, Goodwin, Steffens, & Brown, 1988) One study attempted to differentiate the morphological changes on heterophils that were resulted from endocrine or bacterial stress by TEM. The toxic heterophils of the LPS-treated group exhibited extensive membrane ruffling and pseudopod formation, enlarged ellipsoidal rod-shaped dense granules (may have occurred as a result of the enhancement of a secretory function), and vaccuolation. (Shini, Kaiser, Shini, & Bryden, 2008) (See Appx. 33)

2.5.2 Questions arose from past studies

From the literature, we know that toxic change was used as an indicator for systemic inflammation, especially bacterial infection. However, no descriptions or micrographs of toxic heterophils morphology in sea turtles can be found in published textbook or journal. The only

29

available micrographs in the literature were found on an online summary written by Dr. Nicole Stacy, which were all stained with Wright Giemsa stain, and lack critical information such as descriptions of cellular changes and the clinical information of the individual. Moreover, no ultrastructural studies have been done on the toxic change of reptile heterophils. Therefore, it is unknown whether toxic change is a reliable indicator for clinical inflammation or prognosis in sea turtles, how often are they seen, what are the cellular changes to look for on a blood film, and what exactly changed on a cellular level.
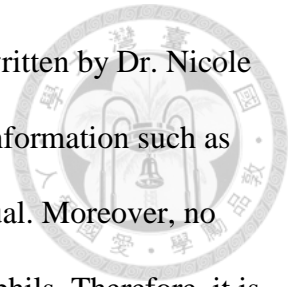
Chapter 3. Material and Method

3.1 Animals

3.1.1 Sea turtles

The subjects of this study were sea turtles that were either stranded, rescued at sea, or victims of fishery bycatch and subsequently entered the sea turtle rescue system under the authority of the Forestry Bureau, Council of Agriculture, Executive Yuan of Taiwan during January 2017 to September 2018. Sea turtles were treated, cared and rehabilitated at the Sea Turtle Rescue Center of Northern Taiwan in National Taiwan Ocean University or the National Museum of Marine Biology and Aquarium under supervision of veterinarians, until released or deceased. Samples were obtained from blood collections at National Taiwan University Veterinary Hospital (NTUVH) or the rehabilitation centers for health examination. The animal use protocols were reviewed and approved by the Institutional Animal Care and Use Committee (IACUC) of National Taiwan University (IACUC Approval No: NTU106-EL-00170).

3.1.2 Yellow pond turtles and Chinese box turtles

The subjects of this study were captive adult yellow pond turtles and Chinese box turtles kept in the laboratory animal house of School of Veterinary Medicine, National Taiwan University (NTU). Samples were obtained from blood collections for health examinations at National Taiwan University Veterinary Hospital (NTUVH). The animal use protocols were reviewed and approved by the Institutional Animal Care and Use Committee (IACUC) of National Taiwan University (IACUC Approval No: NTU106-EL-00171).

3.2 Materials

3.2.1 Blood sampling and laboratory exams

1. 1 ml Syringe with 26 G Needle, TERUMO MEDICAL CORPORATION, Tokyo, Japan

2. 3 ml Syringe with 24 G Needle, TERUMO MEDICAL CORPORATION, Tokyo, Japan

3. 5 ml Syringe with 23 G Needle, TERUMO MEDICAL CORPORATION, Tokyo, Japan

4. 10 ml Syringe with 22 G Needle, TERUMO MEDICAL CORPORATION, Tokyo, Japan

5. Lithium Heparin Tube, Greiner bio-one Co., VACUETTE®, USA

6. HDA Microscope Slides, JIANGSU HUIDA MEDICAL INSTRUMENTS CO., LTD, Jiangsu, China

7. HEMA-TEK 2000^{TM} Slide Stainer, SIEMENS HEALTHCARE DIAGNOSTICS INC., Erlangen, Germany

8. ASK® Liu's Stain A and B, TONYAR BIOTECH. INC., Taoyuan, Taiwan

9. Diff Quik, SYSMEX CORPORATION, Kobe, Japan

10. Distilled Water

11. Immersion Oil for Microscopy (Ordinary Use), OLYMPUS CORPORATION, Tokyo, Japan

12. CX22 LED Upright Microscope, OLYMPUS CORPORATION, Tokyo, Japan

13. RAININ Pipet-Lite XLS, METTLER-TOLEDO LTD., Leicester, UK

14. Axygen T-200-Y Universal Pipet tips, AXYGEN BIOSCIENCE, INC., California, USA

15. Axygen® 1.5mL MaxyClear Snaplock Microcentrifuge Tubes, AXYGEN BIOSCIENCE, INC., California, USA

16. MiniSpin® Personal Microcentrifuge, EPPENDORF AG, Hamburg, Germany

17. SPIFE® 3000 Electrophoresis Analyzer, HELENA LABORATORIES, Texas, USA

3.2.2 Transmission electron microscopy

1. Sodium Phosphate, Monobasic, Dihydrate, NIHON SHIYAKU INDUSTRIES, LTD., Osaka, Japan

2. Disodium Hydrogenphosphate, WAKO PURE CHEMICAL INDUSTRIES, LTD., Osaka, Japan

3. Glutaraldehyde Solution 25%, MERCK, Darmstadt, Germany

4. Osmium Tetroxide 4% Aqueous Solution, ELECTRON MICROSCOPY SCIENCES, Hatfield, USA

5. Ethanol Absolute, MERK, Darmstadt, Germany

6. Low Viscosity Embedding Kit (By Dr. Spurr), ELECTRON MICROSCOPY SCIENCES, Hatfield, USA

7. Orbital Shaker OS701, DEAGLE, New Taipei City, Taiwan

8. BEEM® Embedding Capsules, ELECTRON MICROSCOPY SCIENCES, Hatfield, USA

9. BEEM® Capsule Holders, ELECTRON MICROSCOPY SCIENCES, Hatfield, USA

10. UL 30 Electric Drying Oven, MEMMERT, Schwabach, Germany

11. Stainless Steel Double Edge Blade, ELECTRON MICROSCOPY SCIENCES, Hatfield, USA

12. Zoom Stereo Microscope SZ3060, OLYMPUS, Tokyo, Japan

13. Ultramicrotome Leica EM UC7, LEICA, Wetzlar, Germany

14. DiATOME Diamond Knives Histo, DiATOME, Hatfield, USA

15. DiATOME Diamond Knives Ultra 45°, DiATOME, Hatfield, USA

16. Toluidine Blue O, MERCK, Darmstadt, Germany

17. Reverse-action Tweezers N5, DUMONT, Montignez, Switzerland

18. Gilder Grids Standard Square Mesh (Square 300 Mesh, Copper, 100/vial), ELECTRON MICROSCOPY SCIENCES, Hatfield, USA

19. Gilder Grids Standard Square Mesh (Square 200 Mesh, Copper, 100/vial), ELECTRON

MICROSCOPY SCIENCES, Hatfield, USA

20. Filter Paper, WHATMAN®, Maidstone, UK

21. Grid Storage Box, ELECTRON MICROSCOPY SCIENCES, Hatfield, USA

22. Glass Vials, ELECTRON MICROSCOPY SCIENCES, Hatfield, USA

23. Parafilm M, BEMIS NA, Neenah, US

24. Uranyl Acetate (Crystals), MALLINCKRODT CHEMICAL WORKS, St. Louis, USA

25. SPI-CHEM Lead Citrate, STRUCTURE PROBE, INC., West Chester, USA

26. JEM-1400 Electron Microscope, JEOL, Peabody, USA

27. ORIUS™ SC1000 CCD Camera, GATAN, INC., Pleasanton, USA

Substance	Amount
A: $NaH_2PO_4 \cdot 12H_2O$ 71.6g/L ddH_2O (0.2M)	77ml
B: $Na_2HPO_4 \cdot 2H_2O$ 31.2g/L ddH_2O (0.2M)	23ml
A+B= PBS (0.2M, pH 7.3)	100ml

Table 1. Phosphate buffer solution preparation

Substance	Amount
A: 25% glutaraldehyde	10ml
B: ddH2O	40ml
C: PBS (0.2M, pH 7.3)	50ml
A+B+C= 2.5% glutaraldehyde in 0.1M/ pH 7.3 PBS	100ml

Table 2. Pre-fixative preparation

Substance	Amount
A: 4% osmium tetroxide	10ml
B: ddH2O	10ml
C: PBS (0.2M, pH 7.3)	20ml
A+B+C= 1% osmium tetroxide in 0.1M/ pH 7.3 PBS	40ml

Table 3. Post-fixative preparation

Substance	Amount
A: ERL-4221	10g
B: DER 736	5.5g
C: NSA	26g
D: DMAE	0.3g
A+B+C+D= pure Spurr's resin	41.8g

Table 4. Spurr's resin preparation

Substance	Amount
A: Toluidine Blue	1g
B: Sodium Borate	1g
C: ddH_2O	100ml
A+B+C= 1% Toluidine blue	100ml

Table 5. Toluidine blue stain preparation

3.3 Methods

3.3.1 Blood collection

Venipuncture in sea turtles is a blind technique. The head was manually restrained and the neck was extended and straightened carefully with both hands. 75% ethanol was applied to the puncture site for antiseptic purpose. The jugular veins can be located between the two tendons on each side of the dorsal neck. Different sizes of sterile syringes were selected based on the turtles' body size and used to penetrate the skin at the medial first to middle third neck length.

Adult yellow pond turtles and Chinese box turtles were manually restrained with the neck carefully extended forward. Animals were placed with the lateral neck facing upwards, so the jugular vein can be visualized. Aseptic preparation is as in sea turtles. 1ml sterile syringes with 26G needles were held horizontally to the skin for venipuncture.

A total of 0.4-1ml blood taken from each individual was sufficient for sample analysis.

3.3.2 Sample Preparation

Blood smears were made immediately after sampling using the wedge technique with two microscope slides and left for air dry. Remaining blood samples were infused into lithium heparin anticoagulation tubes following removal of the needles to prevent rupture of blood cells, and shaken evenly to ensure no clot formed. Samples were stored at 4℃, and proceeded to laboratory examinations in 0-6 hours.

Staining of blood films

For each individual, a minimum of 3 blood films were made, each stained with one of the 3 different staining methods. Wright Giemsa stain was produced by the HEMA-TEK 2000^{TM} automatic slide stainer. Diff Quik stain was manually done following user guide provided by

36

manufacturer. First, slides were dipped 5 x 1 second in Fixative Solution, and excess solution was drained by paper towels. The slides were then dipped into Stain Solution I and then Stain Solution II in the same manner. Finally, slides were rinsed with distilled water and left for air dry. Liu's stain was manually done by dripping Liu's stain A onto the slides, left for 1 min, and then mixed with Liu's stain B (double the amount of Liu's stain A). The presence of a greenish lustre on the surface indicates sufficient mixture of the stains. The slides were rinsed with tapped water after 2 minutes and left for air dry.
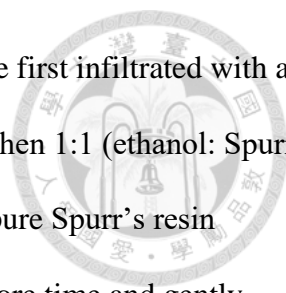
Buffy coat fixation

Heparinized whole blood was transferred into 1.5ml microcentrifuge tubes for centrifugation (1500 rpm, 15 minutes). Plasma was extracted with a pipette and discarded.

2.5% glutaraldehyde in 0.1M/ pH 7.3 PBS was prepared within 1 hour prior to use and stored at 4℃ for buffy coat fixation. The solution was gently added along the inner wall of the microcentrifuge tubes to prevent disturbances between the two layers of blood cells. 1 hour later, an applicator stick with one end shaved into a spatula was used to carefully scraped the cell pellet out of the microcentrifuge tubes, and the samples were placed in 1.5cc 2.5% glutaraldehyde in 0.1M/ pH 7.3 PBS (at least 10 times the sample's volume) at 4℃ overnight. After removing the fixative, samples were rinsed with PBS (0.2M, pH 7.3) for 10 minutes, and repeated 3 times. Samples were then immersed in 1% osmium tetroxide in 0.1M/ pH 7.3 PBS for post-fixation, and rinsed with PBS in the same manner after 1-2 hours.

Serial dehydration and embedding of samples

Fixed samples went through serial dehydration with 35% (repeated twice), 50%, 70%, 85%, 90%, 95% and 100% (repeated 3 times) ethanol, each for 10 minutes. Dehydrated samples were

37

then infiltrated with Spurr's resin also in a serial manner. The samples were first infiltrated with a 3:1 (ethanol: Spurr's resin) mixture under gentle agitation for 90 minutes, then 1:1 (ethanol: Spurr's resin) for 90 minutes, 3:1 (ethanol: Spurr's resin) for 120 minutes, finally pure Spurr's resin overnight. The resin was then replaced with fresh pure Spurr's resin one more time and gently agitated for 1 hour. The infiltrated samples were embedded in BEEM capsules with pure Spurr's resin and placed in a drying oven for polymerization (70°C, 8-15 hours). 2-3 days after polymerization was done, the resin blocks can be removed from the capsules and were ready for trimming.

Trimming and sectioning

Resin blocks were hand-trimmed under a stereo microscope into a trapezoid-topped pyramid (upper base= 0.4mm, lower base= 0.6mm, altitude= 0.5mm, height= 0.2mm) with a blade. When trimming was done, resin blocks were placed on the ultramicrotome for sectioning. Specialized diamond knives were chosen for microtomy (thickness= 77 μ m) and ultramicrotomy (thickness= 70 nm). 1% Toluidine Blue was used to stain the histosections and exam under light microscope to ensure sections contained sufficient proportion of specimen. Quality ultrathin sections (platinum color) floating on the surface of ddH$_2$O were carefully scooped up with 300 or 200 mesh copper grids with dull side facing upwards. The grids containing the sections were placed upon filter papers so the water can be absorbed from below, and dried grids were arranged in specialized storage box placed inside the moisture-proof box for at least 24 hours before proceeded to double staining.

Double staining

Uranyl acetate was dripped on pieces of Parafilm placed inside petri dishes, and the grids with the side of sections facing downwards were placed on the drips for 20 minutes. The stained

grids were dipped 10 times each in 3 beakers filled with distilled water and let dry before double

stained with lead citrate. Approximately a dozen pallets of NaOH were put inside the petri dish

where lead citrate drops were in to absorb CO_2. Contrary to uranyl acetate, the grids were placed on

the bottom of the drops with the section side facing upwards and stained for 4 minutes. The grids

were then rinsed with first CO2-free 0.02N NaOH solutions then distilled water in the same manner

as in uranyl acetate staining. After dehumidification in moisture-proof box for a minimum of 24

hours, the grids can be examined by TEM.
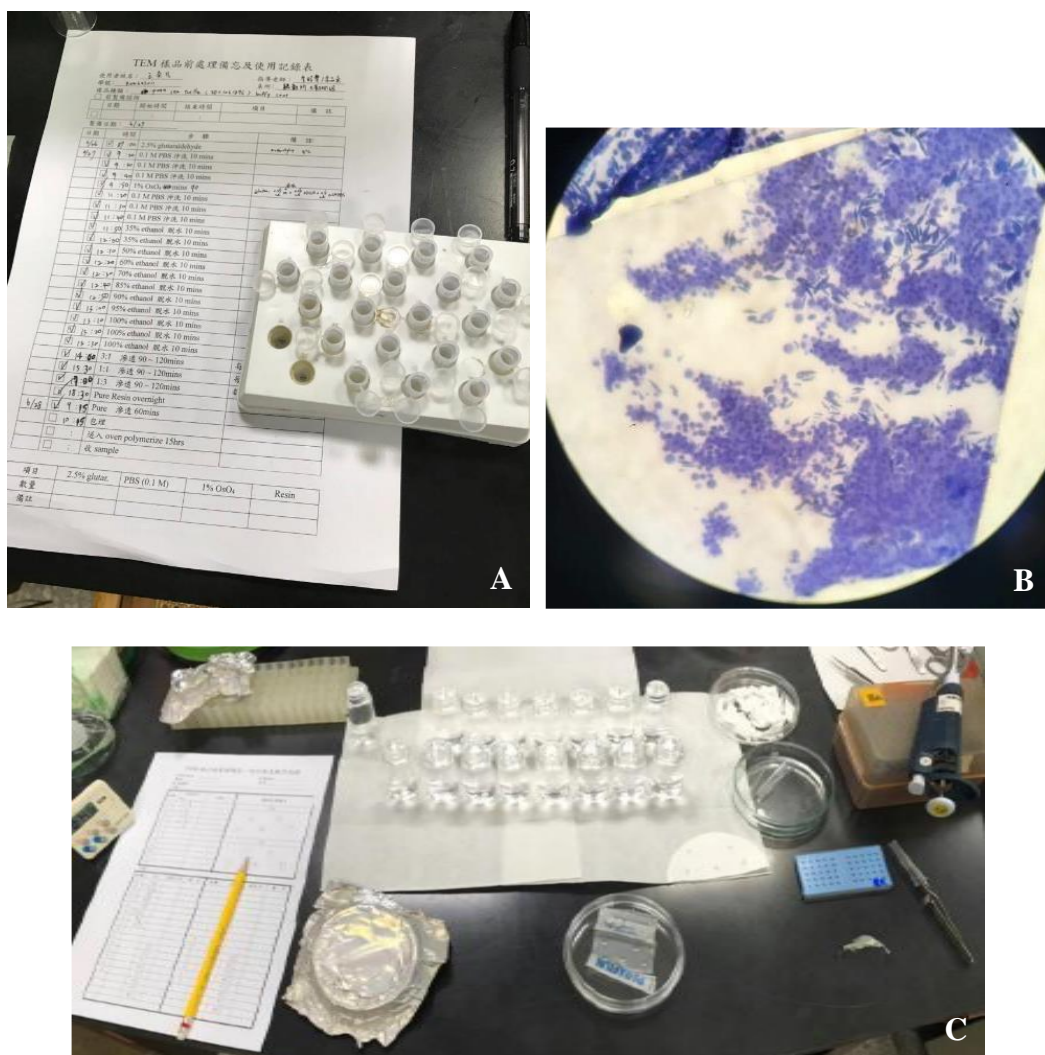
Figure 1. TEM sample preparation

A: embedding with Spurr's resin; B: light microscopic examination of 1% Toluidine Blue stained

histosections; C: double staining with uranyl acetate and lead citrate

3.3.3 Study designs

Morphology and ultrastructure of leukocytes

Blood smears stained with Wright Giemsa stain, Diff-Quik and Liu's stain of all studied individuals were each examined under an OLYMPUS CX22 LED Upright Microscope at 1000 magnification with oil immersion for morphology observation. Intact, appropriately stained leukocytes at the monolayer part of the blood smears were identified, photographed and described.

Processed buffy coat samples were examined on a JEOL JEM-1400 electron microscope at 80kV. Leukocytes were first identified on fluorescent screen then zoomed in to desired size for observation and photography. Transmission electoral micrographs were taken through ORIUS^{TM} SC1000 CCD Camera. Leukocytes ultrastructure were studied and described.
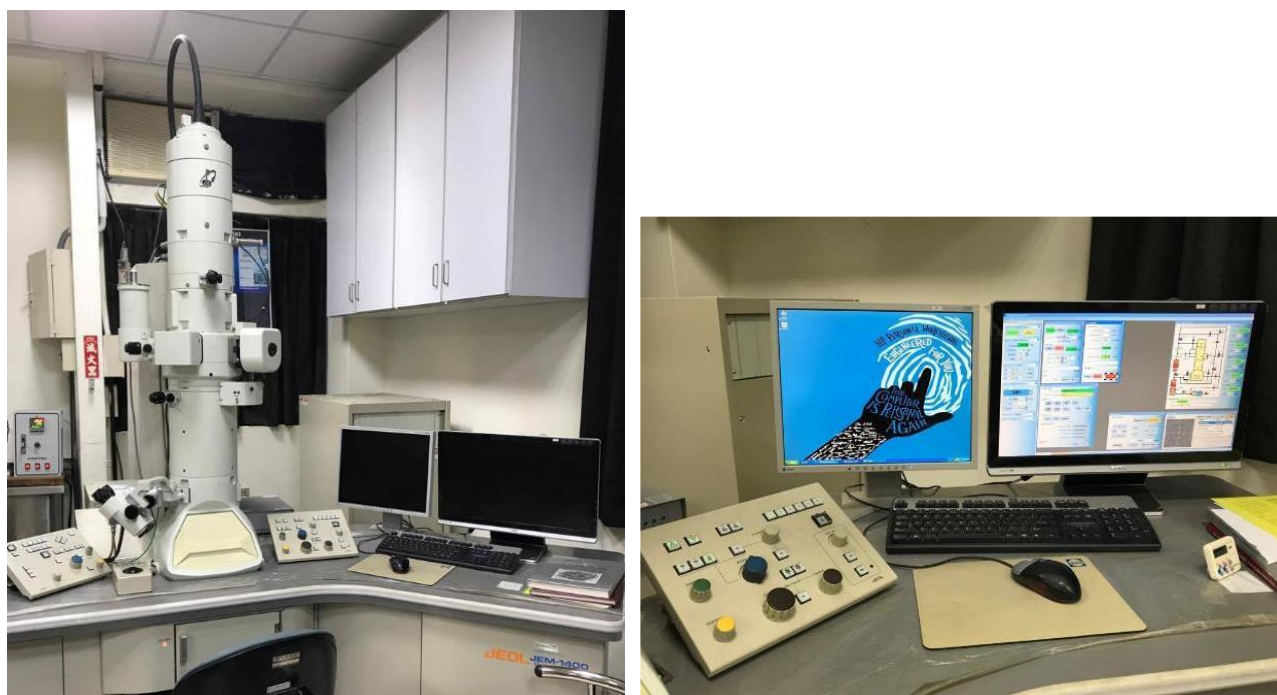
Figure 2. Transmission electron microscope (TEM)

JEM-1400 Electron Microscope, ORIUSTM SC1000 CCD Camera and control panel used in this study

40
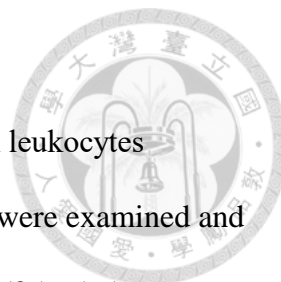
Efficacy of different staining methods

Efficacy of Wright Giemsa stain, Diff-Quik stain and Liu's stain on leukocytes differentiation in sea turtles were evaluated. 100 leukocytes on each slides were examined and graded as excellent (95-100%), good (80-95%), borderline (65-80%), poor (35-65%), or undiagnostic (<35%) on whether the applied stain demonstrate the distinctive colors and morphology of each type of cells.

The three staining methods were also evaluated on the performance of reliable toxic change detection in sea turtles. 100 heterophils on each slides were examined and graded as excellent (95-100%), good (80-95%), borderline (65-80%), poor (35-65%), or undiagnostic (<35%) on whether the applied stain demonstrate a result suitable for cellular changes interpretation. Staining features such as cytoplasmic granules integrity, proper staining and background artifact were taken into account.

Efficacy of blood film examination of toxic change

The efficacy of blood film examination using light microscope on detection of heterophil toxic change during a 100 leukocyte count in sea turtles was evaluated by comparing the results with the ultrastructure seen by TEM examination. Blood samples were categorized as "toxic change present" if toxic heterophils were seen during a 100 leukocyte counts on a blood film, or abnormal heterophil ultrastructure was seen on TEM; while "toxic change absent" means no toxic heterophils were seen during a 100 leukocyte counts on a blood film, or there was no difference of heterophil ultrastructure comparing to the normal ultrastructure presented and described in previous literature.

The efficacy of using blood film examination of toxic change to diagnose systemic inflammation in sea turtles was evaluated by comparing the results with clinical and/or pathological diagnosis. Using a combination of detailed history taking, physical examination, radiology,
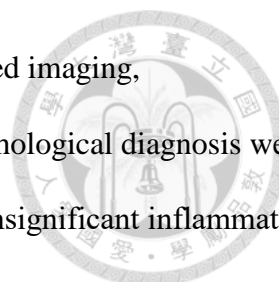
complete hematology exam including CBC and biochemistry, plus advanced imaging, microbiological cultures and/ or histology if warranted; clinical and/ or pathological diagnosis were made, and the inflammatory state of each sea turtle was ranked as "none/ insignificant inflammation (NI)", "less/ slight inflammation (LI)", and "significant/ severe inflammation (SI)". Microscopic examination of toxic change on blood films is considered a reliable indication for systemic inflammation when the presence of toxic change on blood films was strongly associated with more severe clinical inflammatory state, and vice versa.

The efficacy of using blood film examination of toxic change to predict treatment outcomes in sea turtles were also evaluated. The treatment outcomes of sea turtles were classified into "released (R), "treatment and/or rehabilitation continued (T)", and "death (D)".

3.3.4 Statistical analysis

For evaluating the efficacy of different staining methods, Chi-squared test was applied to measure whether there is significant difference (p-value < 0.05) among the 3 staining methods on the performance of leukocytes differentiation, and the performance of producing appropriate morphological and staining properties suitable for the interpretation of heterophil toxic change.

For evaluating the efficacy of blood film examination of toxic change, Cohen's kappa coefficient (κ) was measured to access the degree of agreement between blood film examination and TEM examination on toxic change detection. By definition, $\kappa=1$ means complete agreement; $0<\kappa<1$ means agreement is greater by chance; $\kappa=0$ means observed agreement is equal to chance. Spearman's rank correlation coefficient (also known as Spearman's Rho, or "rs") was used to measure the statistical dependence between the rankings of two variables, namely, the strength of association between the presence of toxic change and the clinical inflammatory state, and the strength of association between the presence of toxic change and the treatment outcome. By

definition, the calculated rs is between -1 and 1. A positive rs represents a positive correlation, while a negative rs represents a negative correlation, and rs=0 means no correlation. The strength of correlation is defined as well, where rs=0.00-0.19 means a "very weak" correlation; rs=0.20-0.39 means a "weak" correlation; rs=0.40-0.59 means a "moderate" correlation; rs=0.60-0.79 means a "strong" correlation; and rs=0.80-1.0 means a "very strong" correlation.

Chapter 4. Results

4.1 Population

4.1.1 Sea turtles

A total of 31 blood samples from 30 individuals were collected between January, 2017 to September, 2018, consisting of 6 olive ridley sea turtles (2 juveniles, 1 subadult, and 3 adults), 21 green sea turtles (1 hatchling, 10 juveniles, 8 subadults, and 2 adults), and 3 hawksbill sea turtles (1 hatchling and 2 juveniles). The results of second blood sampling on 1 green sea turtle hatchling were included in this study because of significant difference in body condition, as well as age and season.

Curved carapace length (CCL)	Age group
CCL≦30cm	Hatchling
30cm< CCL≦75cm	Juvenile
75cm< CCL≦90cm	Subadult
CCL>90cm	Adult

Table 6. Age estimation in green sea turtles using curved carapace length (CCL)

4.1.2 Yellow pond turtles and Chinese box turtles

Blood samples of 8 adult yellow pond turtles and 7 adult Chinese box turtles were collected in November, 2017.

44

4.2 Morphology and ultrastructure of leukocytes

4.2.1 Leukocyte morphology of sea turtles

5 types of leukocytes were identified in each of the studied sea turtle species, including heterophils, eosinophils, basophils, lymphocytes and monocytes.

Heterophils

Heterophils were similar in morphology in green sea turtles, olive ridley sea turtles, and hawksbill sea turtles. These cells were the most commonly found granulocytes on blood films in all samples. Heterophils were usually large (but size can vary significantly), round cells with a small N/C ratio. The single, eccentrically located (rarely centrally located) nucleus was round to elliptical (seldom bi-lobed) and often pushed against the cellular membrane, sometimes the nucleus shape can be difficult to visualized due to its pale or uneven staining properties and/ or the nucleus could be partially obscured by the cytoplasmic granules. The nucleus stained pale blue to bright purple under all 3 types of staining methods (Wright-Giemsa's stain, Diff-Quik and Liu's stain), and when stained deeply, a clumped chromatin pattern could be seen. The clear cytoplasm was packed with eosinophilic, refractile cytoplasmic granules, while vacuoles were not seen. Because of the commonly occurred cytoplasmic drying artifact and the crowdedness of the granules, heterophil granules often appear pleomorphic and less defined in shape.

Heterophil toxic change and left-shifting were rarely seen on the blood films of sea turtles. The most noticeable cellular changes included uneven staining of cytoplasmic granules, degranulation, increased cytoplasmic basophilia, and the presence of basophilic cytoplasmic granules.
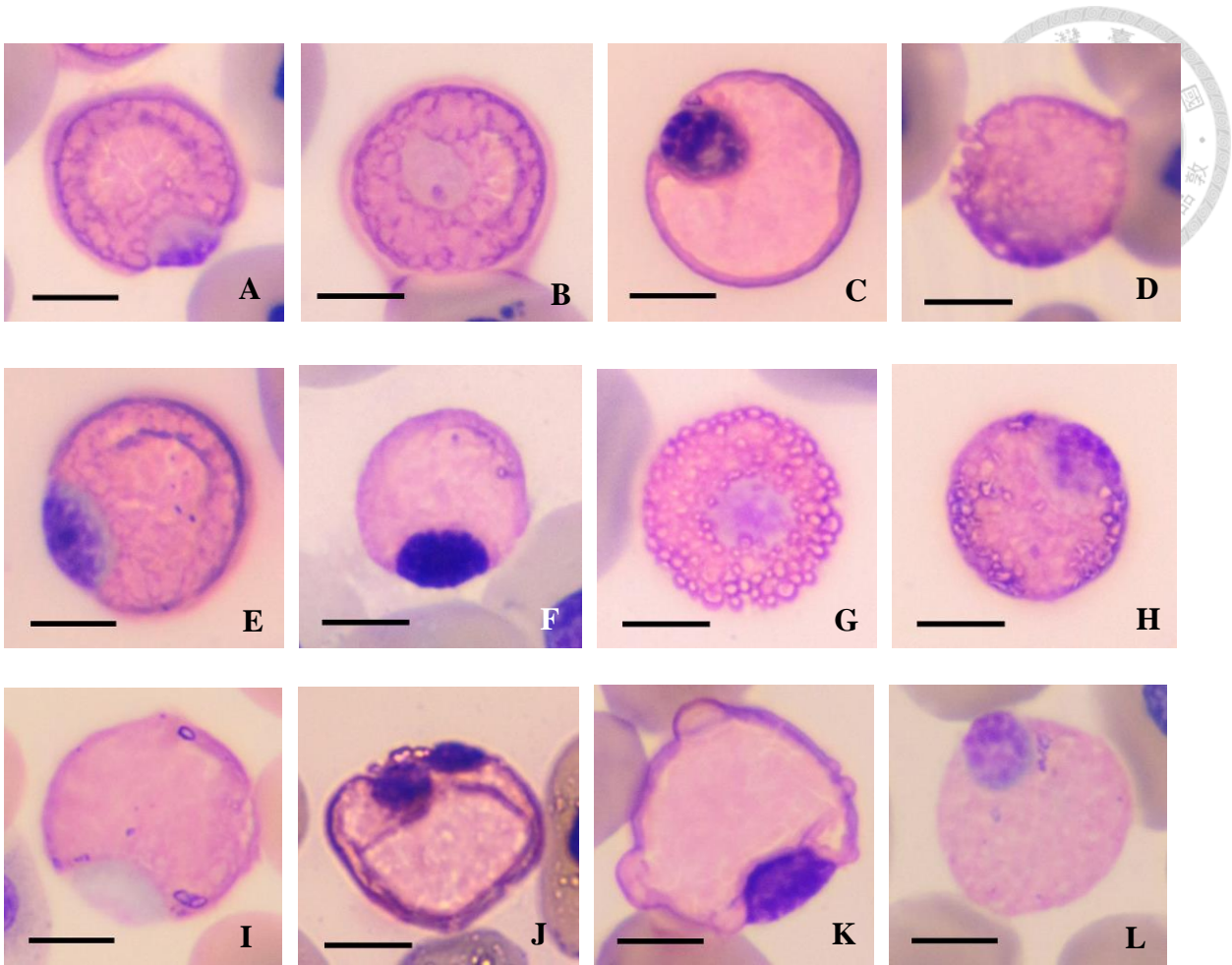
Figure 3. Representative heterophils of studied sea turtles, scale bar=10μm

A-D: green sea turtles; E-H: olive ridley sea turtles; I-L: hawksbill sea turtles

A: the eccentrically located nucleus was pressed against the cellular membrane, Wright-Giemsa stain; B: a centrally located (rare), palely stained nucleus, Wright-Giemsa stain; C: coalescing cytoplasmic granules is often seen with Diff-Quik stain; D: the nucleus had an indistinct border and was partially obscured by cytoplasmic granules, Liu's stain; E: Wright-Giemsa stain; F: Diff-Quik stain; G&H: note the refractile, well-preserved granules with Liu's stain; I: the chromatin pattern couldn't be seen with the pale staining nucleus, Wright-Giemsa stain; J: a bi-lobed nucleus, note the cytoplasmic drying artifact (a refractile pleomorphic ring), Wright-Giemsa stain; K: coalescing cytoplasmic granules, Diff-Quik stain; L: Liu's stain
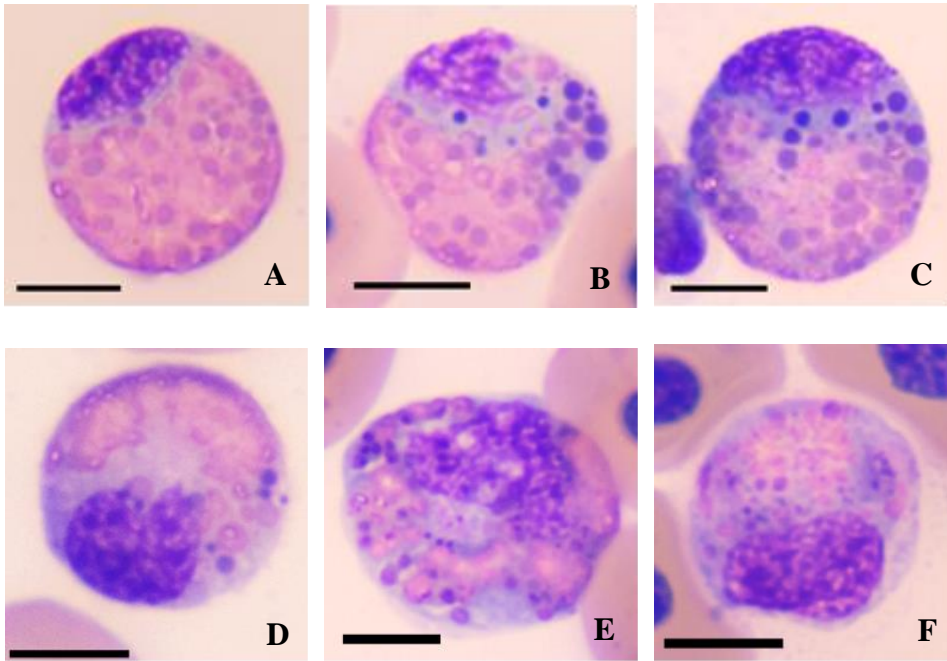
Figure 4. Representative toxic change and/ or left-shifting of heterophils in green sea turtles

Wright-Giemsa stain, scale bar=10μm

A: a mildly toxic heterophil seen with uneven staining of cytoplasmic granules; B: uneven staining of cytoplasmic granules, increased cytoplasm basophilia, and presence of basophilic granules; C: uneven staining of cytoplasmic granules, more prominent cytoplasm basophilia, and presence of basophilic granules; D: decreased number of cytoplasmic granules, marked cytoplasm basophilia, and presence of basophilic granules; E: marked degranulation, marked cytoplasm basophilia, and presence of more basophilic granules; F: marked degranulation and few eosinophilic granules remained, marked cytoplasm basophilia, and presence of more basophilic granules

Eosinophils

In green sea turtles, two distinct types of eosinophils were identified, namely the large eosinophils and the small eosinophils. In olive ridley sea turtles and hawksbill sea turtles, only one type of eosinophils was found, which were similar in morphology to the large eosinophils.

The large eosinophils of the green sea turtles were large (similar to heterophils in size), round cells with a small N/C ratio. The single, eccentrically located (rarely centrally located) nucleus was round to elliptical or irregular in shape, and was often pushed against the cellular membrane. The nucleus stained dark purple under all 3 types of staining methods, and the chromatin pattern was usually dense, sometimes almost smudged. The light blue cytoplasm appears foamy, and contained several (varied in numbers) distinct, rounded and eosinophilic granules that loosely gathered at one part of the cytoplasm. Cytoplasmic granules were pale grayish purple in color, with or without a brightly pink, refractile and smaller core, which may also appear as a second type of granules. With Liu's stain, sometimes only the cores (or the second type of granules) were stained, which resulted in eosinophils that appeared to have less and smaller cytoplasmic granules. In olive ridley sea turtles and hawksbill sea turtles, the cytoplasmic granules were often more consistent in size, generally smaller, and occasionally distributed more evenly within the cytoplasm. The staining properties of the granules and the other cellular features were as in green sea turtles.

Small eosinophils were difficult to find on the blood films of most green sea turtles, except for one individual with severe CNS spirochidae infection. These cells were medium sized, round to pleomorphic, with a N/C ratio around 0.4. The single, eccentrically located (rarely centrally located) nucleus was round to elliptical or irregular in shape, and was often pushed against the cellular membrane. The nucleus stained bright purple, with a clumped chromatin pattern. The cytoplasm was light blue as in the large eosinophils, and was packed with pale to bright pink, rounded granules that sometimes partially obscured the nucleus. Sometimes granules stained pale with Liu's stain.
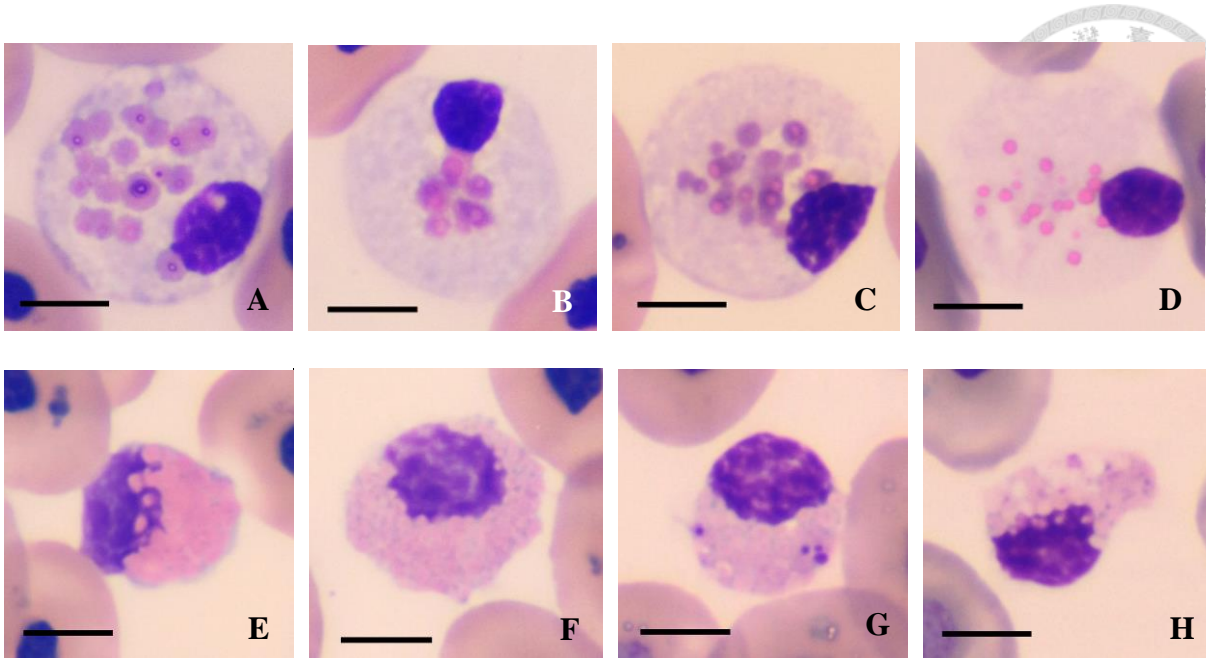
48

Figure 5. Representative eosinophils of green sea turtles, scale bar=10μm

A-D: large eosinophils; E-H: small eosinophils

A: numerous large granules and an elliptical nucleus, Wright-Giemsa stain; B: small numbers of granules, Wright-Giemsa stain; C: the nucleus was pushed against the cellular membrane, Diff-Quik stain; D: sometimes only the cores (or a second type of granules) were stained with Liu's stain, which resulted in eosinophils that appeared to have less and smaller cytoplasmic granules; E: light blue cytoplasm and bright pink granules, some obscured the nucleus, Wright-Giemsa stain; F: large numbers of more fine and pale staining granules comparing to E, Wright-Giemsa stain; G: small eosinophils have higher N/C ratio comparing to heterophils, Diff-Quik stain; H: some granules stained pale with Liu's stain occasionally
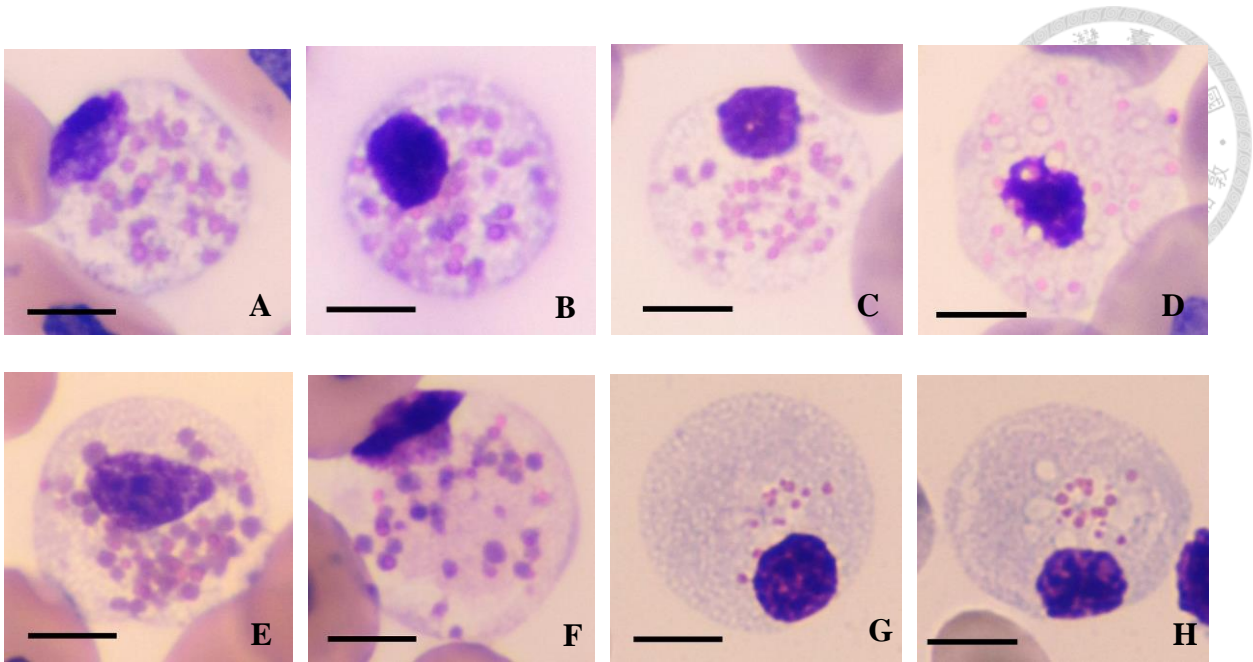
Figure 6. Representative eosinophils of olive ridley and hawksbill sea turtles, scale bar=10μm

A-D: olive ridley sea turtles; E-H: hawksbill sea turtles

A: numerous, more evenly sized and evenly distributed cytoplasmic granules, Wright-Giemsa stain;

B: Diff-Quik stain; C: Liu's stain; D: note the unstained granules sometimes appeared as vacuoles

with Liu's stain, only the cores (or a second type of granules) were stained, which resulted in

eosinophils that appeared to have less and smaller cytoplasmic granules; E: a more centrally located

nucleus, Wright-Giemsa stain; F: a pleomorphic nucleus that was pushed against the cellular

membrane, Diff-Quik stain; G&H: rounded nucleus, note the unstained granules sometimes

appeared as vacuoles with Liu's stain, only the cores (or a second type of granules) were stained,

which resulted in eosinophils that appeared to have less and smaller cytoplasmic granules

Basophils

Basophils, although rarely seen on blood films in sea turtles, were identified in all 3 species in this study. Basophils of sea turtles were small to medium sized, rounded cells with a N/C ratio around 0.5. The single, round to elliptical nucleus was centrally or eccentrically placed, but was difficult to visualize in many cells, being obscured by numerous, deeply basophilic cytoplasmic granules. The granules were generally small and rounded, but size and shape can be indistinct due to compact arrangement and commonly occurred degranulation. Staining properties were identical with Wright-Giemsa's stain, Diff-Quik and Liu's stain.
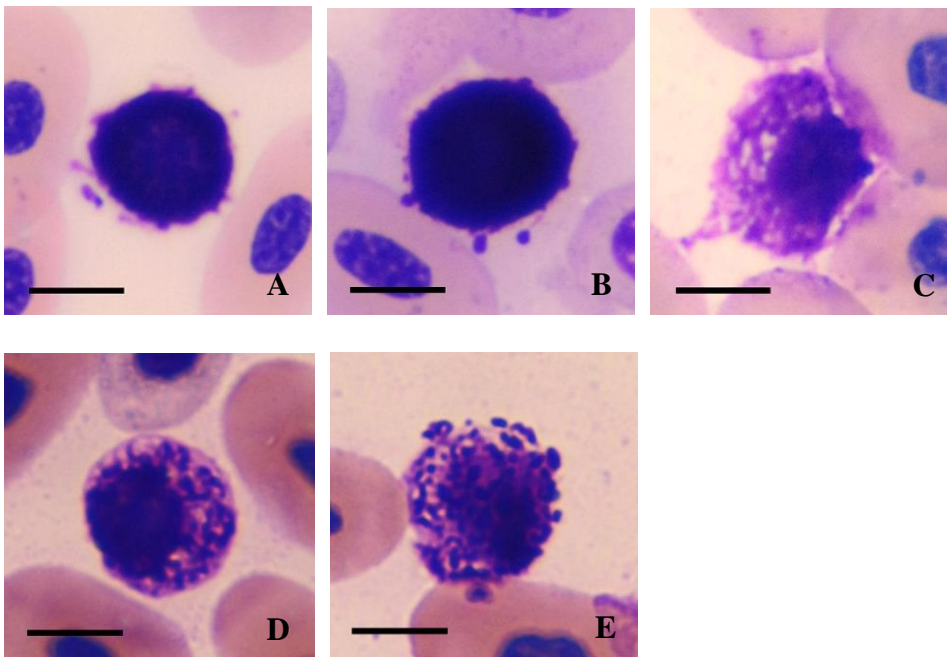
Figure 7. Representative basophils of studied sea turtles, scale bar=10μm

A: a smaller basophil of a green sea turtle, Wright-Giemsa stain; B: a medium-sized basophil of a green sea turtle, Wright-Giemsa stain; C: a degranulated basophil of an olive ridley sea turtle, Diff-Quik stain; D&E: hawksbill sea turtles, Wright-Giemsa stain

Lymphocytes

Lymphocytes morphology were similar in the 3 sea turtle species in this study. Sea turtles' lymphocytes were greatly variable in size (from very small to medium sized) and shape (round to pleomorphic). Usually, lymphocytes had the highest N/C ratio of all blood cells.

Smaller lymphocytes had a N/C ratio close to 1, and the nucleus was round or pleomorphic, with condensed and smudged chromatin that were deeply basophilic. The cytoplasm was scarce, stained blue when seen, and cytoplasmic granules or vacuoles were absent. These cells should be carefully differentiated from thrombocytes by the more basophilic and scant cytoplasm, the more deeply stained and less smooth-margined nucleus, and oftentimes less elongated shapes.

Larger lymphocytes had less condensed chromatin, and more amount of cytoplasm that often created an irregular cell margin by the presence of pseudopodia. The nucleus was frequently irregularly round to oval, stained bright purple, with a clumped chromatin pattern. The cytoplasm is basophilic as in the smaller lymphocytes. These cells should be distinguished from monocytes by the non-lobed nucleus, the higher N/C ratio, the less amount of cytoplasm, the more homogenous and basophilic cytoplasm, and the more condensed or clumped chromatin pattern, which usually resulted in darker staining of the nucleus.

Staining properties of lymphocytes were very similar under all 3 types of stains.
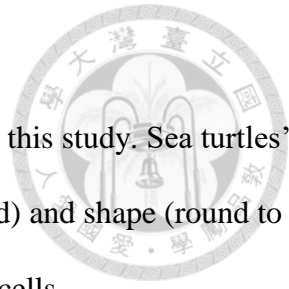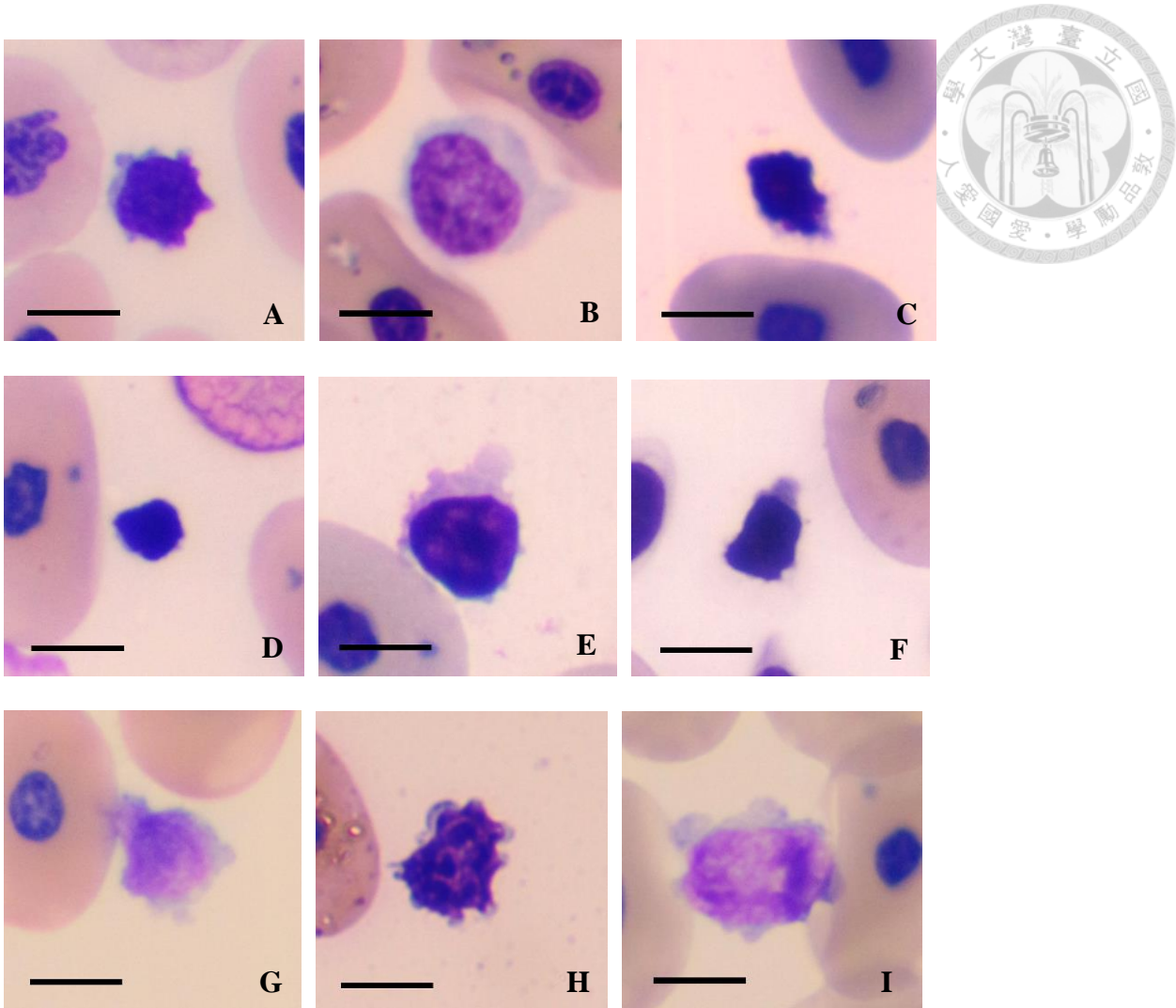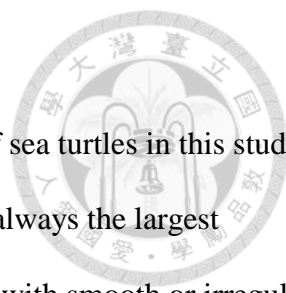
Figure 8. Representative lymphocytes of studied sea turtles, scale bar=10μm

A-C: green sea turtles; D-F: olive ridley sea turtles; G-I: hawksbill sea turtles

A: a small to medium-sized lymphocyte, Wright-Giemsa stain; B: a larger lymphocyte, note the less condensed chromatin, Diff-Quik stain; C: a smaller lymphocyte with condensed and smudged chromatin pattern, Liu's stain; D: a smaller lymphocyte, Wright-Giemsa stain; E: a larger lymphocyte, note the presence of cytoplasmic pseudopodia, Diff-Quik stain; F: a smaller lymphocyte, Liu's stain; G: a medium-sized lymphocyte, Wright-Giemsa stain; H: a medium-sized lymphocyte, note the clumped chromatin pattern, Diff-Quik stain; I: a medium-sized to large lymphocyte, note the presence of cytoplasmic pseudopodia, , Liu's stain

Monocytes

Monocytes were identified on the blood films of all three species of sea turtles in this study. Monocytes were medium-sized to large (unlike in birds and mammals, no always the largest leukocytes seen on blood film), generally rounded to slightly pleomorphic, with smooth or irregular cell borders created by the presence of pseudopodia. The N/C ratio is frequently below 0.5, and the bright purple, frequently eccentrically placed nucleus had a great variety of shapes, ranging from round, elliptical, bean-shaped to pleomorphic. The chromatin pattern was usually lacy, with few or no clumps. The abundant cytoplasm usually stained sky blue with an unevenly mixed pinkish hue, and may contained vacuoles of various size. These cells should be distinguished from immature erythrocytes by the more variable nucleus shape (immature erythrocytes usually had a more rounded nucleus), the more often eccentrically positioned nucleus, the less clumped chromatin, the presence of cytoplasmic pseudopodia, and the usually more abundant cytoplasm with characteristic coloration.

A more immature form of monocytes was also identified in all three species of sea turtles. Immature monocytes were rounded to pleomorphic, with or without pseudopodia, and usually medium sized (smaller than mature monocytes). Comparing to mature monocytes, immature or less matured monocytes had higher N/C ratio, more clumped chromatin, and both the nucleus and the cytoplasm were more intensely stained. Nucleus shape varied from round, elliptical, bean-shaped, lobed to pleomorphic. Cytoplasmic granules were not seen, while small amount of vacuoles sometimes presented.

Staining properties of monocytes were similar under all 3 types of stains.
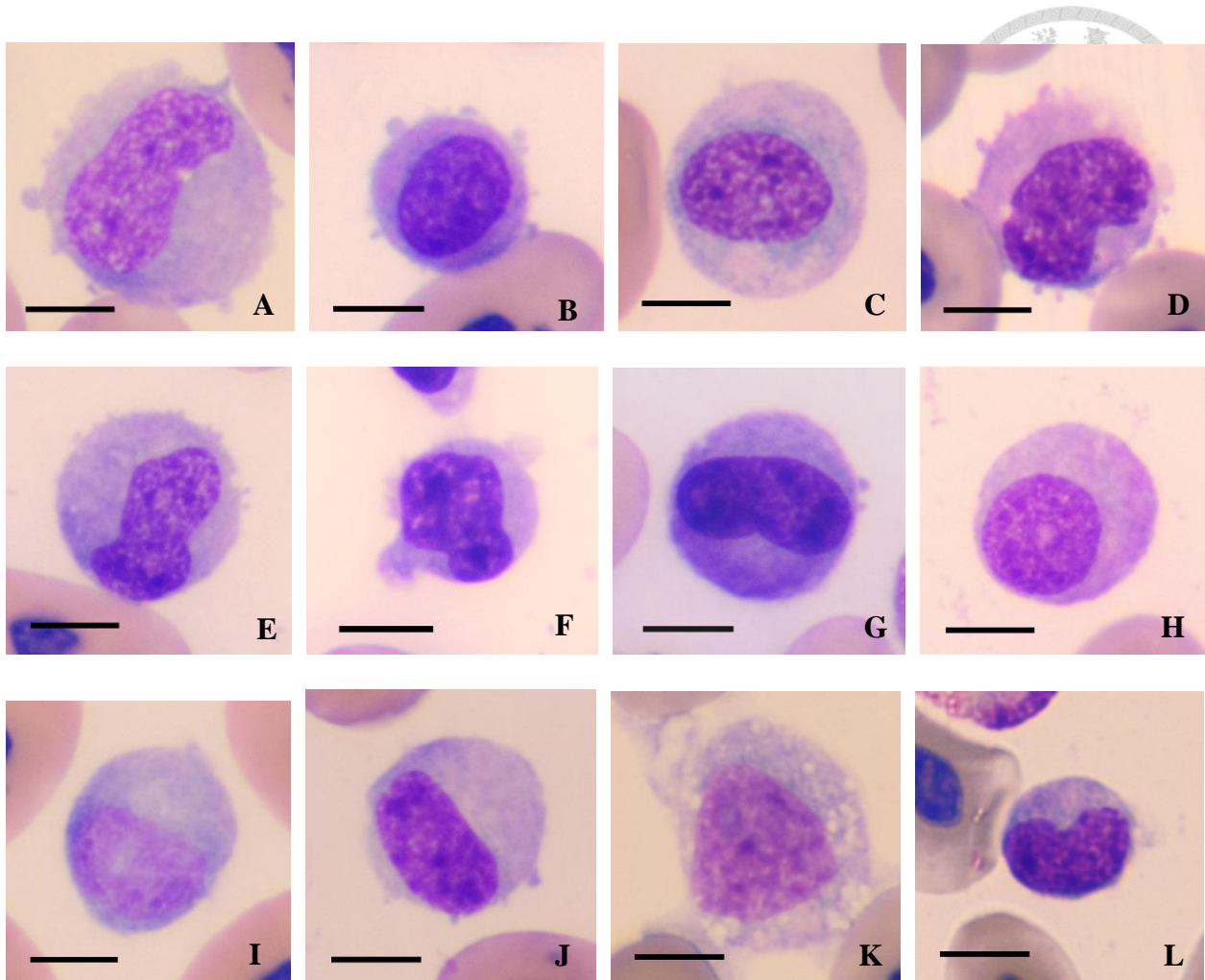
Figure 9. Representative monocytes of studied sea turtles, scale bar=10μm

A-D: green sea turtles; E-H: olive ridley sea turtles; I-L: hawksbill sea turtles

A: lacy chromatin and cytoplasmic pseudopodia, Wright-Giemsa stain; B: an immature monocyte, Wright-Giemsa stain; C: the cytoplasm was stained sky blue with an unevenly mixed pinkish hue, Diff-Quik stain; D: bean-shaped nucleus, Liu's stain; E: pleomorphic nucleus, Wright-Giemsa stain; F: an immature monocyte, Wright-Giemsa stain; G: a less matured monocyte, Diff-Quik stain; H: round nucleus and smooth cellular margins, Liu's stain; I: Wright-Giemsa stain; J: Diff-Quik stain; K: presence of cytoplasmic vacuoles, Liu's stain; L: an immature monocyte, Liu's stain
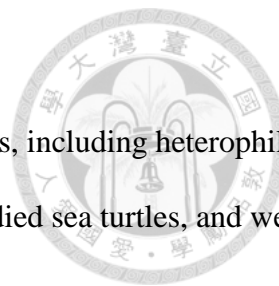
4.2.2 Leukocyte ultrastructure of sea turtles

4 types of leukocytes were identified in the studied sea turtle species, including heterophils, eosinophils, lymphocytes and monocytes. Basophils were scarce in the studied sea turtles, and were not seen on any ultra-sections under TEM examination.

Heterophils

Heterophils were rounded in shape, with few unremarkable small pseudopodia of the cellular membrane. The distinctive nucleus was eccentrically located, irregularly elliptical toward elongated or bi-lobed in shape. Moderate amount of heterochromatin (condensed and inactive form of chromatin, contrary to the uncondensed and active euchromatin, both exist in an interphase nucleus) was seen scattered within the nucleus, and aggregated around the nuclear membrane. Nucleoli was not prominent in most cells examined. The cytoplasm contained numerous round to elliptical or pleomorphic, moderately electron-dense granules (termed as "type I granules"), which were generally homogenous but can also be variable in electron density. Aside from the primary group of granules, a second type of granules were also evident (termed as "type II granules"), which were significantly more electron-dense, more often rounded, and fewer in number. In green sea turtles, type II granules can be comparable to type I granules in size; while in olive ridley sea turtles and hawksbill sea turtles, type II granules were generally smaller. Type I and type II granules distributed unevenly within the cytoplasm, resulted in only one type of granules seen on some ultra-sections. Other cytoplasmic organelles were rare in heterophils of the studied sea turtles. Small number of mitochondria, rare single row of rough-surfaced endoplasmic reticulum (RER) and small vesicles were occasionally found, while free ribosomes and polyribosomes were evenly dispersed within the cytoplasm.
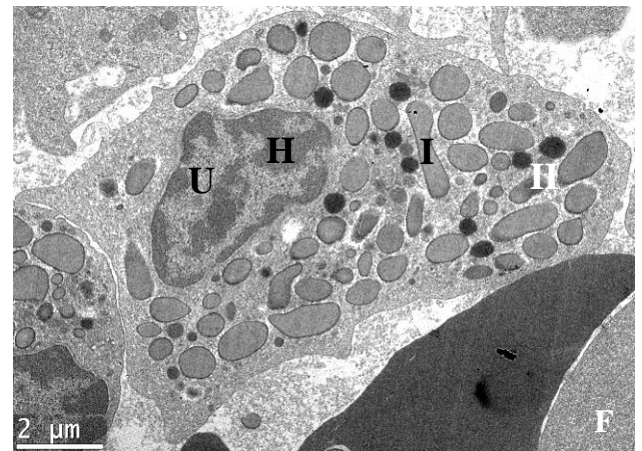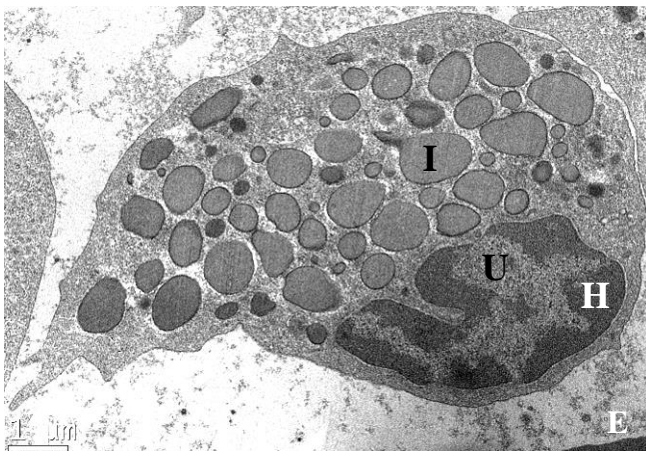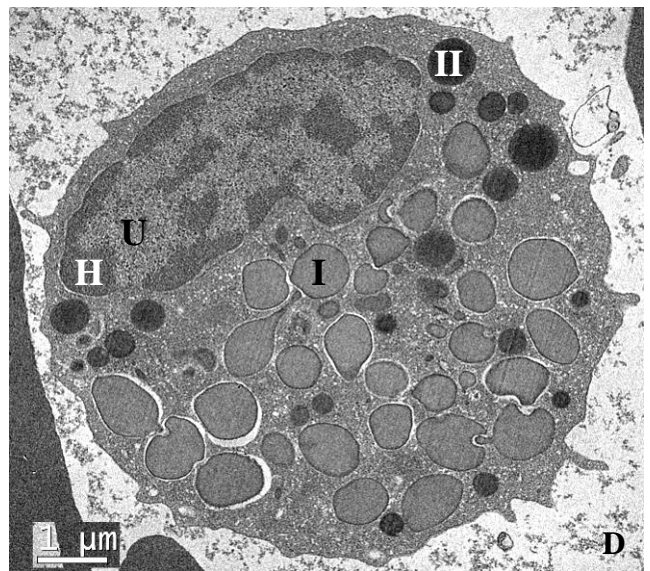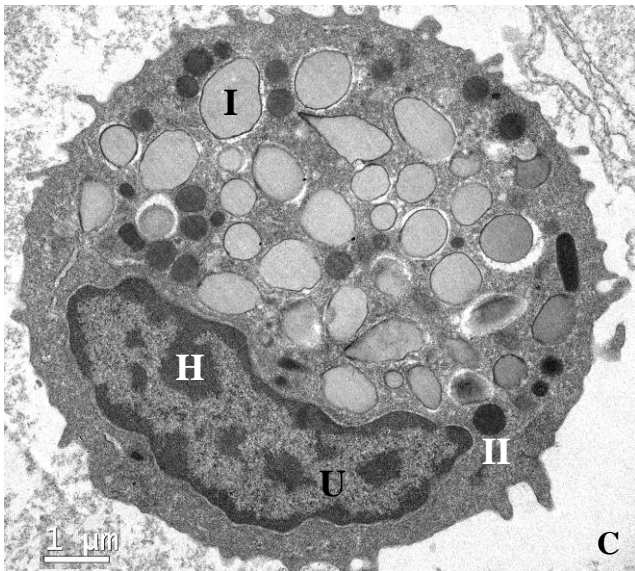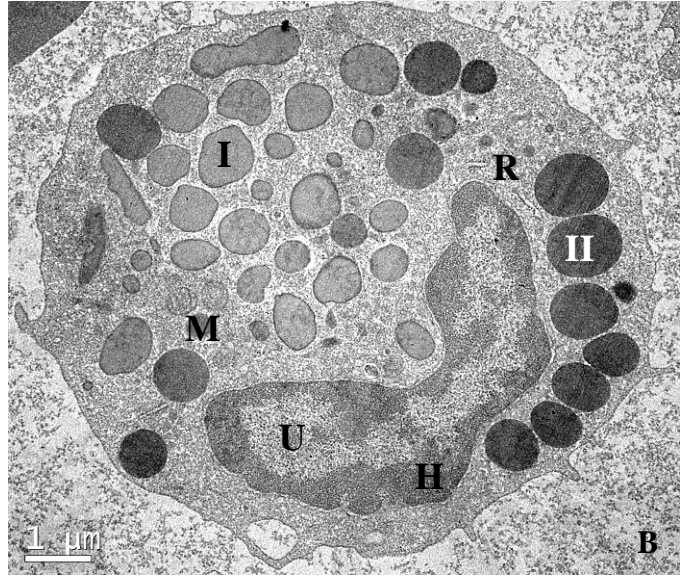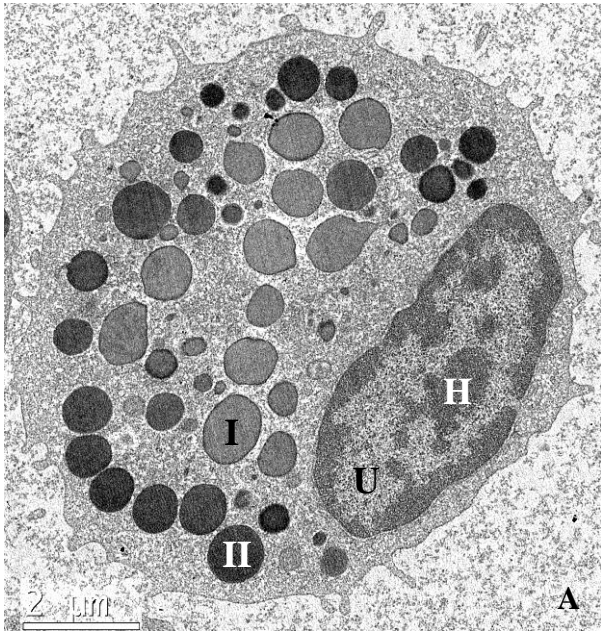
Figure 10. Representative heterophil ultrastructure in studied sea turtles

All cells were stained with uranyl acetate and lead citrate

H: heterochromatin; U: euchromatin; I: type I granules; II: type II granules; M: mitochondria; R: rough-surfaced endoplasmic reticulum (RER)

A&B: green sea turtles; C&D: olive ridley sea turtles; E&F: hawksbill

A: type I granules were generally homogenous in electron density, and type II granules were more electron-dense, fewer in number and comparable to type I granules in size, B: type I and type II granules distributed unevenly within the cytoplasm; C&D: type II granules were generally smaller than type I granules in olive ridley sea turtles; E: type I and type II granules distributed unevenly within the cytoplasm, and type II granules were rarely seen in this ultrasection; F: type II granules were generally smaller than type I granules in hawksbill sea turtles
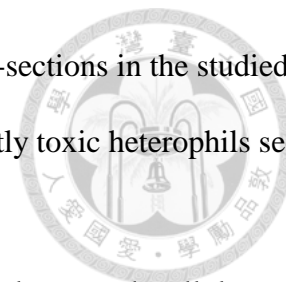
Toxic heterophils were extremely rare and difficult to find on ultra-sections in the studied sea turtles. In the following we described electromicrographs of significantly toxic heterophils seen in green sea turtles.

Toxic heterophils of green sea turtles were rounded in shape and had a smooth cellular membrane. Because of the unsegmented nature of sea turtles' heterophil nucleus, the immaturity of the cells was characterized by the rounded and less indented nucleus, the higher N/C ratio, one or more prominent nucleolus, and a higher proportion of active euchromatin relative to the clumped and condensed, inactive heterochromatin. Of the examined toxic heterophils, left-shifting were commonly observed but not in all cells.

Comparing to normal heterophils, the number of cytoplasmic granules were significantly reduced. Granules generally became smaller or more variable in size; and while some granules remained rounded, others appeared more pleomorphic and had less distinct membrane. As a result, the types of cytoplasmic granules could not be distinguished for certain. Some small, electron-dense granules were seen dispersed within the cytoplasm. Changes of electron density and structure within the primary granules were not apparent.

The cytoplasm of toxic heterophils contained much greater amount of membranous organelles, such as the mitochondria, Golgi apparatus, vesicles, and excessive RER (arranged dispersedly in the form of a single row, not in lamellar form). Clusters of dark polyribosomes were increased and clearly visible.

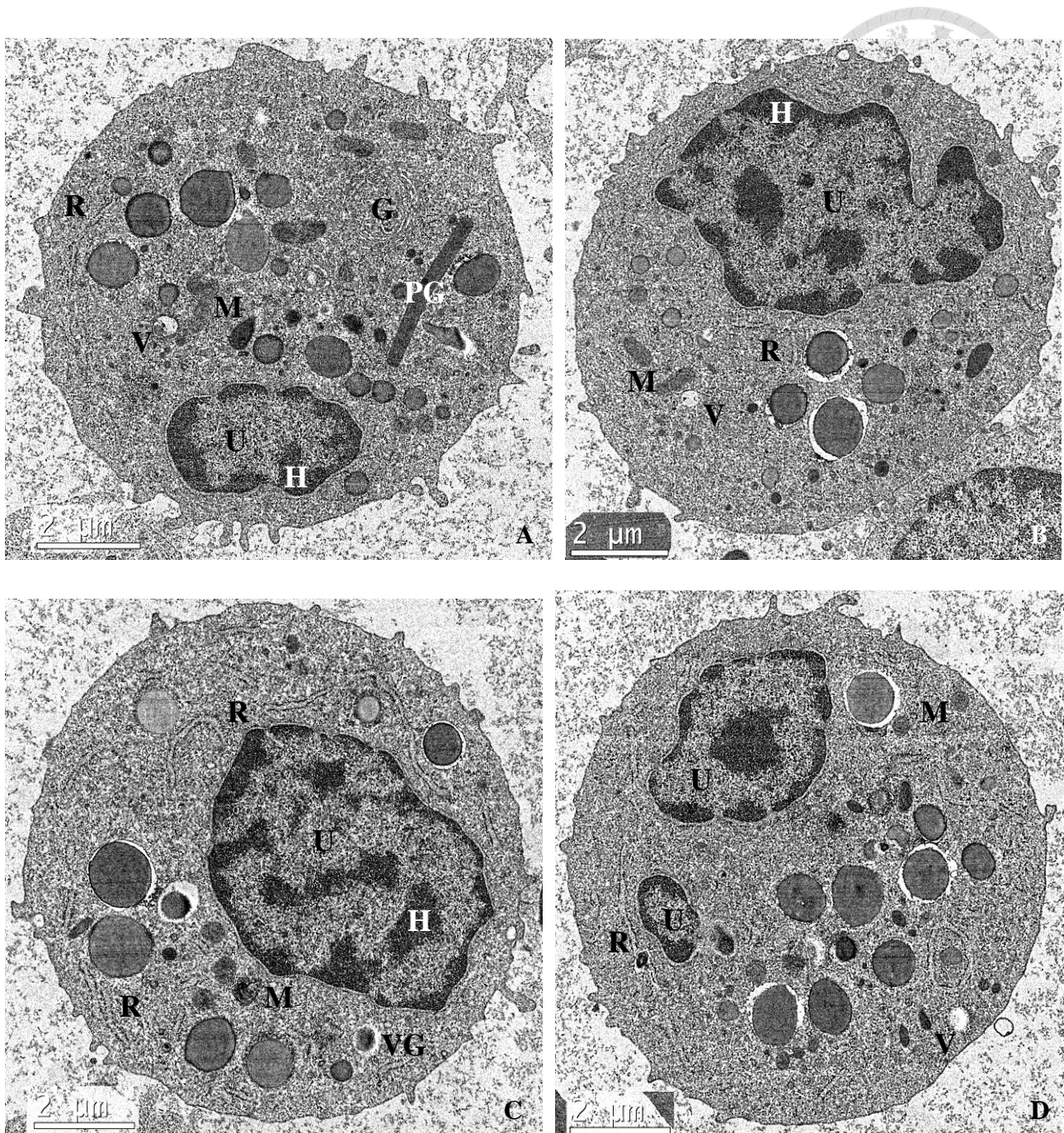No phagocytized materials were observed in the examined toxic heterophils.

Figure 11. Representative toxic heterophil ultrastructure in green sea turtles

All stained with uranyl acetate and lead citrate

H: heterochromatin; U: euchromatin; M: mitochondria; G: Golgi apparatus; V: vesicles; R: endoplasmic reticulum (ER); PG: pleomorphic granules

A: reduced number of cytoplasmic granules, granules became smaller or more variable in size, pleomorphic granules, prominent Golgi apparatus; B: higher N/C ratio and significantly reduced

60

granules; C: reduced granules, abundant RER arranged dispersedly in the form of a single row; D: reduced granules, granules became smaller or more variable in size, prominent RER arranged dispersedly in the form of a single row
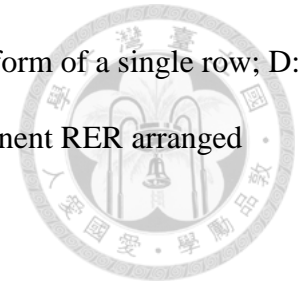
Eosinophils

Large eosinophils were rounded in shape, with few unremarkable pseudopods of the cellular membrane. The distinctive nucleus was frequently eccentrical, irregularly round to elliptical in shape. Moderate amount of condensed heterochromatin was seen scattered within the nucleus, and aggregated around the nuclear membrane. Nucleoli was not prominent in most cells examined. The abundant cytoplasm was filled with consistently small, round and poorly defined (especially evident in stained samples which underwent more processing), coalescing vacuoles. Few large, round (sometimes pushed against each other and appeared more pleomorphic), electron-dense granules; often seen with a very distinct, small, rounded and more electron-dense (sometimes less homogenous) "core"; were found within the cytoplasm. No crystalline structure was identified in the examined eosinophil granules. Free ribosomes and polyribosomes were seen, while membranous organelles were not easily seen.

Small eosinophils were scarce in sea turtles, as a result, these cells were difficult to find on TEM micrographs. Small eosinophils were rounded in shape, and had a smooth cellular membrane. The distinctive nucleus was often eccentrically located, irregularly round to elliptical in shape. Moderate amount of condensed heterochromatin was seen scattered within the nucleus. Nucleoli was not prominent. The cytoplasm was not vacuolated and was packed with multiple large, distinctive, round to elliptical, electron-dense granules without a core or any crystalline structure. Free ribosomes, free polyribosomes, mitochondria and small vesicles were easily found.
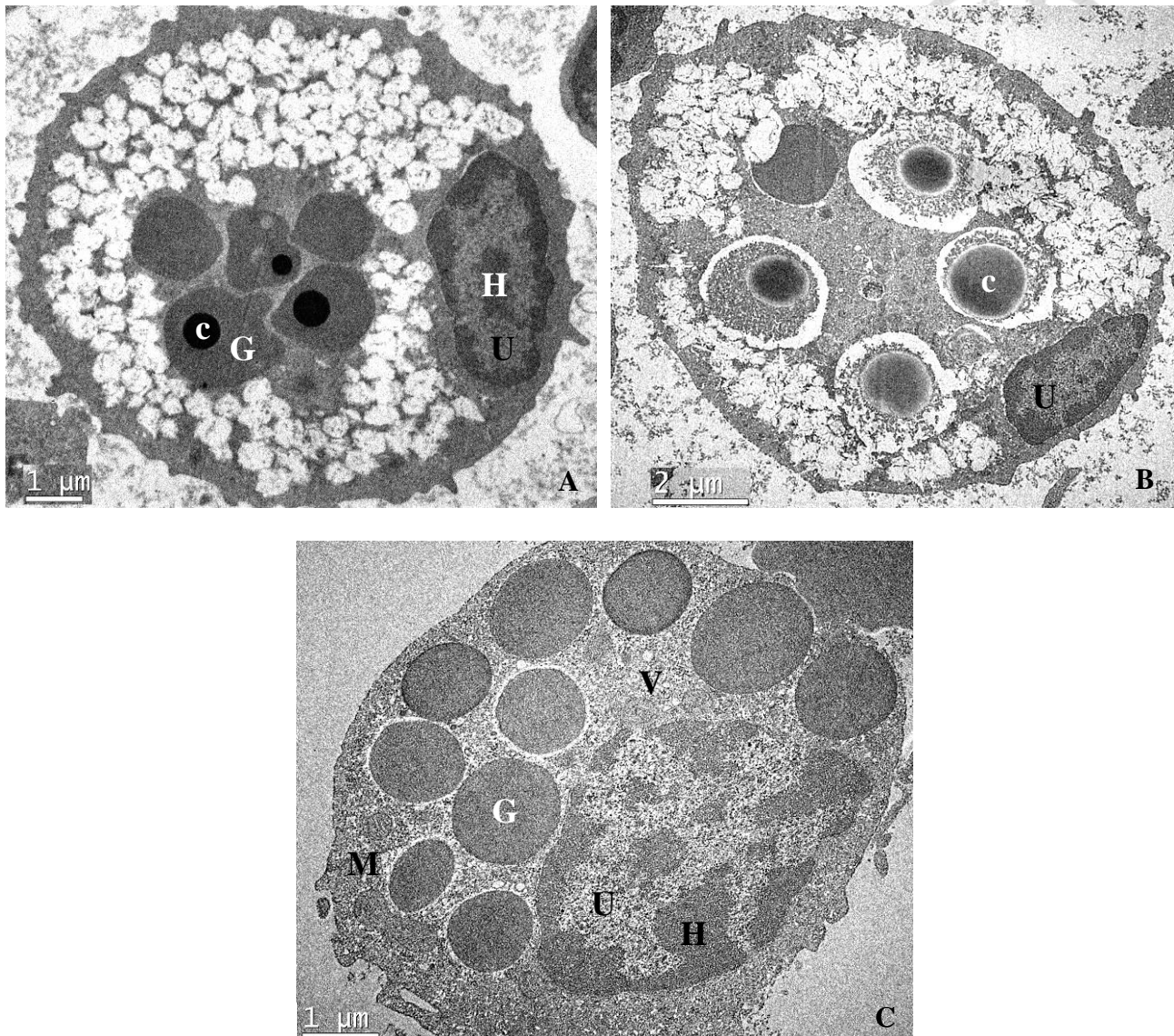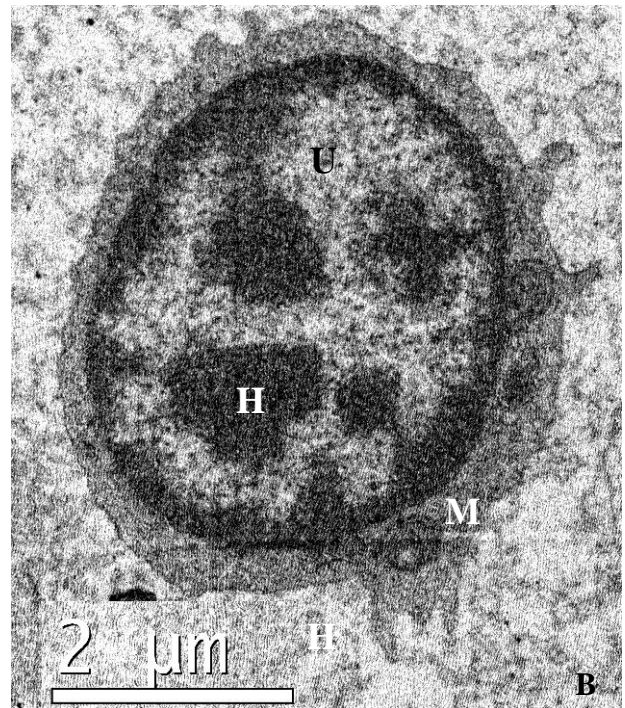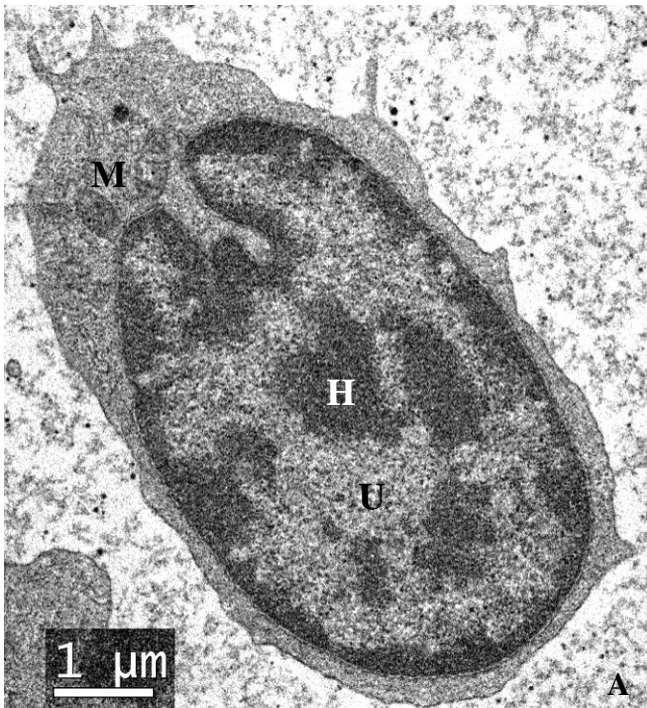
Figure 12. Representative eosinophil ultrastructure in studied sea turtles

H: heterochromatin; U: euchromatin; G: cytoplasmic granules; c: core; M: mitochondria; V: vesicles

A: the cytoplasm of large eosinophils was filled with poorly defined and coalescing vacuoles, and cytoplasmic granules were often seen with a small and strongly electron-dense core, while no crystalline structure was identified within the granules, green sea turtles; B: the vacuoles were less defined when stained with uranyl acetate and lead citrate, while the cores of the cytoplasmic granules were clearly depicted, green sea turtles; C: the cytoplasm of the small eosinophils was not vacuolated and was packed with multiple granules without a core or crystalline structure

62

Lymphocytes

Lymphocytes were round to elliptical in shape, with a generally smooth cellular membrane. The round to indented nucleus took up most of the cellular space, and contained abundant amount of peripherally and centrally clumped heterochromatin. Free ribosomes and polyribosomes were evenly dispersed within the scarce cytoplasm, multiple mitochondria were clearly visible, as well as some rough endoplasmic reticulum, Golgi apparatus and rarely small number of small vesicles.
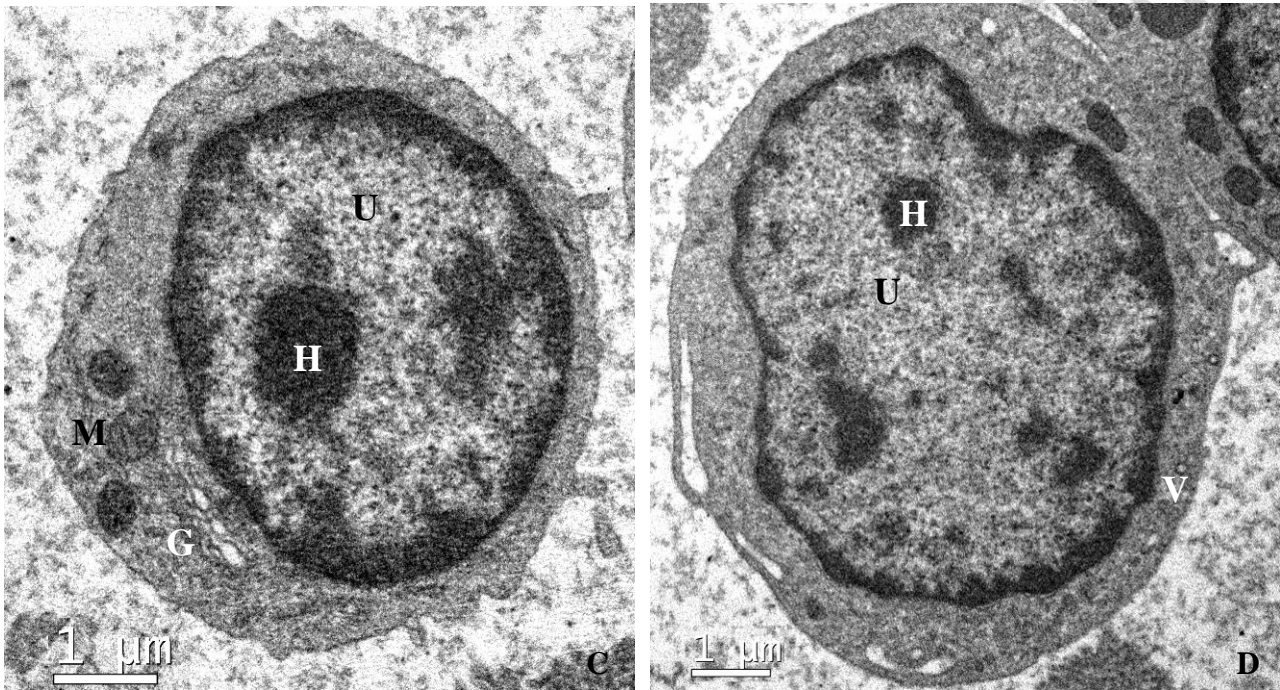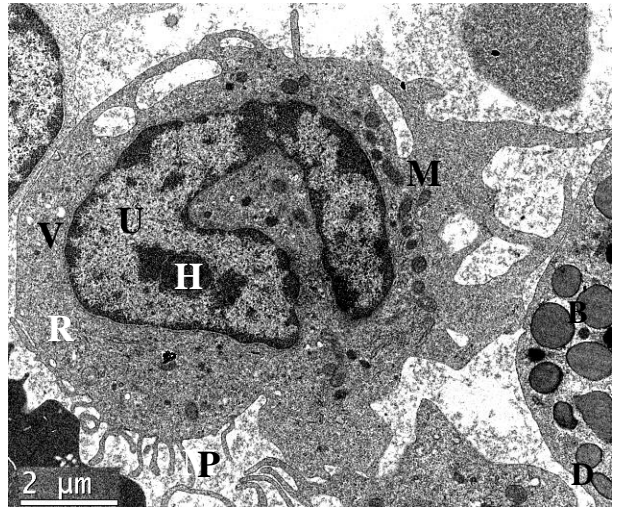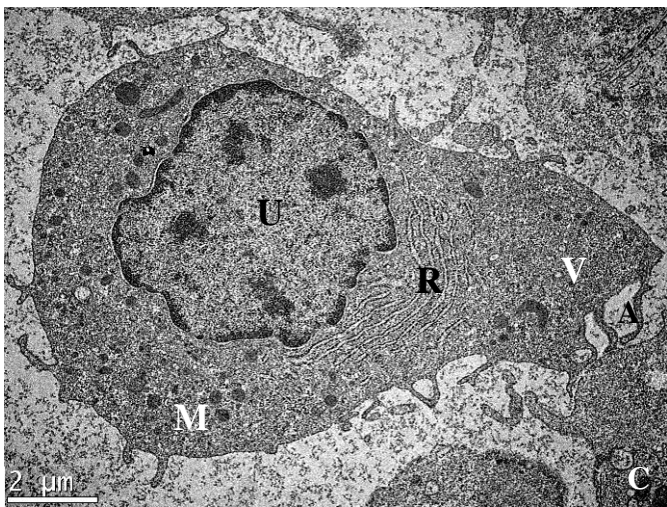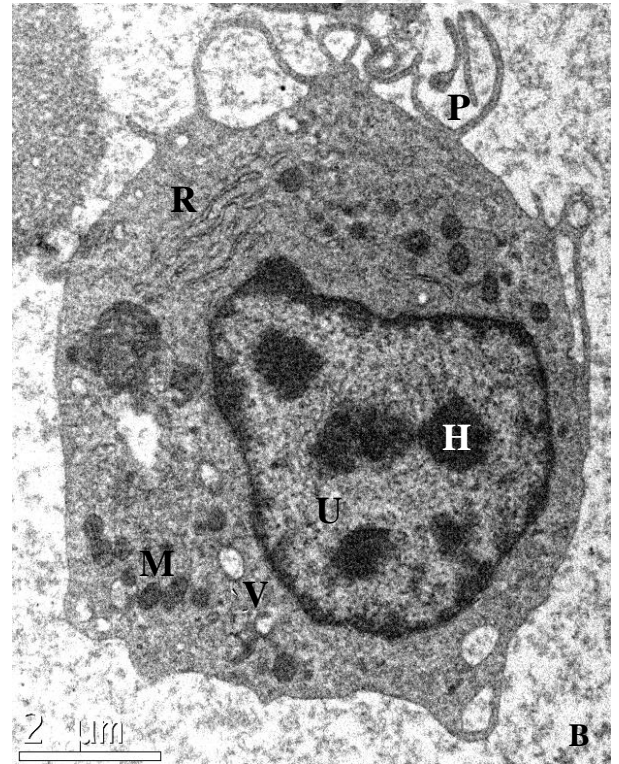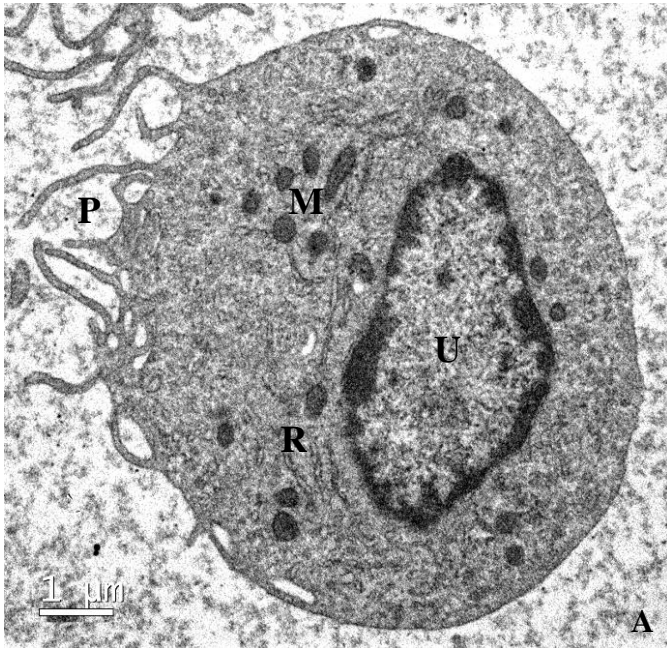
Figure 13. Representative lymphocyte ultrastructure in studied sea turtles

H: heterochromatin; U: euchromatin; M: mitochondria; G: Golgi apparatus; V: vesicles

A: a lymphocyte with a slightly indented nucleus; B: rounded nucleus with highly clumped heterochromatin; C: Golgi apparatus and mitochondria were seen within the cytoplasm; D: a larger lymphocyte with less clumped heterochromatin and slightly more cytoplasm that contained vesicles

Monocytes

Monocytes were irregularly round in shape, often exhibited multiple prominent finger-like pseudopodia extending from the cellular membrane. The nucleus was irregularly round to indented or bean-shaped, containing scant to variable amount of peripherally and centrally clumped heterochromatin. The abundant cytoplasm was rich in mitochondria, endoplasmic reticulum (sometimes prominent), vesicles of various size, and free ribosomes and polyribosomes. Sometimes a Golgi apparatus and small number of small, rounded, electron-dense granules were seen within the cytoplasm. Monocytes exhibited phagocytic properties, and on rare occasion were seen engulfing apoptotic cells or foreign materials.
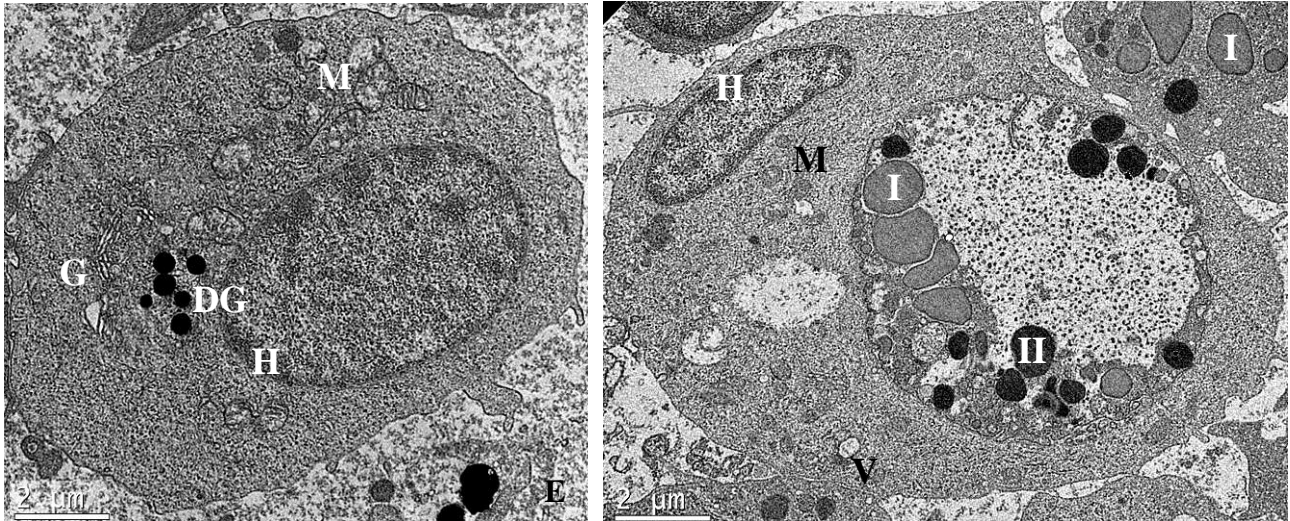
64

Figure 14. Representative monocyte ultrastructure in studied sea turtles

H: heterochromatin; U: euchromatin; P: pseudopodia; M: mitochondria; V: vesicles; R: rough-surfaced endoplasmic reticulum (RER); G: Golgi apparatus; DG: dense granules; I: type I granules of heterophil; II: type II granules of heterophil

A: pseudopodia, scant heterochromatin, and cytoplasm filled with membranous organelles; B: the cytoplasm was rich in mitochondria, endoplasmic reticulum, vesicles of various size, and free ribosomes and polyribosomes; C: abundant cytoplasm with a prominent rough endoplasmic reticulum (RER); D: an indented nucleus seen in a monocyte of a hawksbill sea turtle, stained with uranyl acetate and lead citrate; E: small number of small, rounded, electron-dense granules were seen within the cytoplasm of a monocyte of a green sea turtle; F: a phagocytic monocyte and a degenerated heterophil (note the characteristic cytoplasmic granules), stained with uranyl acetate and lead citrate

66

4.2.3 Leukocyte morphology of yellow pond turtles and Chinese box turtles

5 types of leukocytes were identified in both yellow pond turtles and Chinese box turtles, including heterophils, eosinophils, basophils, lymphocytes and monocytes.
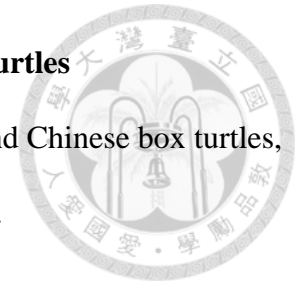
Heterophils

Heterophils of yellow pond turtles and Chinese box turtles were very similar to that of sea turtles. They were usually larger (but cell size can vary), round cells with a small N/C ratio. The single, eccentrically located nucleus was round to elliptical or bi-lobed, and often pushed against the cellular membrane. Sometimes the nucleus border can be difficult to identified due to its pale or uneven staining properties. The nucleus stained pale blue to dark purple under Wright-Giemsa's stain, Diff-Quik stain and Liu's stain, and when stained deeply, a clumped chromatin pattern could be seen. The clear cytoplasm was packed with eosinophilic, refractile cytoplasmic granules, while vacuoles were not seen. Because of the commonly occurred cytoplasmic drying artifact and the crowdedness of the granules, heterophil granules often appear pleomorphic and less defined in shape.
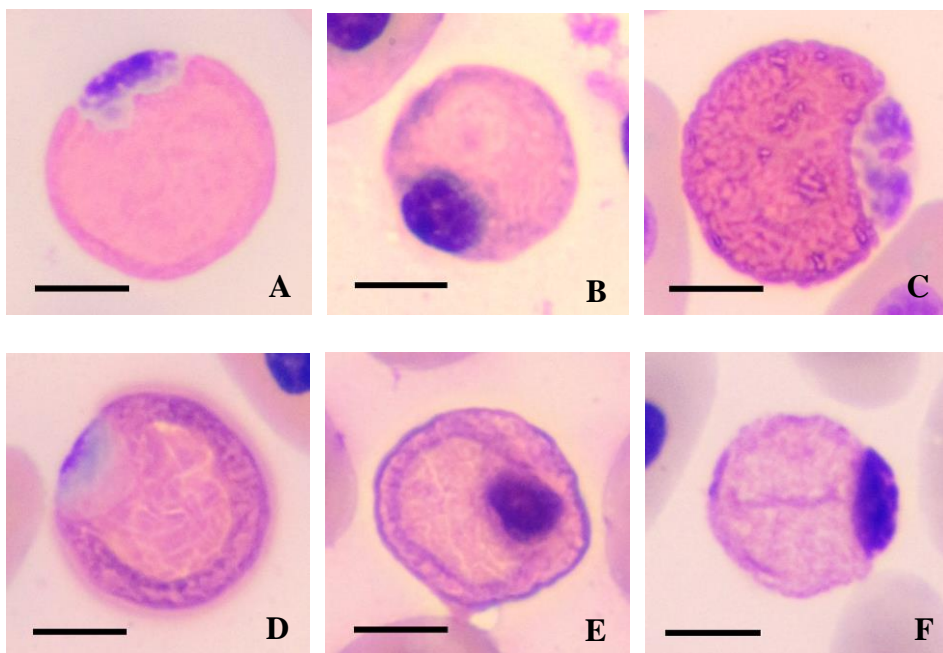
Figure 15. Representative heterophils of studied yellow pond turtles and Chinese box turtles, scale bar=10μm

A-C: yellow pond turtles; D-F: Chinese box turtles; A: the nucleus was pushed against the cellular membrane, Wright-Giemsa stain; B: a more rounded nucleus, Diff-Quik stain; C: a bilobed nucleus, note the packed and refractile granules, Liu's stain; D: note the common presence of drying artifact, Wright-Giemsa stain; E: Diff-Quik stain; F: Liu's stain

Eosinophils

Eosinophils of yellow pond turtles and Chinese box turtles could be mistaken for heterophils by inexperienced examiners. At first glance, eosinophils seemed identical to heterophils judging on their compact, small and indistinct in shape, brightly eosinophilic cytoplasmic granules, and the eccentrically located, basophilic nucleus that was frequently pushed against the cell border. However, eosinophils could be distinguished by the significantly smaller cell size, the light blue cytoplasm, and the relatively homogenously stained, intensely basophilic nucleus. The chromatin pattern was clumped or smudged. Sometimes some scattered granules could be seen obscuring the nucleus. Staining properties were identical with Wright-Giemsa's stain, Diff-Quik and Liu's stain.
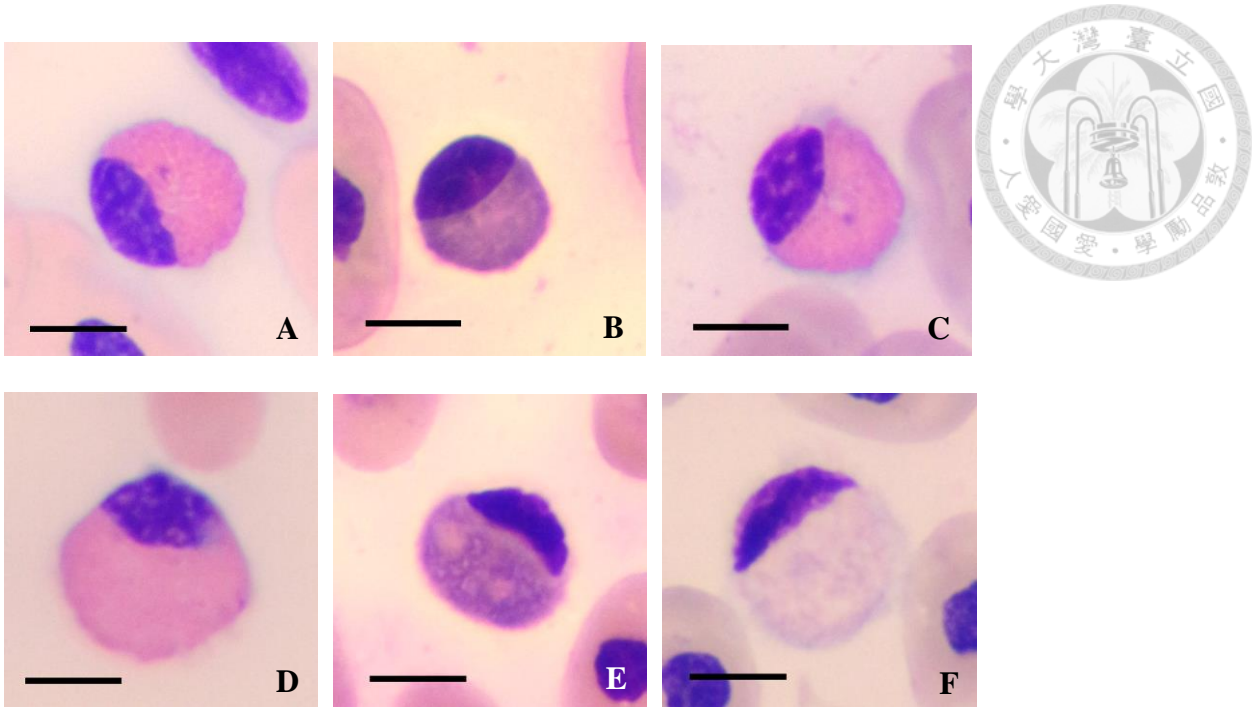
Figure 16. Representative eosinophils of studied yellow pond turtles and Chinese box turtles, scale bar=10μm

A-C: yellow pond turtles; D-F: Chinese box turtles; A: eosinophils could be distinguished from heterophils by the significantly smaller cell size and the light blue cytoplasm, Wright-Giemsa stain; B: the N/C ratio is larger in eosinophils comparing to heterophils, Diff-Quik stain; C: note the light blue cytoplasm, Liu's stain; D: some scattered granules could be seen obscuring the nucleus, Wright-Giemsa stain; E: Diff-Quik stain; F: Liu's stain

Basophils

    Basophils, contrary to those of sea turtles, were commonly seen on the blood films of yellow pond turtles and Chinese box turtles, as in many other freshwater turtles. Basophils of yellow pond turtles and Chinese box turtles were similar to sea turtles in morphology. These cells were small, rounded cells with a high N/C ratio. The single, round to elliptical nucleus was difficult to visualize in many cells, being obscured by numerous, deeply basophilic cytoplasmic granules. The granules were generally fine to small and rounded, but size and shape can be indistinct due to compact arrangement and commonly occurred degranulation. Staining properties were identical with Wright-Giemsa's stain, Diff-Quik and Liu's stain.
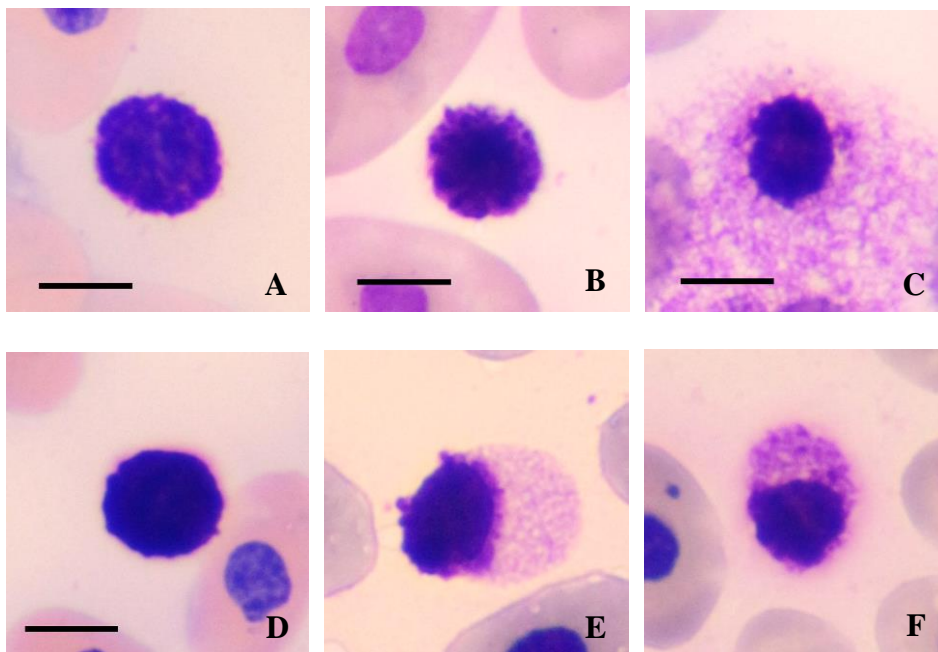

Figure 17. Representative basophils of studied yellow pond turtles and Chinese box turtles, scale bar=10μm

A-C: yellow pond turtles; D-F: Chinese box turtles; A: the nucleus was obscured by cytoplasmic granules, Wright-Giemsa stain; B: Diff-Quik stain; C: commonly occurred degranulation, Liu's stain; D: Wright-Giemsa stain; E: degranulation, Diff-Quik stain; F: degranulation, Liu's stain

Lymphocytes

Lymphocytes were the smallest cells found on the blood films of yellow pond turtles and Chinese box turtles in this study, however, these cells were still variable in size (from very small to small-medium sized) and shape (round to pleomorphic). Lymphocytes had very high N/C ratio (close to 1), and the nucleus was round or pleomorphic, with condensed and clumped to smudged chromatin that were deeply basophilic. The blue cytoplasm was scant, sometimes only seen as wispy edges of the nucleus, created an irregular cellular border. These cells should be carefully differentiated from thrombocytes by the more bluish, scant cytoplasm, the more deeply stained and less smooth-margined nucleus, and oftentimes less elongated shapes.
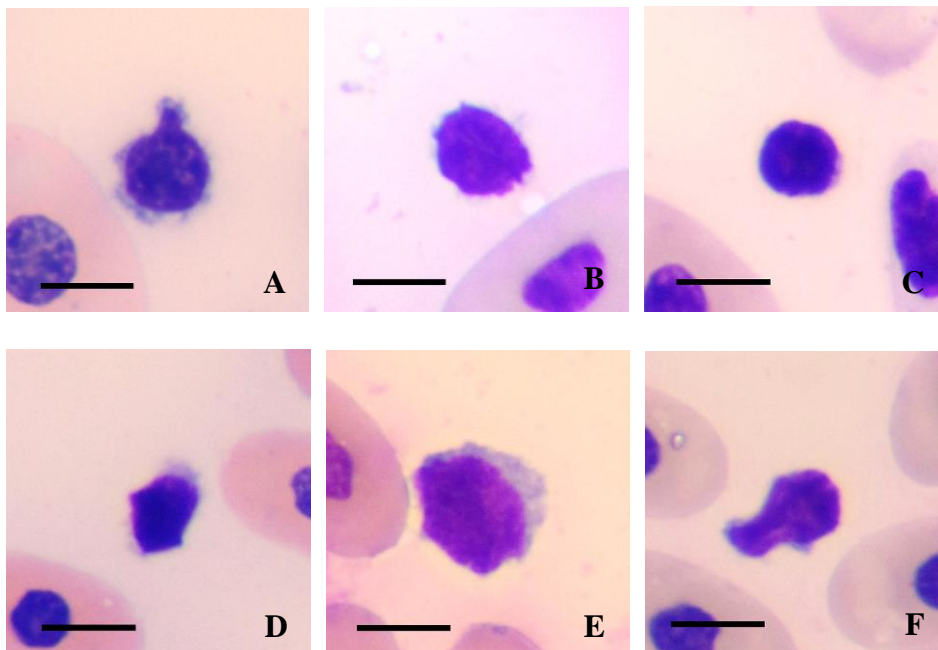

Figure 18. Representative basophils of studied yellow pond turtles and Chinese box turtles, scale bar=10μm

A-C: yellow pond turtles; D-F: Chinese box turtles; A: blue cytoplasm, Wright-Giemsa stain; B: scarce cytoplasm, Diff-Quik stain; C: rounded nucleus, Liu's stain; D: pleomorphic nucleus, Wright-Giemsa stain; E: a larger lymphocyte, Diff-Quik stain; F: pleomorphic nucleus, Liu's stain

Monocytes

Monocytes were medium-sized to large (generally slightly smaller comparing to heterophils), generally rounded, with smooth to slightly irregular cell borders created by the presence of pseudopodia. The N/C ratio is generally close to 0.4 to 0.5, and the bright purple, frequently eccentrically placed nucleus was frequently lobed, although nucleus shape could also range from elliptical, bean-shaped to pleomorphic. The chromatin pattern was usually lacy to coarse and mildly clumped. The abundant cytoplasm usually stained sky blue with an unevenly mixed pink to purplish hue, and may contained vacuoles of various size. Staining properties of monocytes were similar under all 3 types of stains.
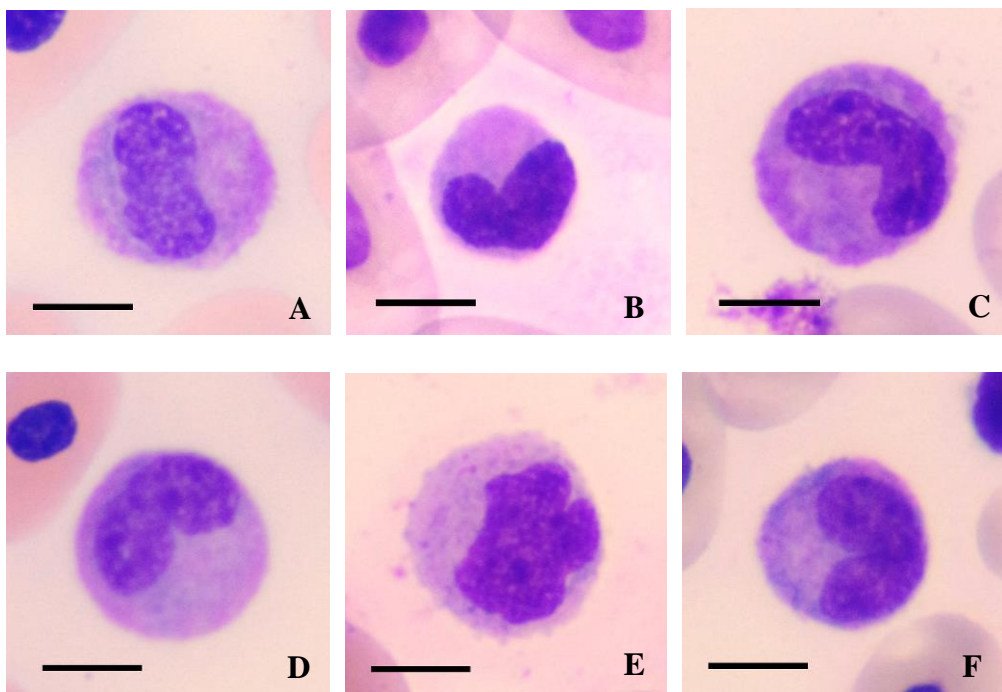
Figure 19. Representative monocytes of studied yellow pond turtles and Chinese box turtles, scale bar=10μm

A-C: yellow pond turtles; D-F: Chinese box turtles; A: elliptical to bean-shaped nucleus, note the lacy chromatin pattern and foamy cytoplasm, Wright-Giemsa stain; B: a less mature monocyte, Diff-Quik stain; C: slightly clumped chromatin pattern, Liu's stain; D: Wright-Giemsa stain; E: pleomorphic nucleus, Diff-Quik stain; F: Liu's stain

72

4.2.4 Leukocyte ultrastructure of yellow pond turtles and Chinese box turtles

Heterophils

Yellow pond turtles had irregularly rounded heterophils with a generally smooth cytoplasmic membrane, which sometimes exhibited small, finger-like pseudopodia. The eccentrically located nucleus was pleomorphic, with moderate amount of peripheral heterochromatin. The cytoplasm was packed with numerous large, irregularly spindle-shaped (even elongated) and electron-dense granules. One or more small, round and strongly electron-dense cores were frequently seen within the cytoplasmic granules. Free ribosomes and polyribosomes were dispersed within the cytoplasm. Mitochondria were seen in small numbers, and vacuoles were also found; while endoplasmic reticulum was difficult to find.

Heterophils of the Chinese box turtles also had a generally smooth cytoplasmic membrane with few small pseudopodia. The eccentrically located nucleus was irregularly round to pleomorphic, with moderate amount of peripherally or centrally clumped heterochromatin. The cytoplasm was packed with primarily large, oval-shaped and moderately electron-dense granules (type I granules). As in the yellow pond turtles, these granules were also frequently found with one or more small, rounded and strongly electron-dense cores. A second population of granules (type II granules) were also seen, which were fewer in number, smaller in size, round to elliptical in shape, and significantly less electron-dense. Free ribosomes and polyribosomes were dispersed within the cytoplasm. Other membranous organelles such as mitochondria and endoplasmic reticulum were not commonly found, while vacuoles were clearly present.
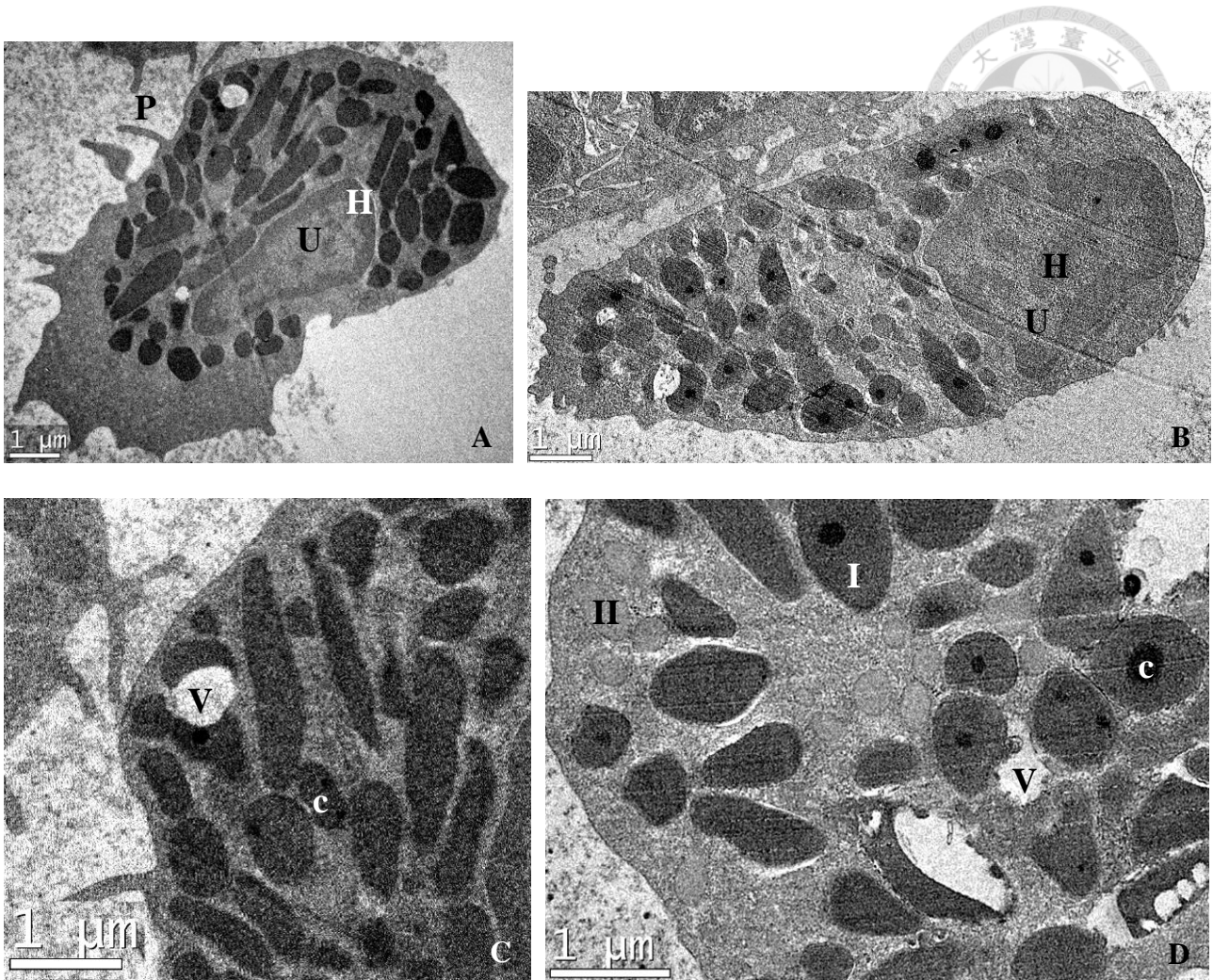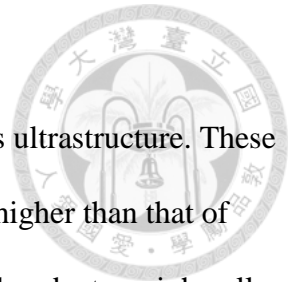
Figure 20. Representative heterophil ultrastructure in yellow pond turtles and Chinese box turtles

H: heterochromatin; U: euchromatin; V: vacuoles; c: core; I: type I granules; II: type II granules

A: irregularly spindle-shaped and electron-dense granules, yellow pond turtles; B: the cytoplasm was packed with primarily large, oval-shaped granules with one or more strongly electron-dense cores, Chinese box turtles; C: close up details of the cytoplasmic granules, one or more strongly electron-dense cores were frequently seen, yellow pond turtles; D: close up details of the cytoplasmic granules, a second population of granules (type II granules) were also seen, which were significantly less electron-dense, Chinese box turtles

Eosinophils

Yellow pond turtles and Chinese box turtles had similar eosinophils ultrastructure. These cells were rounded with some finger-like pseudopodia. The N/C ratio was higher than that of heterophils, and the large nucleus was irregularly round to indented, with abundant, peripherally and centrally aggregated heterochromatin. The cytoplasm was packed with numerous evenly sized, rounded granules with variable electron density (generally homogenously electron-dense). No cores or crystalline structure were identified within the granules, but vacuoles were frequently presented. Free ribosomes and polyribosomes were dispersed within the cytoplasm, few mitochondria and vesicles were seen, but endoplasmic reticulum was difficult to find.
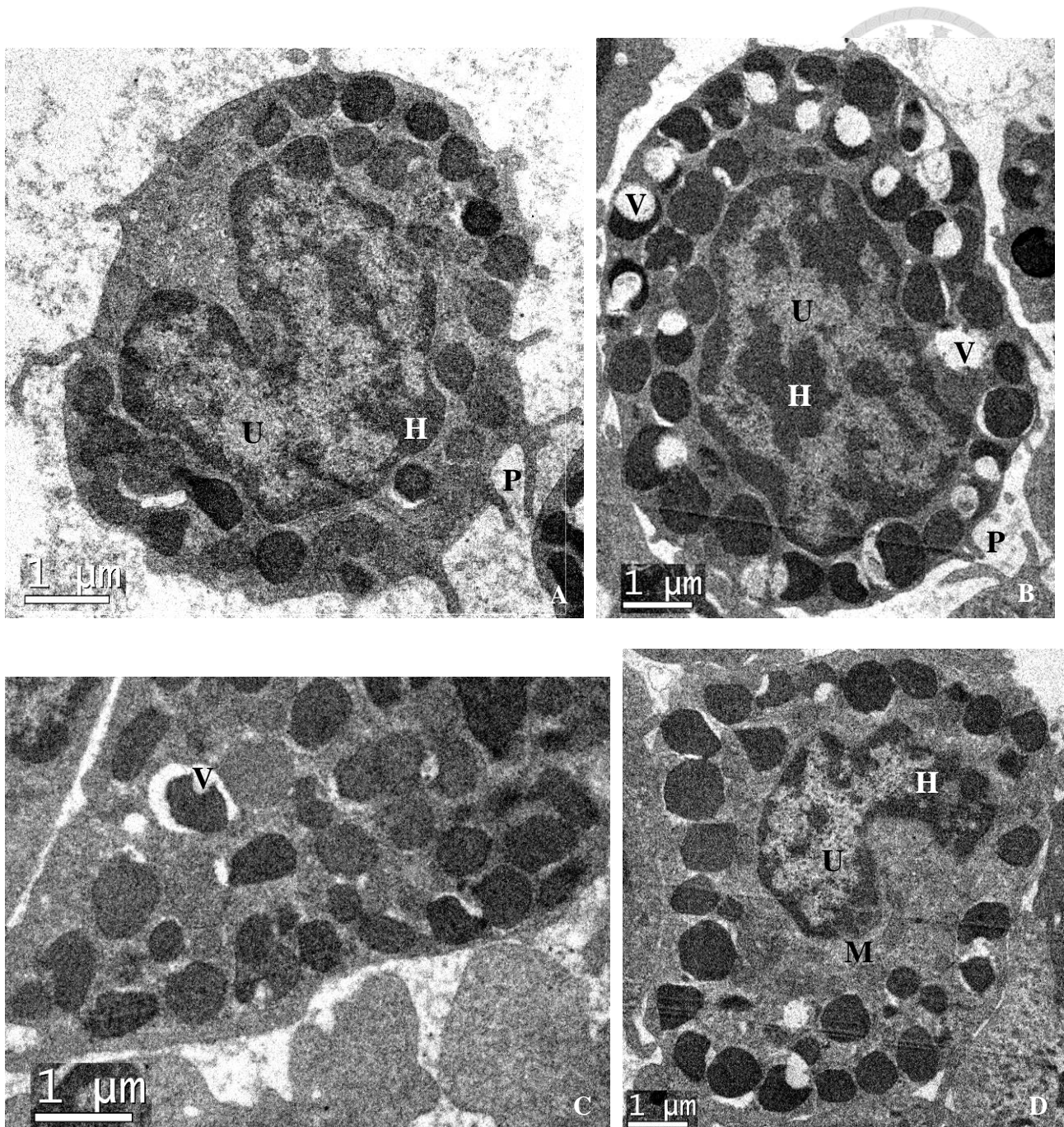
Figure 21. Representative eosinophil ultrastructure in yellow pond turtles and Chinese box turtles

H: heterochromatin; U: euchromatin; P: pseudopodia; V: vacuoles; M: mitochondria

A: indented nucleus and evenly sized granules, yellow pond turtles; B: an irregularly rounded

nucleus, cores or crystalline structure were not seen within the granules, but vacuoles were

frequently presented, Chinese box turtles; C: close up details of the cytoplasmic granules, yellow

pond turtles; D: indented nucleus and a few mitochondria were seen, Chinese box turtles

76

Basophils

Yellow pond turtles and Chinese box turtles had similar basophils ultrastructure. These cells were rounded with a smooth cellular membrane, but occasionally few finger-like pseudopodia was present. The N/C ratio was high, and the large nucleus was irregularly round to pleomorphic, with abundant heterochromatin. The cytoplasm was packed with a highly heterogenous population of rounded to pleomorphic granules of varying size. Although identically basophilic under light microscope, it was fascinating to see the diversity of these granules on an ultra-microscopic level. Many of them had a finely stippled content (type I granules), while a fewer but very conspicuous group of granules exhibited delicate patterns (sometimes termed as "honeycomb-like" or "reticular" in literature) of unique kinds and different electron density (type II granules). These structures were identified as microtubules. The third group of cytoplasmic granules appeared irregularly round, relatively homogenous and electron-dense, while vacuoles were sometimes presented (type III granules). However, with uranyl acetate and lead citrate double staining, one or more crystalline inclusions were clearly seen within many of the type III granules. The crystalline structures were homogenously electron-dense, polygonal in shape, giving some type III granules an angular appearance. Yellow pond turtles seemed to have dominant type I granules and less, smaller type III granules comparing to Chinese box turtles, but type II granules were rarest in both species. Other cytoplasmic organelles were not prominent in basophils of these species. Free ribosomes and polyribosomes were dispersed within the cytoplasm, short segments of rough endoplasmic reticulum were occasionally seen, while other membranous organelles were difficult to find.
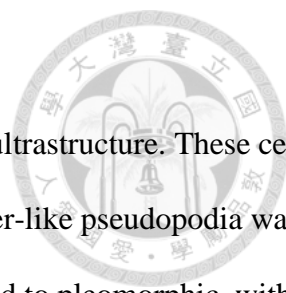
Figure 22. Representative basophil ultrastructure in yellow pond turtles and Chinese box turtles

H: heterochromatin; U: euchromatin; V: vacuoles; I: type I granules; II: type II granules; III: type III granules; cs: crystalline structure

A: type I granules have finely stippled content, yellow pond turtles; B: type II granules have honeycomb-like pattern, Chinese box turtles; C&D: crystalline inclusions were seen within many of the type III granules stained with uranyl acetate and lead citrate, Chinese box turtles

Lymphocytes

Lymphocytes were similar between yellow pond turtles and Chinese box turtles. These cells were round to elliptical in shape, with an irregular cellular membrane. The large, rounded nucleus took up most of the cellular space, and contained abundant amount of peripherally and centrally clumped heterochromatin. Free ribosomes and polyribosomes were dispersed within the scarce cytoplasm. Membranous organelles were scant in small lymphocytes, while multiple mitochondria, rough endoplasmic reticulum and small vesicles were clearly seen in large lymphocytes.
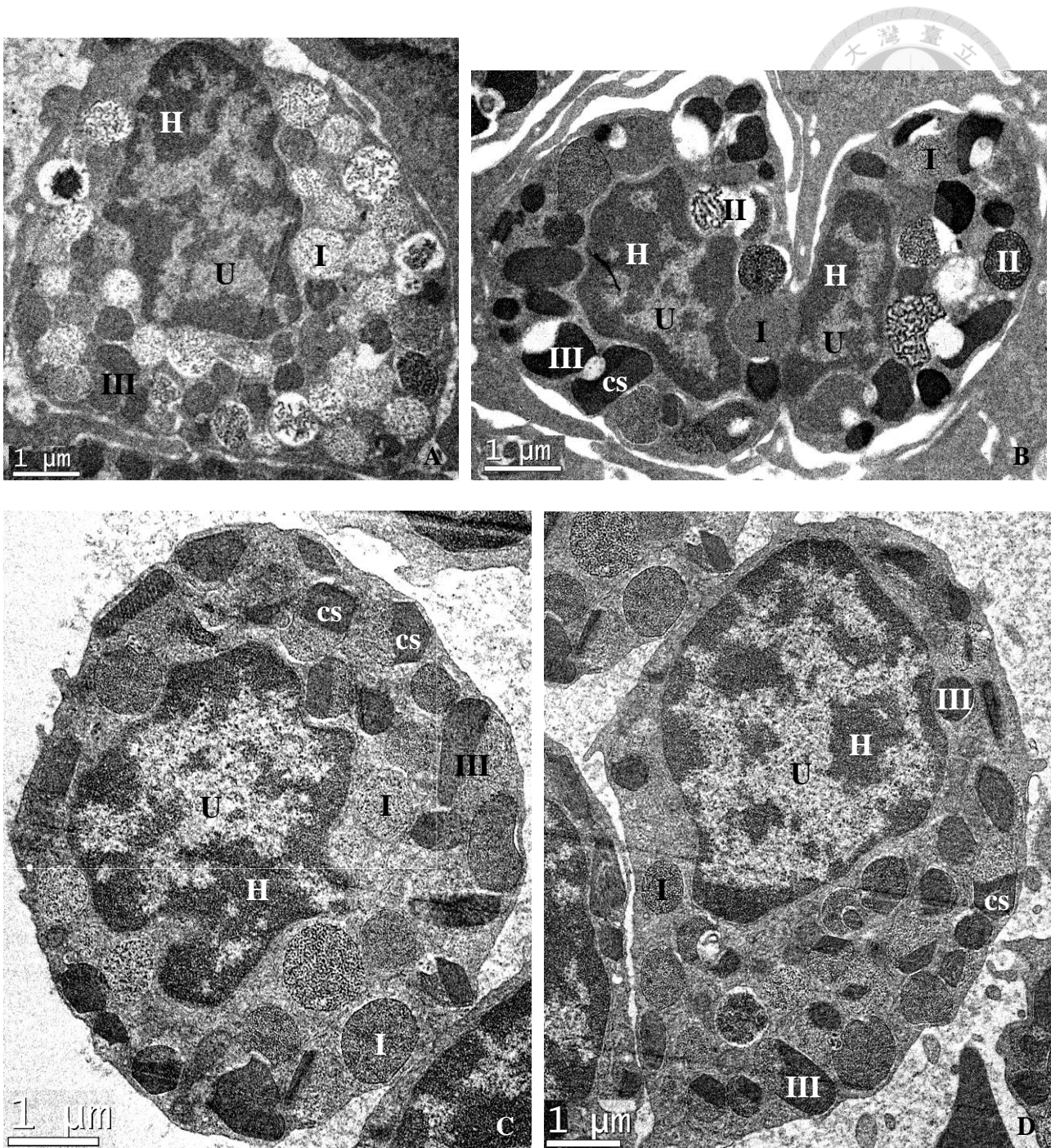

Figure 23. Representative lymphocyte ultrastructure in yellow pond turtles and Chinese box turtles

H: heterochromatin; U: euchromatin; M: mitochondria; R: rough endoplasmic reticulum (RER); V: vesicles

A: scant cytoplasm and membranous organelles in a small lymphocyte; B: abundant amount of clumped chromatin, multiple mitochondria, rough endoplasmic reticulum and small vesicles in a large lymphocyte, stained with uranyl acetate and lead citrate

Monocytes

Monocytes were similar between yellow pond turtles and Chinese box turtles. These cells were irregularly round in shape, with a lower N/C ratio. The nucleus was irregularly round to indented, containing scant to variable amount of peripherally and centrally clumped heterochromatin. The abundant cytoplasm was rich in membranous organelles. Numerous mitochondria, endoplasmic reticulum, vesicles of various size, small number of small, rounded, electron-dense granules, free ribosomes and polyribosomes were easily seen.
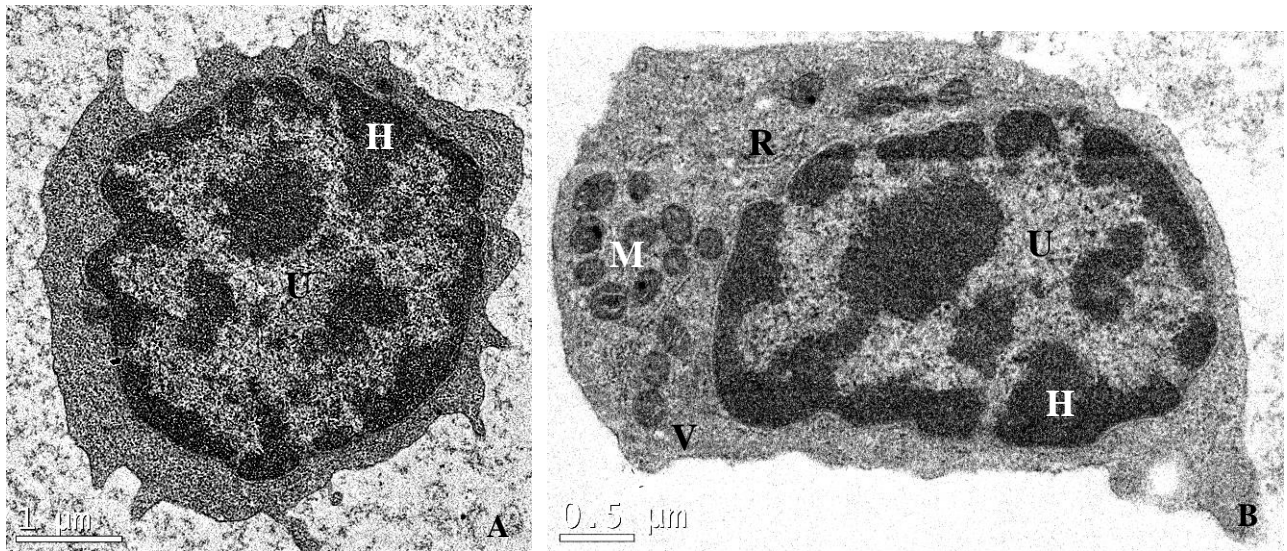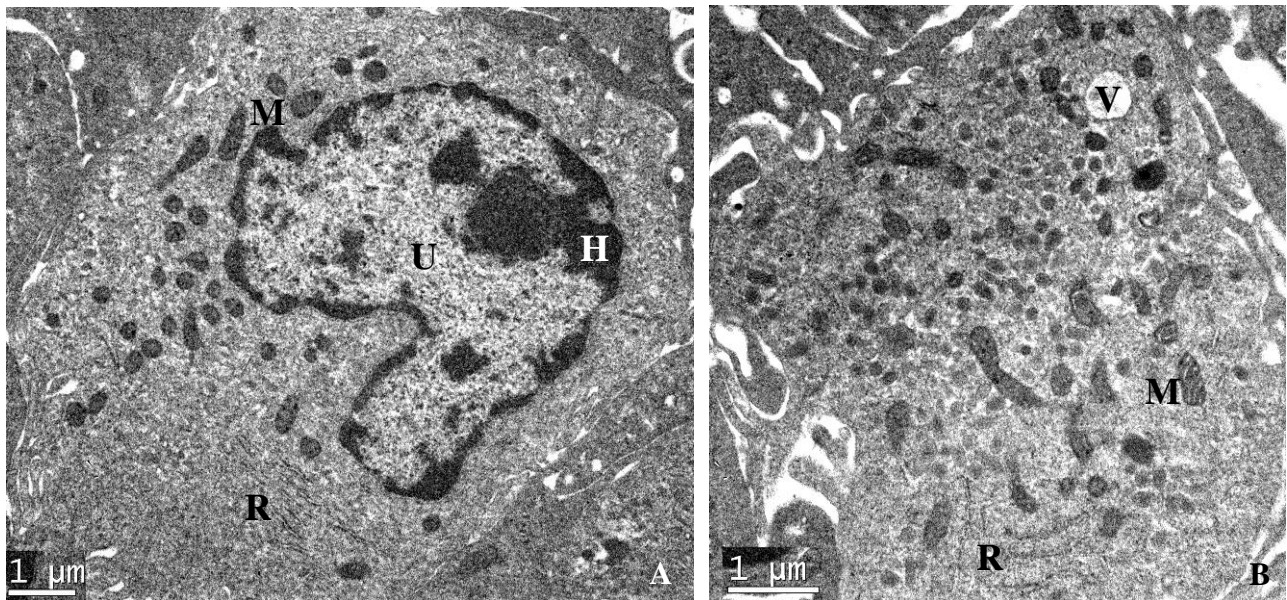

Figure 24. Representative monocyte ultrastructure in yellow pond turtles and Chinese box turtles

H: heterochromatin; U: euchromatin; M: mitochondria; R: rough endoplasmic reticulum (RER); V: vesicles

A: the indented nucleus contained mainly euchromatin, note the abundant cytoplasmic membranous organelles; B: abundant cytoplasmic membranous organelles

4.3 Efficacy of different staining methods

4.3.1 Leukocyte differentiation

Blood films from all 30 sea turtles were stained with Wright Giemsa stain, Diff-Quik stain, and Liu's stain; except for one individual, of which only Wight Giemsa stained blood films were obtained. All three staining methods demonstrated excellent staining properties for leukocyte differentiation, with about 90% or more slides ranked diagnostic (above borderline) or better. Specifically, with Wright Giemsa stain, 29 of 30 (96.67%) slides were excellent on staining properties for leukocyte differentiation. With Diff-Quik stain, 25 of 29 (86.21%) slides were excellent, and 3 of 29 (10.34%) slides were good. Finally, with Liu's stain, 26 of 29 (89.66%) slides were excellent. No significant difference was found among the three staining methods (Chi-squared P-value=0.965, >0.05) regarding the performance of leukocyte differentiation. Slides rendered poor or undiagnostic were due to overstaining (Diff-Quik stain and Liu's stain) or lack of basophilic stain (Wright Giemsa stain).
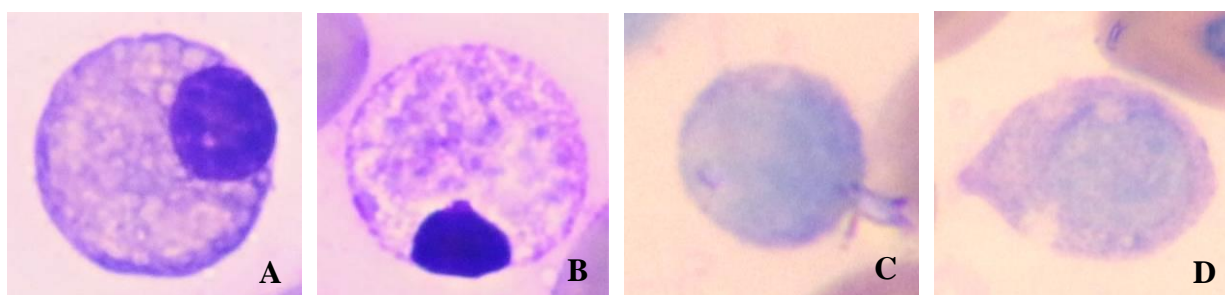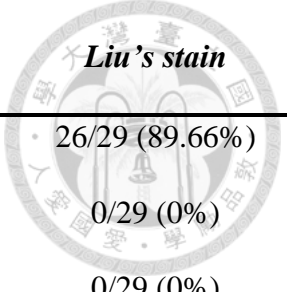

Figure 25. Examples of staining properties unsuitable for leukocyte differentiation

A-D: Examples of failure to demonstrate cell specific colors and/ or morphology. During the 100 leukocyte count, the more percentage these kind of cells were seen on a stained slide, the slide is regarded as less diagnostic; A: the eosinophilic heterophil granules were not presented due to overstaining, Diff-Quik stain; B: the eosinophilic granules and light blue cytoplasm of an eosinophil were not presented due to overstaining, Diff-Quik stain; C&D: lack of basophilic stain resulted in difficulties of leukocyte differentiation, Wright Giemsa stain

100 leukocytes per slide	*Wright Giemsa stain*	*Diff-Quik stain*	*Liu's stain*
Excellent (95-100)	29/30 (96.67%)	25/29 (86.21%)	26/29 (89.66%)
Good (80-95)	0/30 (0%)	3/29 (10.34%)	0/29 (0%)
Borderline (65-80)	0/30 (0%)	0/29 (0%)	0/29 (0%)
Poor (35-65)	0/30 (0%)	1/29 (3.45%)	3/29 (10.34%)
Undiagnostic (<35)	1/30 (3.33%)	0/29 (0%)	0/29 (0%)

Table 7. Performance of 3 staining methods on leukocyte differentiation

All three staining methods demonstrated excellent staining properties for leukocyte differentiation, with about 90% or more slides ranked diagnostic (above borderline) or better. No significant difference was found among the three staining methods (Chi-squared P-value=0.965, >0.05) regarding the performance of leukocyte differentiation.

4.3.2 Toxic change diagnosis

With Wright Giemsa stain, 80% of the slides were ranked diagnostic (above borderline) or better on producing appropriate morphological and staining properties that are suitable for the interpretation of heterophil toxic change. With Liu's stain, 48.28% of the slides were diagnostic, and only 3.45% when using Diff-Quik stain. That is to say, over 96% of the slides were ranked as poor or undiagnostic using Diff-Quik stain. No significant difference was found between Wright Giemsa stain and Liu's stain (Chi-squared P-value=0.307, >0.05) regarding the performance of toxic change diagnosis. Significant difference was found between Diff-Quik stain and Wright Giemsa stain (Chi-squared P-value=0.000, <0.05), and also between Diff-Quik stain and Liu's stain (Chi-squared P-value=0.000, <0.05). Slides rendered poor or undiagnostic were due to significant drying artifact, coalescing of granules, or overstaining.
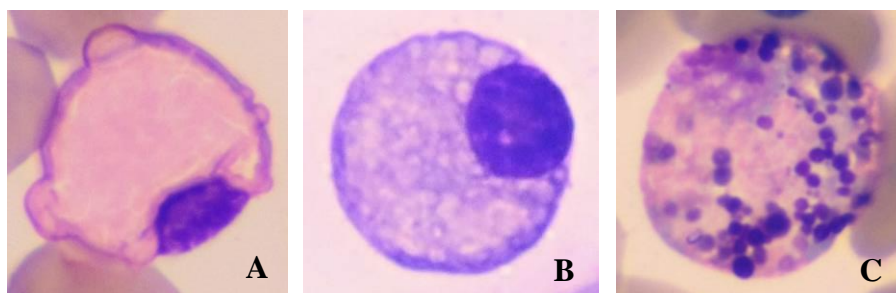
Figure 26. Examples of staining properties unsuitable for toxic change diagnosis

A-D: Examples of failure to demonstrate appropriate staining properties for reliable interpretation of cellular changes. During the 100 heterophil count, the more percentage of these kind of cells were seen on a stained slide, the slide is regarded as less diagnostic; A: granule coalescence caused the loss of cytoplasmic details, thus the changes of the granule number/ staining properties/ size and shape could not be reliably assessed, Diff-Quik stain; B: overstaining caused abnormal colors of the cell, thus cytoplasmic basophilia and changes of the granule staining properties could not be reliably assessed, Diff-Quik stain; C: overstaining caused abnormal colors of the granules, thus changes of the granule staining properties could not be reliably assessed, Liu's stain

100 heterophils per slide	*Wright Giemsa stain*	*Diff-Quik stain*	*Liu's stain*
Excellent (95-100)	8/30 (26.67%)	0/29 (0%)	4/29 (13.79%)
Good (80-95)	7/30 (23.33%)	0/29 (0%)	7/29 (24.14%)
Borderline (65-80)	9/30 (30%)	1/29 (3.45%)	3/29 (10.34%)
Poor (35-65)	5/30 (16.67%)	2/29 (6.90%)	7/29 (24.14%)
Undiagnostic (<35)	1/30 (3.33%)	26/29 (89.66%)	8/29 (27.59%)

Table 8. Performance of 3 staining methods on reliable toxic change diagnosis

80% of the slides were ranked diagnostic (above borderline) or better on producing reliable toxic

change diagnosis with Wright Giemsa stain, 48.28% with Liu's stain, and over 96% of the slides were ranked as poor or undiagnostic using Diff-Quik stain. No significant difference was found between Wright Giemsa stain and Liu's stain (Chi-squared P-value=0.307, >0.05) regarding the performance of toxic change diagnosis. Significant difference was found between Diff-Quik stain and Wright Giemsa stain (Chi-squared P-value=0.000, <0.05), and also between Diff-Quik stain and Liu's stain (Chi-squared P-value=0.000, <0.05)

## 4.4 Efficacy of blood film examination of toxic change

4.4.1 Agreement between blood film exam and TEM exam

From each of the total 31 blood samples, blood films were stained and examined for the presence of heterophil toxic change in a 100 leukocyte count using light microscope, while 21 of the 31 blood samples were examined for ultrastructure changes using TEM. The degree of agreement between the blood film exam and TEM examination of the 21 blood samples was measured. Cohen's kappa coefficient (κ)=1, indicated complete agreement between the two exams.

4.4.2 Correlation of toxic change and clinical inflammatory state

Clinical and/ or pathological diagnosis of sea turtles were ranked on the severity of clinical inflammatory state from "none/ insignificant inflammation (NI)", to "less/ slight inflammation (LI)", and finally "significant/ severe inflammation (SI)" (for details see **3.3.3**).

6 subjects were categorized in group NI, including 5 healthy individuals and 1 juvenile green sea turtle with uncomplicated cornea ulceration. 10 subjects were categorized in group LI, including 1 juvenile green sea turtle and 1 subadult green sea turtle with mild and uncomplicated pneumonia that resolved within a few weeks; 2 juvenile green sea turtle with mild wounds caused by fishhook within the gastrointestinal tract (excreted or surgically removed soon after presentation); 1 juvenile olive ridley sea turtle, 2 subadult green sea turtles, and 1 juvenile hawksbill sea turtle with simple or superficial traumatic soft tissue injury; 2 subadult green sea turtles with superficial fibropapillomas that underwent multiple surgical excisions but healthy otherwise. 15 subjects were categorized in group SI, including 1 juvenile olive ridley sea turtle and 1 juvenile green sea turtle with traumatic bone fractures (the green sea turtle also had osteomyelitis); 1 subadult olive ridley sea turtle, 1 adult olive ridley sea turtle, and 1 juvenile green sea turtle with osteomyelitis (the adult olive ridley sea turtle also had pneumonia); 1 adult olive ridley sea turtle and 1 juvenile hawksbill sea turtle with

85
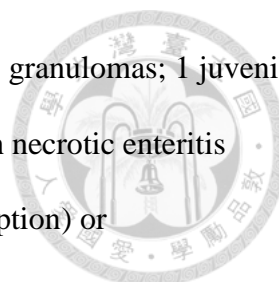
systemic bacterial infection; 1 green sea turtle hatchling with necrotic renal granulomas; 1 juvenile green sea turtle, 1 subadult green sea turtle and 1 adult green sea turtle with necrotic enteritis (caused by gastrointestinal foreign body obstruction or ileocolic intussusception) or pseudomembranous enteritis; 1 juvenile green sea turtle with serious wounds from neuroblastoma of one eye and secondary bacterial infection, systemic Spirorchiidae infection and enteritis; 1 subadult green sea turtle with capture myopathy and multiple wounds from web trapping; 1 adult green sea turtle with severe CNS Spirorchiidae infection; and 1 subadult green sea turtle with complete carapace fracture, multiple full thickness plastron wounds, coelomitis and bacteremia.

Heterophil toxic change was present in the 100 leukocyte count blood film exams of 2 subadult green sea turtles. One had ileocolic intussusception and necrotic enteritis, and the other had complete carapace fracture, multiple full thickness plastron wounds, coelomitis and bacteremia, both categorized in the SI group. Toxic change was absent in all other samples, regardless of the clinical inflammatory state.

The correlation of the presence of toxic change and the clinical inflammatory state of the sea turtles was measured. Spearman's rank correlation coefficient (r_s)=0.255, indicated a weak positive (r_s=0.20 to 0.39 by definition) and insignificant (p=0.166, >0.05) correlation between the two. (N=31)

4.4.3 Correlation of toxic change and treatment outcome

The treatment outcome of all sea turtles were documented and ranked on the prognosis from "released (R)", to "treatment and/or rehabilitation continued (T)", and "death (D)". Given that the data were collected through a course of 21 months, and that recovery and rehabilitation of sea turtles were generally gradual in speed, subjects were only categorized in group T and not the definite R or D when they have been under treatment or rehabilitation for longer than 6 months at the time of data
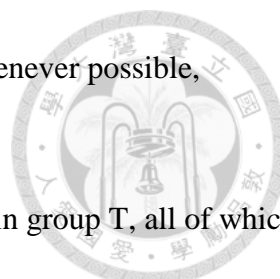
analysis. Final outcomes (R and D) of the individuals were represented whenever possible, regardless of the treatment time course.

15 sea turtles were categorized in group R, and 5 were categorized in group T, all of which toxic change was absent during the 100 leukocyte count. 7 subjects were categorized in group D, of which toxic change was present in a subadult green sea turtle with ileocolic intussusception and necrotic enteritis, but was absent in all others. 4 samples were collected less than 2 months prior to data analysis, thus the outcome of these 4 sea turtles were considered unrepresentative and was excluded from statistical analysis. This included 1 juvenile olive ridley sea turtle with traumatic soft tissue injury and 1 subadult green sea turtle with complete carapace fracture, multiple full thickness plastron wounds, coelomitis and bacteremia which were still receiving medical care; 1 juvenile green sea turtle which had ingested and excreted a fish hook and was scheduled for release; and 1 juvenile hawksbill sea turtle with traumatic soft tissue injury that had finished medical treatment and was gaining weight in the rehabilitation center. Toxic change was present in the subadult green sea turtle but absent in the other three.

The correlation of the presence of toxic change and the treatment outcome of the sea turtles was measured. Spearman's rank correlation coefficient (r_s)=-0.280, indicated a weak negative (r_s=-0.20 to -0.39 by definition) and insignificant (p=0.156, >0.05) correlation between the two. (N=27)

ID	Age & species	Toxic change LM	TEM	Diagnosis	Inflammatory state	Outcome
O11	juvenile, olive	-	-	bone fracture	SI	R
1072256	juvenile, olive	-	ND	deep tissue wound, emaciation	LI	t

87

O6	subadult, olive	-	-	osteomyelitis	SI	R
O8	adult, olive	-	-	healthy	NI	R
O9	adult, olive	-	-	pneumonia, osteomyelitis	SI	T
O12	adult, olive	-	-	systemic infection	SI	T
1063973	hatchling, green	-	-	healthy	NI	D
1063973 (6/21)	hatchling, green	-	ND	necrotic renal granuloma	SI	D
1054660	juvenile, green	-	-	necrotizing enteritis (foreign body obstruction), pneumonia, systemic spirorchidiasis, chronic nephritis	SI	D
1064184	juvenile, green	-	-	healthy	NI	R
1070022	juvenile, green	-	-	healthy	NI	R
1070856	juvenile, green	-	-	open fracture and osteomyelitis, hypocalcemia	SI	R
1071086	juvenile,	-	-	uncomplicated cornea	NI	R

88

	green			ulceration		
1071085	juvenile, green	-	ND	uncomplicated pneumonia	LI	R
1071150	juvenile, green	-	ND	osteomyelitis	SI	R
1071443	juvenile, green	-	ND	fishhook in esophagus	LI	R
PH2337	juvenile, green	-	ND	O.D neuroblastoma, periophthalmitis, bacterial infection, systemic Spirorchiidae infection, entritis	SI	D
1072633	juvenile, green	-	ND	GI foreign body	LI	t
G9	subadult, green	-	-	trauma	LI	T
G46	subadult, green	-	-	herpes infection, papilloma	LI	T
G47	subadult, green	-	-	herpes infection, papilloma	LI	T
G48	subadult, green	-	-	capture myopathy and wounds by web trapping	SI	R
G49	subadult, green	-	-	superficial traumatic wounds, malnutrition	LI	R

89

|					
1061896	subadult, green	+	+	ileocolic intussusception, ulcerative and necrotizing enteritis, spirorchid infection	SI	D
1070170	subadult, green	-	ND	pneumonia	LI	R
1072678	subadult, green	+	+	complete carapace fractures, full thickness plastron wounds, coelomitis and bacteremia	SI	t
1070557	adult, green	-	-	CNS spirochidae infection (meningoencephalitis and ventriculitis, spinal cord -megingitis), aortitis, hepatitis	SI	D
268307111	adult, green	-	ND	pseudomembranous enteritis	SI	D
1063668	hatchling, hawksbill	-	-	healthy	NI	R
1063699	juvenile, hawksbill	-	-	systemic infection, severe dehydration, ileus, pneumonia	SI	R
1072602	juvenile, hawksbill	-	ND	superficial wounds, GI foreign body	LI	t

90
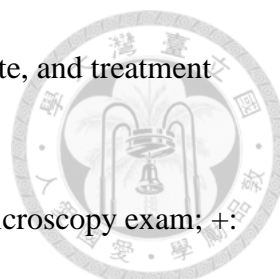
Table 9. Results of blood film exam, TEM exam, clinical inflammatory state, and treatment outcome of the studied sea turtles

LM: light microscopy exam of blood films; TEM: transmission electron microscopy exam; +: presence of toxic change; -: absence of toxic change; ND: exams not done; NI: none/ insignificant inflammation; LI: less/ slight inflammation; SI: significant/ severe inflammation; R: released; T: treatment and/or rehabilitation continued; D: death; t: subjects undergoing treatment and/or rehabilitation but samples were collected less than 2 months prior to data analysis, thus considered unrepresentative and was excluded from statistical analysis; O.D.: right eye; GI: gastrointestinal tract; CNS: central nervous system

Chapter 5. Discussion

5.1 Leukocytes classification, morphologic and ultrastructural findings

5.1.1 Sea turtles

Contradictions and confusions have been presented in previous studies regarding the classification and morphological characteristics of sea turtle's circulating leukocytes. The results of this study agreed with those by Work et al (Work et al., 1998), Casal and Orós (Casal & Orós, 2007), and Zhang et al (Zhang et al., 2011) on differentiating the leukocytes of sea turtles into heterophils, eosinophils, basophils, lymphocytes and monocytes; as well as the general morphological descriptions of these cells under light microscope. Considering the characteristics and criteria on identifying azurophils and neutrophils, previous descriptions of these cells in sea turtles did not fit well, nor did the cells examined in this study on morphological or ultrastructural level. As a result, differentiation of these cells in sea turtles is no longer considered necessary or appropriate.

Heterophil granules had always been described as fusiform, spindle-shape or elongated in literature, not only many reptile and avian species but also specifically in sea turtles. This feature had been a useful way for avian and reptile veterinarians to differentiate heterophils from the other group of eosinophilic granulocytes, aka the eosinophils, which had more rounded granules. In this study, the heterophil granules appeared indistinct in shape under light microscope due to cytoplasmic compactness; and even when the sectioning axials were taken into account, these granules often looked round to elliptical rather than spindle-shaped and elongated under TEM. This is further supported by comparing Fig. 43 with Fig. 17, when better-preserved cells in this study were evident by the symmetrical, rounded cellular margin and the clear, intact cellular and granular membrane. While this difference in granule shapes is true in many avian and reptile species, it may

92

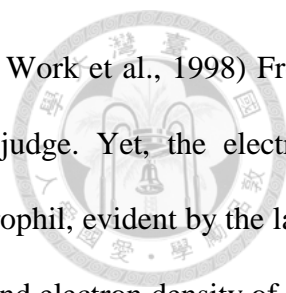not be as apparent in some sea turtle species.

Unique among reptiles, two types of eosinophils (namely the large and the small eosinophils) had been documented in green sea turtles and juvenile olive ridley sea turtles, and the morphological descriptions were similar in this two species. (Work et al., 1998; Zhang et al., 2011) In this study, large eosinophils and small eosinophils were both found in the green sea turtles, but only one type of eosinophils (resembling the large eosinophils of the green sea turtles) were found in olive ridley sea turtles and hawksbill turtles. This was most likely explained by, and the author would like to emphasize on this fact, that small eosinophils were relatively scarce. Small eosinophils were rarely seen under blood film examinations in sea turtles in this study. In many green sea turtles, not one small eosinophil was found despite extensive search on multiple blood films. Although there are chances that such type of cell doesn't exist in olive ridley sea turtles and hawksbill turtles, the possibility is low due to previous documentation in olive ridley sea turtles, the small sample size of these turtles in this study, and the straightforward fact that these cells are originally rare.

Work et al (Work et al., 1998) had begun an interesting discussion on the functional difference between the two morphologically distinct eosinophils in green sea turtles. They've made a hypothesis that the large eosinophils were activated cells reacting to parasitic infection or other inflammatory stimulus. However, no investigations have been made to confirm this hypothesis, nor have other discussions provided by other studies. The answer to which eosinophil is more mature than the other need microscopic examination of granulopoietic sites, as suggested by Work et al, and is beyond the extent of this study. However, in this study the author did notice that the large eosinophils have smaller nucleus with a very clumped and compact chromatin pattern, which represent the inactive heterochromatin; while the small eosinophils have large and rounded nucleus with a significantly lighter and less clumped chromatin pattern, which represent more amount of active euchromatin and nuclear immaturity. Furthermore, the only individual in this study that had

93

significant amount of small eosinophils had severe spirochidae infection of the central nervous system that was later confirmed by pathology; while large eosinophils were easily found in all studied sea turtles, regardless of their health status. These findings were far from evident to overturn the hypothesis made by Work et al, but were interesting inputs to the discussion and did suggest otherwise.

As described in the results of this study, different types of granules existed and distributed unevenly within the cytoplasm of heterophils, leading to the appearance that only one type of granules were present on some ultrathin sections. This phenomenon was also mentioned in the study of Asian water monitors (Salakij et al., 2014), as showed in Appendix 34. In such circumstances, the identification of a granulocyte should be made very cautiously because the sections of a same cell can exhibit distinct types of granules. In this sense, the loggerhead sea turtles eosinophil ultrastructure presented by Casal and Orós (Casal et al., 2007; Casal & Orós, 2007; Orós et al., 2010) seemed likely the case. In their studies, Casal and Orós presented micrographs of the vacuolated large eosinophils commonly identified in sea turtles and described accordingly; adversely, the electron micrographs of eosinophils they presented were not at all vacuolated and exhibited abundant cytoplasm. Casal and Orós explained in text that the one type of eosinophils they documented were ultrastructurally more similar to that describing small eosinophils in green sea turtles. However, unlike the loosely arranged granules in their electron micrographs, small eosinophils often had very compact granules, as shown in this study; not to mention the rareness of this type of cells. It is more likely that the electron micrographs presented by Casal and Orós were heterophils seen only with a single type of granules.

Crystalloid granulation is a distinguished characteristic of human eosinophils, however it has been rarely reported in reptiles. Of all the eosinophils examined in this study, regardless of sea turtle species or eosinophil types, no crystalline structure was seen. This is contrary to two studies that

94

have reported crystalloid granulation in sea turtles. (Di Santi et al., 2013; Work et al., 1998) From the electron micrograph provided by Work et al, it was difficult to judge. Yet, the electron micrograph of an eosinophil presented by Di Santi et al was clearly a heterophil, evident by the lack of vacuolated cytoplasm and distinctive size, shape, number, distribution and electron density of the cytoplasmic granules; while the "paracrystalloid core" of the granules in the presented image was easily identified as typical artifact caused by scratches from sectioning with an unsmooth knife edge, as the stripes were continuous and parallel across the whole section/ cell. (Di Santi et al., 2013) From what we know now, sea turtles are not considered exceptional among the majority of reptile species that do not have eosinophil crystalloid granulations.

The clear documentation of all three species of sea turtles' basophils is also important in this study. Due to the rareness of basophils in sea turtles, veterinarians were very unfamiliar with the morphology of this type of cells. Combined with the unique morphology of other granulocytes in these species, examiner can easily make a mistake and falsely classified other cells as basophils. Although basophils have been documented in sea turtles in a few studies previously, some micrographs were dated and not in the best resolution (see Fig. 8) (Wood & Ebanks, 1984; Work et al., 1998), making identification less easy for the readers. This study demonstrated that basophils of sea turtles were in fact, very similar with those typical of other avian and reptile species. This finding is very different from the morphologic descriptions and the quality micrographs provided by Stacy and Boylan (Stacy Nicole I., 2014), in which basophils morphology were described as "very variable", while the presented micrographs of green sea turtles were more likely small eosinophils.

5.1.2 Yellow pond turtles and Chinese box turtles

To date, no leukocytes morphologic or ultrastructural studies have been done in yellow pond turtles or Chinese box turtles to the author's knowledge. On the basis of morphologic, cytochemical

95

and ultrastructural studies on numerous other species of freshwater turtles (cited in chapter 2), this study was able to provide the first detailed description on the morphologic and ultrastructural characteristics of the circulating leukocytes in these two endangered freshwater turtles.

Reptile leukocytes morphology is of great variety, and differentiation have been important but problematic for veterinarians. As in many other species of freshwater turtles, five types of leukocytes were identified in yellow pond turtles or Chinese box turtles, including heterophils, eosinophils, basophils, lymphocytes and monocytes. Contrary to previous studies on yellow-headed temple turtles (Chansue et al., 2011), Geoffroy's side-necked turtle (Zago et al., 2010) and some Amazon freshwater turtles (Oliveira-Júnior et al., 2009; Oliveira et al., 2011), azurophils and neutrophils were not classified in this study. There is possibility that this is the result of species differences, but was mainly due to terminological issue, as azurophils were occasionally used instead of monocytes while describing the same type of cell. (Chansue et al., 2011; Oliveira-Júnior et al., 2009; Oliveira et al., 2011) As in the study by Zago et al, both the neutrophil and azurophil presented in the micrographs were likely lymphocytes of varying sizes. This was supported by the presence of typical lymphocyte features such as high N/C ratio, small cell size, scarce and irregular cytoplasm, and basophilic staining; while lacking the typical morphologic features of neutrophils or azurophils in these cells. (Zago et al., 2010)

From the review of literature and the results of this study, it is interesting that while the mononuclear lymphocytes and monocytes appeared consistent ultrastructurally among most species, granulocytes were very heterogenous and species specific. Still, resemblance was recognized in similar species. The small, round and deeply electron-dense cores seen in the heterophil granules in this study were not unique of the yellow pond turtles and Chinese box turtles, but were also described in yellow-bellied sliders (J. D. Hernández et al., 2016) and yellow-headed temple turtles (Chansue et al., 2011). The heterogenous granules seen in basophils of the yellow pond turtles and

96

Chinese box turtles were also similar to those of yellow-bellied sliders (J. D. Hernández et al., 2016) and yellow-headed temple turtles (Chansue et al., 2011). However, the polygonal crystalloid structures seen in the basophil granules of Chinese box turtles have not been documented in other species of freshwater turtles before.

5.1.3 Limitations of this study

In this study, detailed morphologic and ultrastructural characteristics were described in the hawksbill sea turtles, the yellow pond turtles, and the Chinese box turtles for the first time. Although morphology and TEM ultrastructure are two of the most important tools in classifying and characterizing leukocytes, a triple-method with the addition of cytochemical staining provides the most reliable (not definite due to the lack of a standard reference) result. Increasing the sample size (in this study the sample size is comparable to cited studies), sampling at different seasons of the year, and a strict subjects' criteria regarding age, sex, and body conditions will also make the results more convincing.

A great challenge faced in this study is the difficulty to obtain electron micrographs of targeted cell types of sufficient quality and quantity. Blood cells were separated by centrifugation according to cell densities. However, unlike the clearly layered mammal blood cells in the buffy coat, separation of layers was much less evident and ineffective in reptiles. Heterophils, for instance, were presence among erythrocytes and mononuclear cells; while erythrocytes were normally presence in the buffy coat and contaminated throughout all layers. (See Appx. 35) (Fontes Pinto, Lopes, Malhão, & Marcos, 2018) It is therefore nearly impossible to target a specific cell type – or even leukocytes- prior to examination of the sections. The complicated TEM sample processing added even more risk of creating artifacts or damaging the samples. For example, the repeated rinsing necessary for staining with uranyl acetate and lead citrate often lead to creases on the

97

ultrathin sections, in the worst case loss of sections can also occurred. This study relied on repeated sectioning and examinations to obtain a desired result, however some cell types were difficult to find on TEM, and unstained electron micrographs were provided instead. The contrast of double staining is important to the classification of granulocytes and the precise description of the granules, and should be applied if possible.

5.2 Staining Methods

5.2.1 Application of different staining methods

Wright Giemsa stain, Diff-Quik stain and Liu's stain were all acceptable for leukocytes classification and morphological evaluation in the studied species. Multiple clear micrographs of leukocytes of studied species stained with Diff-Quik and Liu's stain were provided by this study for the first time, for the purpose of practical use by reptile veterinarians. In order to obtain consistent, quality staining results, blood films should be dried and stained as soon as possible, and stains should be flushed with distilled water thoroughly. Increased dips in the stains or prolong staining against the guidelines provided by manufacturers should be avoided. It is advised that Wright Giemsa stain or Liu's stain should be used instead of Diff-Quik stain when the examiner is aimed for detailed cytoplasmic change evaluation. With Liu's stain, some eosinophil granules were normally unstained and may appear morphologically different from normal eosinophils. It is advised that a single stain should be used through the course of treatment to evaluate the improvement of a patient, unless the examiner is experienced and familiar with the staining properties of different types of stains.
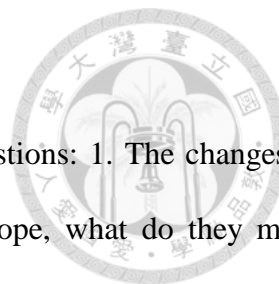
5.3 Toxic Change in Sea Turtles
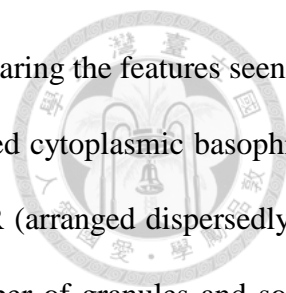
Through this study, the author tried to answer two important questions: 1. The changes of cytoplasm, granulation and staining properties we see on light microscope, what do they mean exactly on a cellular level? 2. The presence of toxic change is widely used among veterinarians to access a patient's clinical inflammatory state or prognosis, is it a reliable indicator in sea turtles?

5.3.1 Morphology and ultrastructure

This study documented and described toxic change in the green sea turtles on both morphologic and ultrastructural level for the first time, and this is also the first ultrastructural presentation of toxic change in reptiles.

Heterophil toxic change in green sea turtles were morphologically similar to other species. Increased cytoplasm basophilia, degranulation, and the presence of prominent basophilic cytoplasmic granules were seen; while vacuolization was not evident. The most important skill relevant to correctly evaluate toxic change is to minimize and identify artifacts. Heterophils of sea turtles are fragile and prone to alternations from artifacts. The presence of a single "toxic" change without the others should be very carefully interpreted. Degranulation and vacuolization easily occurred during sample handling and making of the blood films. Increased staining time or dipping in the stains resulted in basophilic staining of cytoplasmic granules. A bluish hue can occur due to use of anticoagulant or staining.

To overcome challenges and limitations (ie. magnitude and artifact) of identifying true toxic change, TEM was used to confirm cellular changes on the ultrastructural level. This study found that blood film examination by light microscope were compatible to TEM examinations, that is to say, toxic heterophils with ultrastructural changes can be readily identified with a 100 leukocyte count on a light microscope.
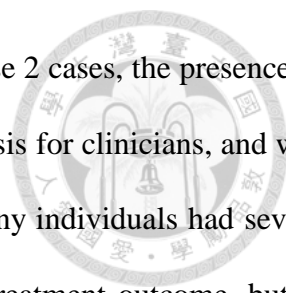
Based on previous studies on mammals and avian species, by comparing the features seen on light microscope and TEM, this study was able to confirmed that increased cytoplasmic basophilia was resulted from increased clusters of polyribosomes and excessive RER (arranged dispersedly in the form of a single row, not in lamellar form), and while reduced number of granules and some changes in shape was observed, no significant ultrastructural difference were seen between toxic and normal granules. These findings agreed with previous studies on mammals, while the extensive membrane ruffling and pseudopod formation, enlarged ellipsoidal rod-shaped dense granules and vaccuolation observed in chickens' toxic heterophils ultrastructurally were not seen in sea turtles.

As stated previously by other investigators, toxic change remained a well-recognized but poorly understood phenomenon. Regarding what we've known, the increase of polyribosomes and RER indicated increased protein synthesis; while toxic granulations are presence in a more primary state of heterophil development, and are resulted from altered affinity for Wright stain possibly due to alternations in the membrane or composition but no ultrastructural difference were found comparing to normal granules. To date, our best answers to why toxic granulations were more severe than cytoplasm basophilia was primarily because the former changes were observed in patients with more severe inflammation/ infection.

5.3.2 Correlation with clinical inflammatory state and prognosis

To answer the question on whether toxic change is a sensitive and reliable indicator for systemic inflammation in sea turtles, this study presents the correlations between each individual's clinical inflammatory state, whether toxic change was present on blood film examination, and the treatment outcome.

As demonstrated in the results, toxic change was present in only two individual – a subadult green sea turtle with necrotizing enteritis and a subadult green sea turtle complete carapace fracture,

multiple full thickness plastron wounds, coelomitis and bacteremia. In these 2 cases, the presence of toxic heterophils did ring the alarm for a severe infection and poor prognosis for clinicians, and was also confirmed afterward. However, in the same SI class and D class, many individuals had severe systemic inflammation confirmed by pathology and also had the worst treatment outcome, but in none of these samples were toxic heterophils present. Micrographs and electron micrographs of heterophils were grouped according to the inflammatory state of the studied sea turtles, and no significant difference was found between the groups except for the two aforementioned green subadult sea turtle. This might give an idea of how toxic change is not as sensitive and reliable in evaluating a sea turtle's inflammatory/ infectious state or prognosis as in many species, but the presence of toxic change did truthfully represent severe infection and poor outcome of an individual. Statistical analysis further proved that toxic change had a weak correlation with both clinical inflammatory state and treatment outcome in sea turtles of this study.

The reasons behind this result is intriguing. Veterinarians working on sea turtle rescue recognized that sometimes these animals were surprisingly resilient to infections. In many sea turtles, deeply wounded tissue healed well even when the animal stayed in water, and oftentimes no aggressive wound care (ie. routine surgical debridement) were necessary. Whether this phenomenon is related to the rarely present toxic change is unknown, but this suggest an interesting aspect for future studies on sea turtle immunity.

Chapter 6. Conclusion

In this study, the differentiation and characteristics of circulating leukocytes of the studied species was clarified and described in details, each complemented with micrographs.

Most morphological and ultrastructural findings in this study agree with previous studies in similar species, while some discoveries were made. Specifically, heterophil granules were more rounded and less elongated in sea turtles, contrary to earlier descriptions. Heterophil granules in sea turtles were unevenly distributed, and distinct types of granules see on ultra-thin sections can lead to false identification of the granulocytes. Two types of eosinophils were only found in green sea turtles, presumably due to the rareness of small eosinophils. Whether the presence of one type of eosinophils represents immune activation or immaturity remains unknown. Crystalloid granulations were not seen in eosinophils of sea turtles in this study, and previous statement was questionable. Basophils were rare in sea turtles, but was well documented in this study in the hope to clarify on its morphology for veterinarians. The granulocytes ultrastructure of yellow pond turtles and Chinese bow turtles were similar to those of yellow-bellied sliders and yellow-headed temple turtles. However, the polygonal crystalloid structures seen in the basophil granules of Chinese box turtles have not been seen in other species of freshwater turtles.

Wright Giemsa stain, Diff-Quik stain and Liu's stain had similar staining properties and were all suitable for leukocyte differentiation. However, Wright Giemsa satin and Liu's stain were preferred over Diff-Quik stain for reliable interpretation of heterophil toxic change.

Toxic change morphology in sea turtles and toxic change ultrastructure in reptile species were described for the first time in this study. The characteristics of these cellular changes were demonstrated with both morphologic and ultrastructural descriptions. It is known among

veterinarians working with sea turtles that toxic change was rare in these species, but this study provided evidence on how the presence toxic change was not a sensitive or reliable indicator for a sea turtle's clinical inflammatory state or prognosis/ treatment outcome.

This study provides fundamental hematologic information and subsequently more sophisticated medical diagnosis and treatment for these endangered species, as well as insights to further investigations on clinical pathology and immunity of these species.

References

Arizza, V., Russo, D., Marrone, F., Sacco, F., & Arculeo, M. (2014). Morphological characterization of the blood cells in the endangered Sicilian endemic pond turtle, Emys trinacris (Testudines: Emydidae). *Italian Journal of Zoology, 81*(3), 344-353.

Azevedo, A., & Lunardi, L. O. (2003). Cytochemical characterization of eosinophilic leukocytes circulating in the blood of the turtle (Chrysemys dorbignih). *Acta histochemica, 105*(1), 99.

Bradley, T. A., Norton, T. M., & Latimer, K. S. (1998). Hemogram values, morphological characteristics of blood cells and morphometric study of loggerhead sea turtles, Caretta caretta, in the first year of life. *Bulletin of the Association of Reptilian and Amphibian Veterinarians, 8*(3), 8-16.

Cambell, T. (2006). Clinical pathology of reptiles. *Reptile medicine and surgery, 2nd ed. St. Louis (MO): Saunders*, 453-470.

Campbell, T. (2015). Peripheral blood of birds. *Exotic Animal Hematology and Cytology. 4th ed. Ames, Iowa, USA: Wiley-Blackwell*, 37-66.

Campbell, T. W. (2012). Hematology of reptiles. *Veterinary hematology and clinical chemistry. Philadelphia: Lippincott Williams & Wilkins*, 277-297.

Campbell, T. W. (2015). Peripheral Blood of Reptiles *Exotic Animal Hematology and Cytology. 4th ed. Ames, Iowa, USA: Wiley-Blackwell* (pp. 67-88).

Cannon, M. S. (1992). The morphology and cytochemistry of the blood leukocytes of Kemp's ridley sea turtle (Lepidochelys kempi). *Canadian Journal of Zoology, 70*(7), 1336-1340.

Casal, A., Freire, F., Bautista-Harris, G., Arencibia, A., & Orós, J. (2007). Ultrastructural characteristics of blood cells of juvenile loggerhead sea turtles (Caretta caretta). *Anatomia,*

histologia, embryologia, 36(5), 332-335.
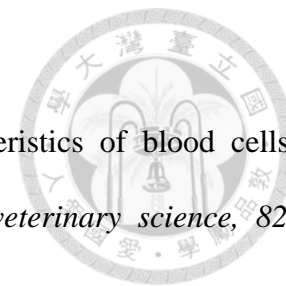
Casal, A., & Orós, J. (2007). Morphologic and cytochemical characteristics of blood cells of juvenile loggerhead sea turtles (Caretta caretta). *Research in veterinary science, 82*(2), 158-165.

Chansue, N., Sailasuta, A., Tangtrongpiros, J., Wangnaitham, S., & Assawawongkasem, N. (2011). Hematology and clinical chemistry of adult yellow-headed temple turtles (Hieremys annandalii) in Thailand. *Veterinary clinical pathology, 40*(2), 174-184.

Chung, C.-s., Cheng, C.-h., Chin, S.-c., Lee, A.-h., & Chi, C.-h. (2009). Morphologic and cytochemical characteristics of Asian yellow pond turtle (Ocadia sinensis) blood cells and their hematologic and plasma biochemical reference values. *Journal of Zoo and Wildlife Medicine, 40*(1), 76-85.

Claver, J. A., & Quaglia, A. I. (2009). Comparative morphology, development, and function of blood cells in nonmammalian vertebrates. *Journal of exotic pet medicine, 18*(2), 87-97.

Di Santi, A., Basile, F., Ferretti, L., Bentivegna, F., Glomski, C., & Pica, A. (2013). Morphology, cytochemistry and immunocytochemistry of the circulating granulocytes of the loggerhead sea turtle Caretta caretta. *Comparative Clinical Pathology, 22*(3), 481-490.

Fontes Pinto, F., Lopes, C., Malhão, F., & Marcos, R. (2018). Unraveling avian and reptilian hematology: An optical and electron microscopic study of the buffy coat. *Veterinary clinical pathology*.

Hernández, J., Castro, P., Saavedra, P., Ramírez, P., & Orós, J. (2017). Morphologic and Cytochemical Characteristics of the Blood Cells of the Yellow-bellied Slider (trachemys scripta scripta). *Anatomia, histologia, embryologia, 46*(5), 446-455.

Hernández, J. D., Orós, J., Artiles, M., Castro, P., & Blanco, A. (2016). Ultrastructural characteristics of blood cells in the Yellow-Bellied Slider Turtle (Trachemys scripta scripta).
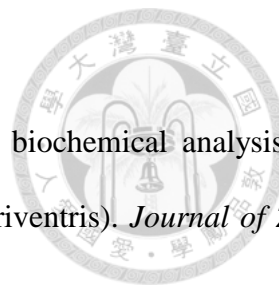
Veterinary clinical pathology, 45(1), 106-109.

Innis, C. J., Tlusty, M., & Wunn, D. (2007). Hematologic and plasma biochemical analysis of juvenile head-started northern red-bellied cooters (Pseudemys rubriventris). *Journal of Zoo and Wildlife Medicine*, 425-432.

IUCN. (2018). The IUCN Red List of Threatened Species. Version 2018-2.
.   Retrieved 13 November 2018 http://www.iucnredlist.org

Javanbakht, H., Vaissi, S., & Parto, P. (2013). The morphological characterization of the blood cells in the three species of turtle and tortoise in Iran. *Research in Zoology, 3*(1), 38-44.

Latimer, K. S., Tang, K.-N., Goodwin, M. A., Steffens, W., & Brown, J. (1988). Leukocyte changes associated with acute inflammation in chickens. *Avian Diseases*, 760-772.

Maxwell, M., & Robertson, G. (1998). The avian heterophil leucocyte: a review. *World's Poultry Science Journal, 54*(2), 155-178.

McCall, C. E., Katayama, I., Cotran, R. S., & Finland, M. (1969). Lysosomal and ultrastructural changes in human" toxic" neutrophils during bacterial infection. *Journal of Experimental Medicine, 129*(2), 267-293.

Mead, K. F., & Borysenko, M. (1984). Surface immunoglobulin on granular and agranular leukocytes in the thymus and spleen of the snapping turtle, Chelydraserpentina. *Developmental & Comparative Immunology, 8*(1), 109-120.

Metin, K., Türkozan, O., Kargin, F., Basumoglu, Y., Taskavak, E., & Koca, S. (2006). Blood cell morphology and plasma biochemistry of the captive European pond turtle Emys orbicularis. *Acta Veterinaria Brno, 75*(1), 49-55.

Montali, R. (1988). Comparative pathology of inflammation in the higher vertebrates (reptiles, birds and mammals). *Journal of comparative pathology, 99*(1), 1-26.

Nardini, G., Leopardi, S., & Bielli, M. (2013). Clinical hematology in reptilian species. *Veterinary*

Clinics: Exotic Animal Practice, 16(1), 1-30.
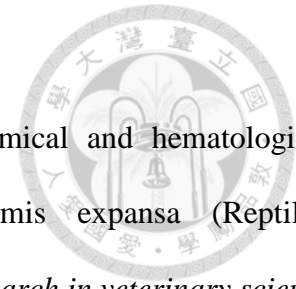
Oliveira-Júnior, A., Tavares-Dias, M., & Marcon, J. (2009). Biochemical and hematological reference ranges for Amazon freshwater turtle, Podocnemis expansa (Reptilia: Pelomedusidae), with morphologic assessment of blood cells. *Research in veterinary science, 86*(1), 146-151.

Oliveira, A. T., Cruz, W. R., Pantoja-Lima, J., Araújo, S. B., Araújo, M. L., Marcon, J. L., & Tavares-Dias, M. (2011). Morphological and cytochemical characterization of thrombocytes and leukocytes in hatchlings of three species of Amazonian freshwater turtles. *Veterinarski arhiv, 81*(5), 657-670.

Orós, J., Casal, A., & Arencibia, A. (2010). Microscopic studies on characterization of blood cells of endangered sea turtles. *Microscopy: Science, technology, applications and education, 1*(4), 75-84.

Pitol, D. L., Issa, J. P. M., Caetano, F. H., & Lunardi, L. O. (2007). Morphological characterization of the leukocytes in circulating blood of the turtle (Phrynops hilarii). *International Journal of Morphology*, 677-682.

Salakij, C., Salakij, J., Prihirunkit, K., Narkkong, N. A., Sanyathitiseree, P., & Kranjanapitukkul, K. (2014). Quantitative and qualitative morphologic, cytochemical, and ultrastructural characteristics of blood cells in captive Asian water monitors. *Veterinary clinical pathology, 43*(4), 538-546.

Schofield, K., Stone, P., Beddall, A., & Stuart, J. (1983). Quantitative cytochemistry of the toxic granulation blood neutrophil. *British journal of haematology, 53*(1), 15-22.

Shini, S., Kaiser, P., Shini, A., & Bryden, W. L. (2008). Differential alterations in ultrastructural morphology of chicken heterophils and lymphocytes induced by corticosterone and lipopolysaccharide. *Veterinary immunology and immunopathology, 122*(1-2), 83-93.
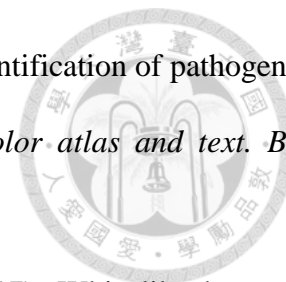
Stacy, B., & Pessier, A. (2007). Host response to infectious agents and identification of pathogens in tissue section. *Infectious diseases and pathology of reptiles: color atlas and text. Boca Raton: CRC Press, Taylor & Francis Group, 200*, 257-298.

Stacy, N., Fredholm, D., Rodriguez, C., Castro, L., & Harvey, J. (2017). Whip-like heterophil projections in consecutive blood films from an injured gopher tortoise (Gopherus polyphemus) with systemic inflammation. *Veterinary Quarterly, 37*(1), 162-165.

Stacy, N. I., Alleman, A. R., & Sayler, K. A. (2011). Diagnostic hematology of reptiles. *Clinics in laboratory medicine, 31*(1), 87-108.

Stacy, N. I., & Raskin, R. E. (2015). Reptilian eosinophils: beauty and diversity by light microscopy. *Veterinary clinical pathology, 44*(2), 177-178.

Stacy Nicole I., B. S. (2014). Clinical Pathology of Sea Turtles. Retrieved 2018/7/3, from WIDECAST Technical Report No. 16.

Strik, N., Alleman, A., & Harr, K. (2007). Circulating inflammatory cells. *Infectious diseases and pathology of reptiles: color atlas and text*, 167-218.

Sykes, J. M., & Klaphake, E. (2015). Reptile hematology. *Clinics in laboratory medicine, 35*(3), 661-680.

Taylor, K., & Kaplan, H. M. (1961). Light microscopy of the blood cells of pseudemyd turtles. *Herpetologica, 17*(3), 186-192.

Tristan, T. (2008). *Introduction to Hematology and Biochemistry in Sea Turtles.* Paper presented at the ACVP/ASVCP Concurrent Annual Meetings, San Antonio, Texas, USA.

Velásquez, J. C., Cartagena, H. N., Bolaño, C. R., Otero, G. Á ., Pacheco, J. C., & Arias, J. L. (2014). Caracterización hematológica de hicoteas (Trachemys callirostris Gray, 1856) en Córdoba, Colombia. *Revista de Medicina Veterinaria*(28), 43-55.

Wilkinson, R., McArthur, S., & Meyer, J. (2004). Clinical pathology. *Medicine and surgery of*

tortoises and turtles, 141-186.

Wood, F. E., & Ebanks, G. K. (1984). Blood cytology and hematology of the green sea turtle, Chelonia mydas. *Herpetologica*, 331-336.

Work, T. M., Raskin, R. E., Balazs, G. H., & Whittaker, S. (1998). Morphologic and cytochemical characteristics of blood cells from Hawaiian green turtles. *American journal of veterinary research, 59*, 1252-1257.

Zago, C. E. S., Da Silva, T. L., Da Silva, M. I. A., Venancio, L. P. R., Mendonça, P. P., Junior, L. R. F., . . . de Azeredo-Oliveira, M. T. V. (2010). Morphological, morphometrical and ultrastructural characterization of Phrynops geoffroanus'(Testudines: Chelidae) blood cells, in different environments. *Micron, 41*(8), 1005-1010.

Zhang, F.-Y., Li, P.-P., Gu, H.-X., & Ye, M.-B. (2011). Hematology, morphology, and ultrastructure of blood cells of juvenile olive ridley sea turtles (Lepidochelys olivacea). *Chelonian Conservation and Biology, 10*(2), 250-256.

Appendix

Appendix 1: Heterophils of loggerhead sea turtles
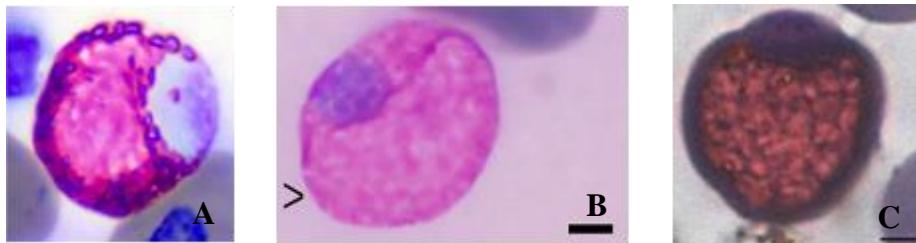
A: Wright-Giemsa stain (Stacy Nicole I., 2014); B: Diff-Quik, scale bar= 3.6μm (Casal & Orós,

2007); C: May–Grünwald–Giemsa stain, scale bar=4μm (Di Santi et al., 2013)

Appendix 2: Eosinophils of loggerhead sea turtles
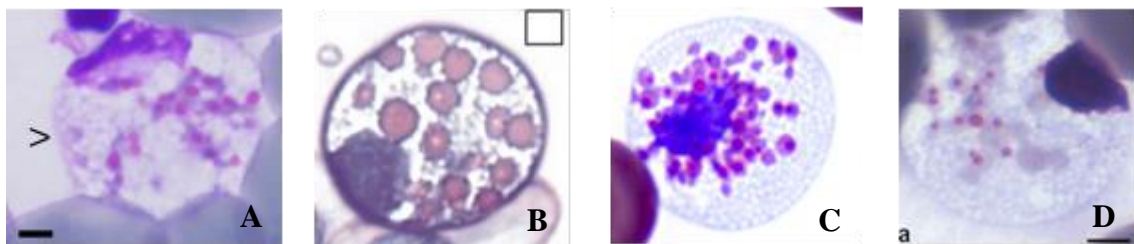
A: Diff-Quik, scale bar= 3.3μm (Casal & Orós, 2007); B: Wright-Giemsa stain (N. I. Stacy &

Raskin, 2015); C: Wright-Giemsa stain (Stacy Nicole I., 2014); D: May–Grünwald–Giemsa stain,

scale bar=4μm (Di Santi et al., 2013)

Appendix 3. Lymphocytes of loggerhead sea turtles
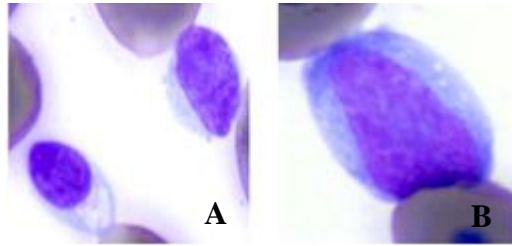
A: Wright-Giemsa stain, comparing to a thrombocyte (lower left); B: Wright-Giemsa stain, a reactive lymphocyte (Stacy Nicole I., 2014)

Appendix 4. Monocytes of loggerhead sea turtles
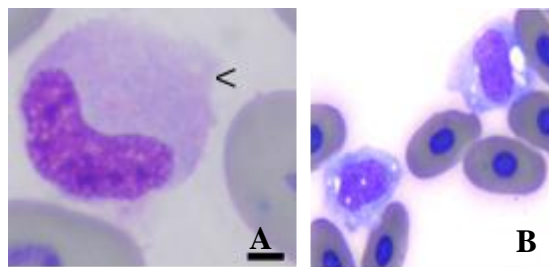
A: Diff-Quik stain, scale bar= 3.2μm (Casal & Orós, 2007); B: Wright-Giensa stain, reactive monocytes (Stacy Nicole I., 2014)

Appendix 5. Heterophils of green sea turtles

A: Leokostat stain (Work et al., 1998); B: modified May-Grünwald-Giemsa stain (Wood & Ebanks, 1984); C: Wright-Giemsa stain (Stacy Nicole I., 2014)

Appendix 6. Eosinophils of green sea turtles
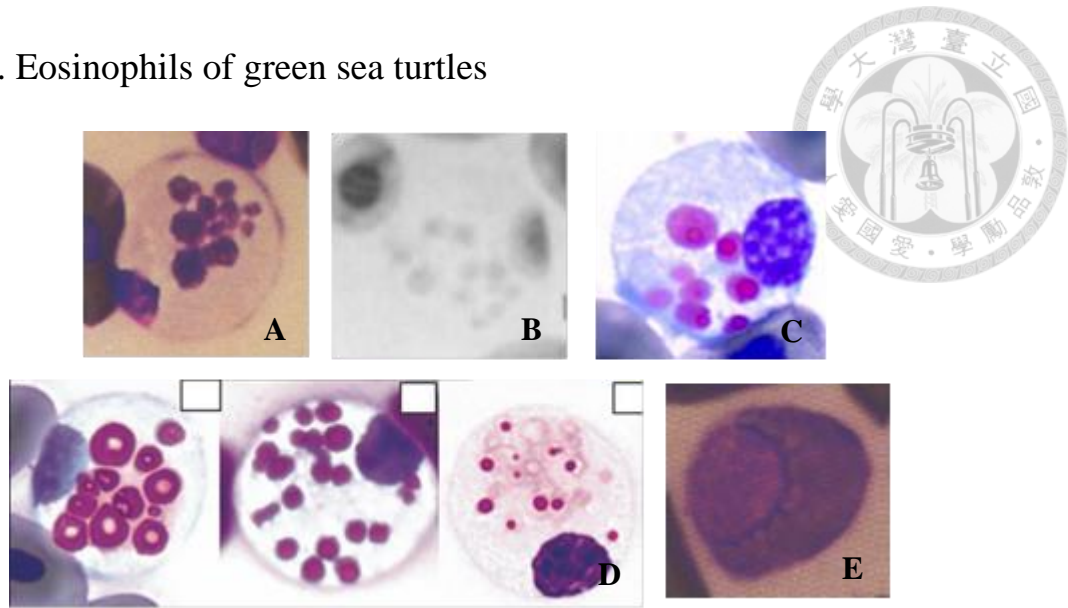
A: Leokostat stain (Work et al., 1998); B: modified May-Grünwald-Giemsa stain (Wood & Ebanks, 1984); C: Wright-Giemsa stain (Stacy Nicole I., 2014); D: Wright-Giemsa stain (N. I. Stacy & Raskin, 2015); E: a small eosinophil, Leokostat stain (Work et al., 1998)

Appendix 7. Basophils of green sea turtles
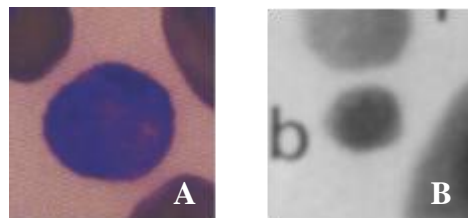
A: Leokostat stain (Work et al., 1998); B: modified May-Grünwald-Giemsa stain (Wood & Ebanks, 1984)

Appendix 8. Lymphocytes of green sea turtles
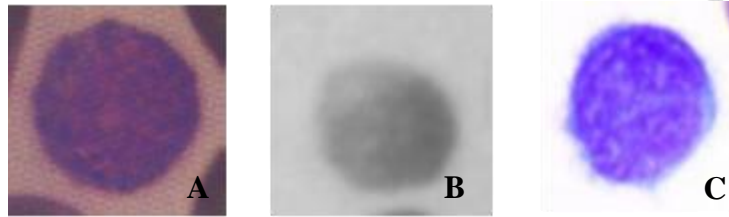
A: Leokostat stain (Work et al., 1998); B: modified May-Grünwald-Giemsa stain (Wood & Ebanks, 1984); C: Wright-Giemsa stain (Stacy Nicole I., 2014)

Appendix 9. Monocytes of green sea turtles
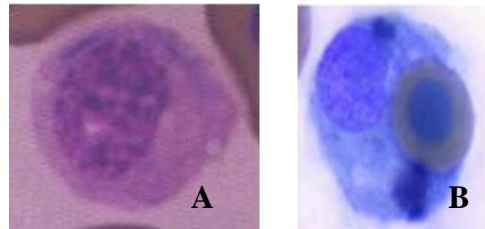
A: Leokostat stain (Work et al., 1998); B: Wright-Giemsa stain, a monocyte exhibiting a phagocytized erythrocyte and hemosiderin (Stacy Nicole I., 2014)

Appendix 10. Heterophils of olive ridley sea turtles
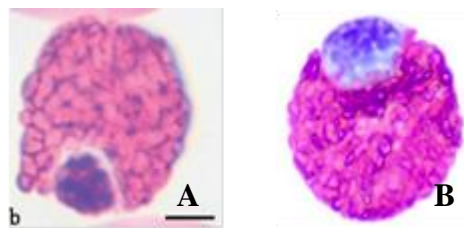
A: Wright-Giemsa stain, scale bar=4μm (Zhang et al., 2011); B: Wright-Giemsa stain (Stacy Nicole I., 2014)

Appendix 11. Eosinophils of olive ridley sea turtles
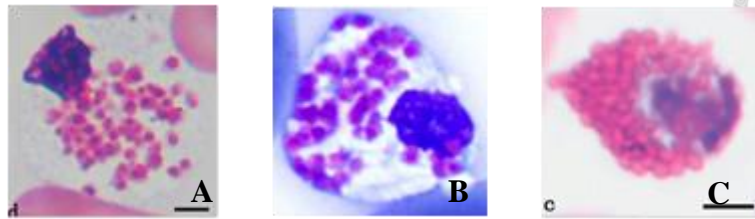
A: a large eosinophil, Wright-Giemsa stain, scale bar=4μm (Zhang et al., 2011); B: a large

eosinophil, Wright-Giemsa stain (Stacy Nicole I., 2014); C: a small eosinophil, Wright-Giemsa

stain, scale bar=4μm (Zhang et al., 2011)

Appendix 12. A basophil of a juvenile olive ridley sea turtle
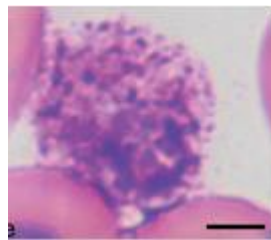
Wright-Giemsa stain, scale bar=4μm (Zhang et al., 2011)


Appendix 13. Lymphocytes of juvenile olive ridley sea turtles
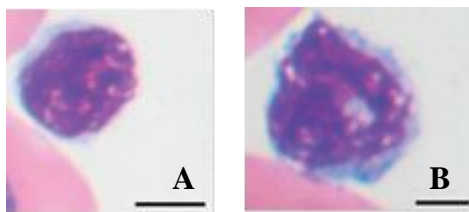
A: a small lymphocyte, Wright-Giemsa stain, scale bar=4μm; B: a medium-sized lymphocyte,

Wright-Giemsa stain, scale bar=4μm (Zhang et al., 2011)

Appendix 14. Monocytes of juvenile olive ridley sea turtles
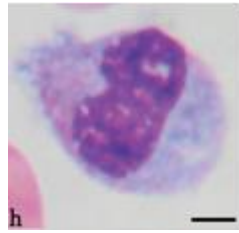
Wright-Giemsa stain, scale bar=4μm (Zhang et al., 2011)

Appendix 15. Leukocytes of Kemp's ridley sea turtles
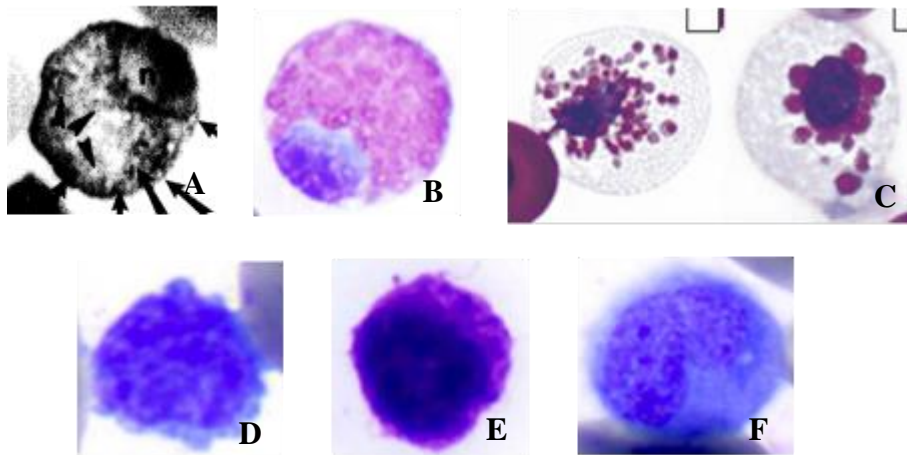
A: a heterophil, Wright-Giemsa stain (Cannon, 1992); B: a heterophil, Wright-Giemsa stain; C: 2 eosinophils, Wright-Giemsa stain (Stacy Nicole I., 2014) D: a lymphocyte, Wright-Giemsa stain; E: a basophil, Wright-Giemsa stain; F: a monocyte, Wright-Giemsa stain (Stacy Nicole I., 2014)

Appendix 16. Heterophil ultrastructure in sea turtles
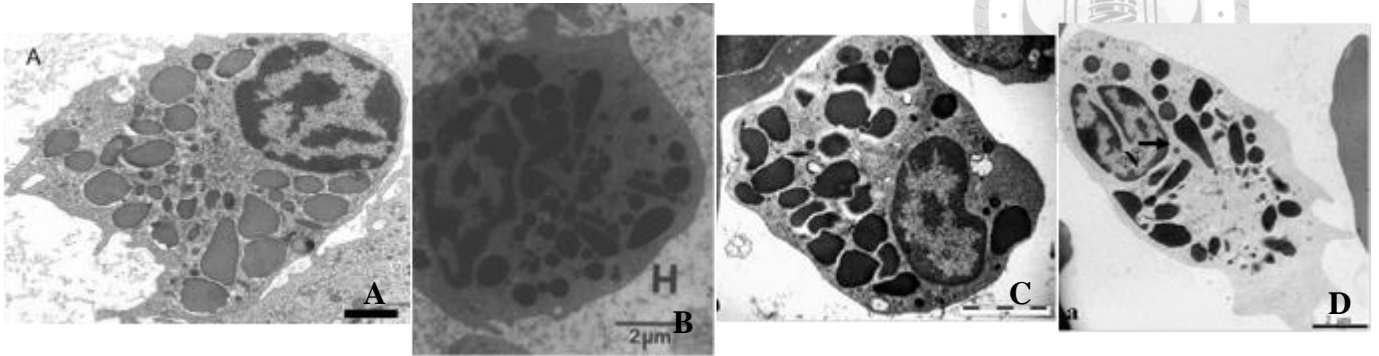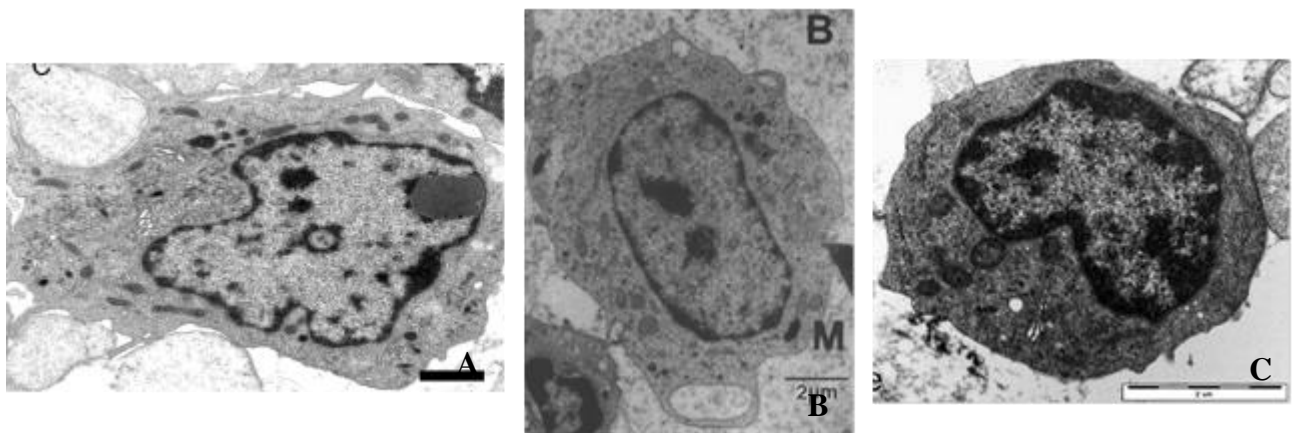

A: a heterophil of a juvenile loggerhead sea turtle, stained with uranyl acetate (1% methanol) and Stato´s lead solution, scale bar=1.6μm (Orós et al., 2010); B: a heterophil of a green sea turtle, stained with 2% aqueous uranyl acetate and Reynold's lead citrate, scale bar =2μm (Work et al., 1998); C: a heterophil of a juvenile olive ridley sea turtle, stained with uranyl acetate and lead citrate, scale bar =2μm (Zhang et al., 2011); D: a heterophil of a loggerhead sea turtle, stained with uranyl acetate and lead citrate, scale bar =2μm (Di Santi et al., 2013)

# Appendix 17. Eosinophil ultrastructure in sea turtles
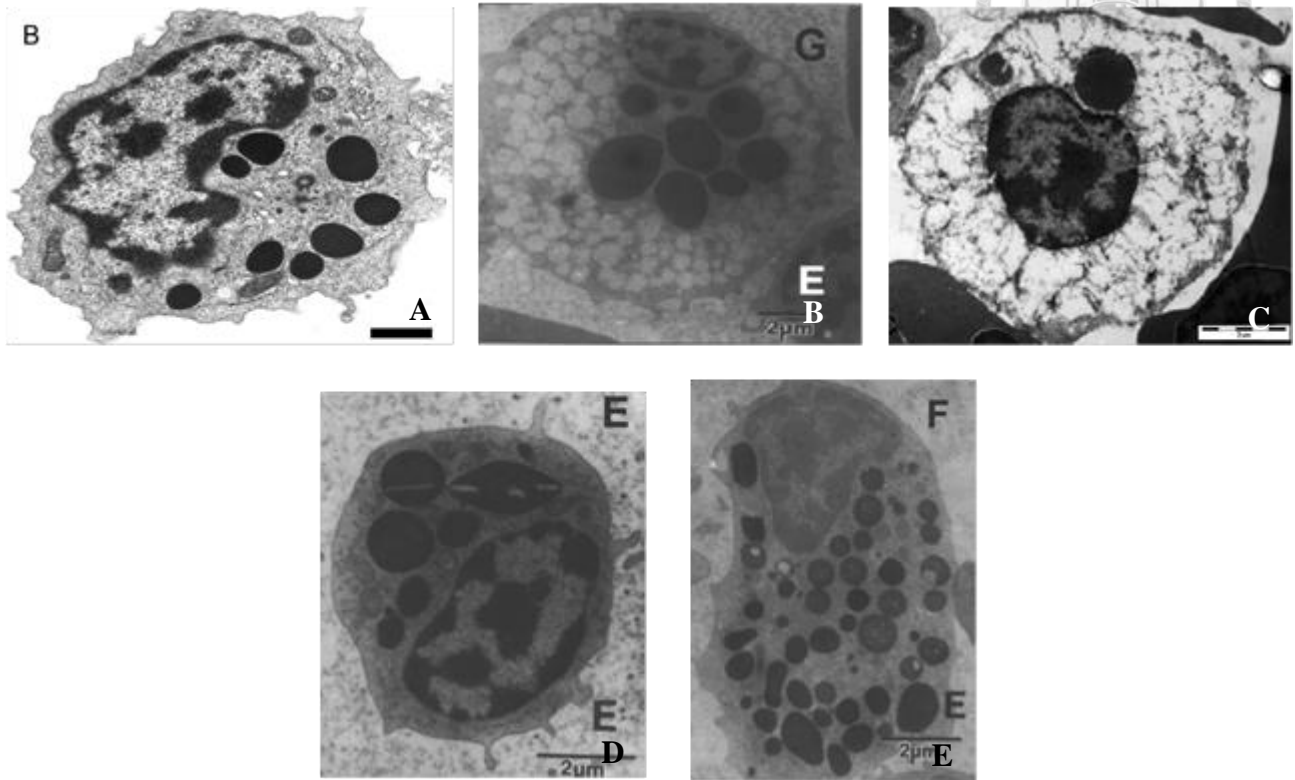
A: an eosinophil of a juvenile loggerhead sea turtle, stained with uranyl acetate (1% methanol) and Stato´s lead solution, scale bar=1.3μm (Orós et al., 2010); B: a large eosinophil of a green sea turtle, stained with 2% aqueous uranyl acetate and Reynold's lead citrate, scale bar =2μm (Work et al., 1998); C: a large eosinophil of a juvenile olive ridley sea turtle, stained with uranyl acetate and lead citrate, scale bar =2μm (Zhang et al., 2011); D: a small eosinophil of a green sea turtle with crystalline structures seen in granules, stained with 2% aqueous uranyl acetate and Reynold's lead citrate; E: a small eosinophil of a green sea turtle with partially vacuolated granules, stained with 2% aqueous uranyl acetate and Reynold's lead citrate, scale bar =2μm (Work et al., 1998)

Appendix 18. Lymphocyte ultrastructure in sea turtles
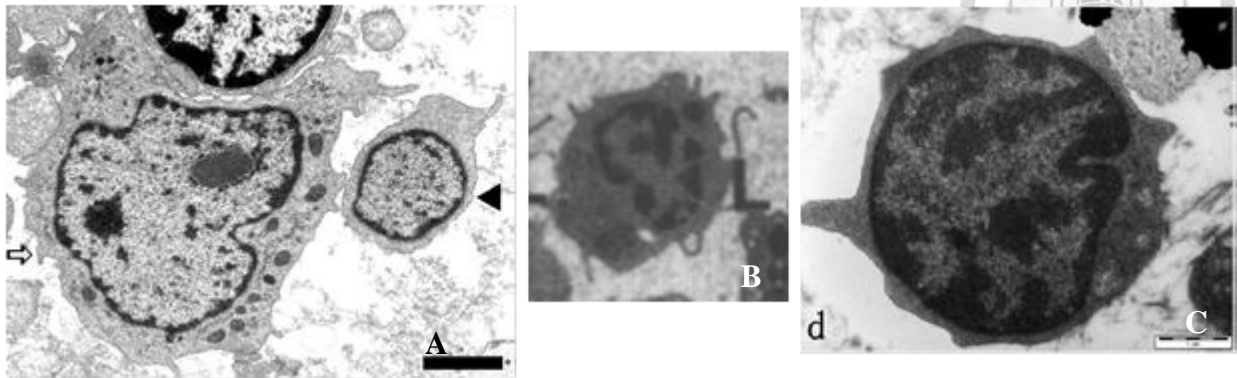
A: a lymphocyte of a juvenile loggerhead sea turtle, comparing to a thrombocyte on the right (arrowhead), stained with uranyl acetate (1% methanol) and Stato´s lead solution, scale bar=1.8μm (Orós et al., 2010); B: a lymphocyte of a green sea turtle, stained with 2% aqueous uranyl acetate and Reynold's lead citrate (Work et al., 1998); C: a lymphocyte of a juvenile olive ridley sea turtle, stained with uranyl acetate and lead citrate, scale bar =1μm (Zhang et al., 2011)

Appendix 19. Monocyte ultrastructure in sea turtles

A: a monocyte of a juvenile loggerhead sea turtle, stained with uranyl acetate (1% methanol) and Stato´s lead solution, scale bar=1.7μm (Orós et al., 2010); B: a monocyte of a green sea turtle, stained with 2% aqueous uranyl acetate and Reynold's lead citrate, scale bar=2μm (Work et al., 1998); C: a monocyte of a juvenile olive ridley sea turtle, stained with uranyl acetate and lead citrate, scale bar =2μm (Zhang et al., 2011)

# Appendix 20. Heterophils of freshwater turtles
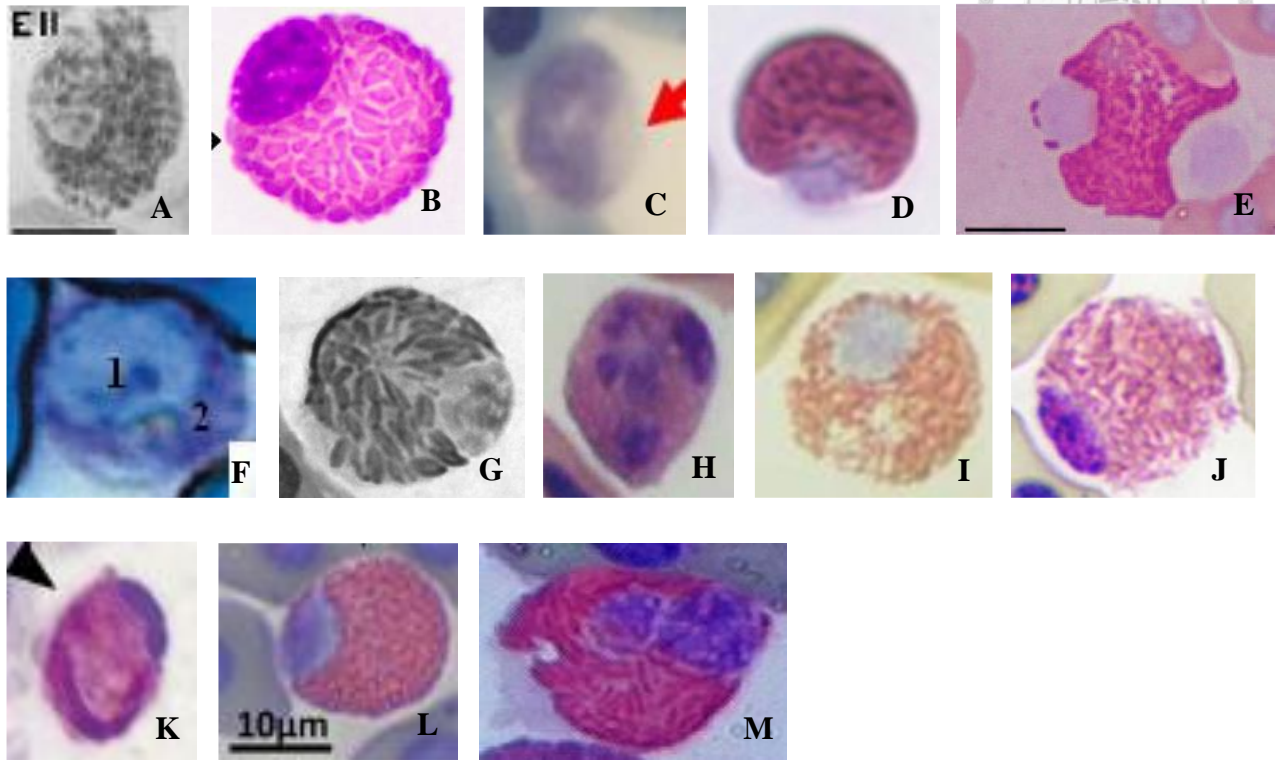
A: the D'Orbigny's sliders, Giemsa stain, scale bar=10.0μm (Azevedo & Lunardi, 2003); B: the yellow-bellied sliders, Diff-Quick stain (J. Hernández et al., 2017); C: the common tortoises (*Testudo graeca*) or the Caspian turtles or the European pond turtles, Giemsa stain (Javanbakht et al., 2013); D: the Sicilian pond turtle, May-Grünwald Giemsa stain (Arizza et al., 2014); E: the Chinese stripe-necked turtle, Wright–Giemsa stain, scale bar=10μm (Chung et al., 2009); F: the Hilaire's side-necked turtle, Leishmann stain (Pitol et al., 2007); G: the European pond turtles, Wright's stain (Metin et al., 2006); H: the Colombian slider, Wright's stain (Velásquez et al., 2014); I: the yellow-spotted river turtles, May-Grünwald Giemsa stain (Oliveira et al., 2011); J: the Arrau turtles, May-Grünwald Giemsa stain (Oliveira-Júnior et al., 2009); K: the yellow-headed temple turtles, Wright–Giemsa stain (Chansue et al., 2011); L: yellow-headed temple turtles, Wright's stain, scale bar=10.0μm (Chansue et al., 2011); M: the Geoffroy's side-necked turtle, Panoptic stain (Zago et al., 2010)

Appendix 21. Eosinophils of freshwater turtles
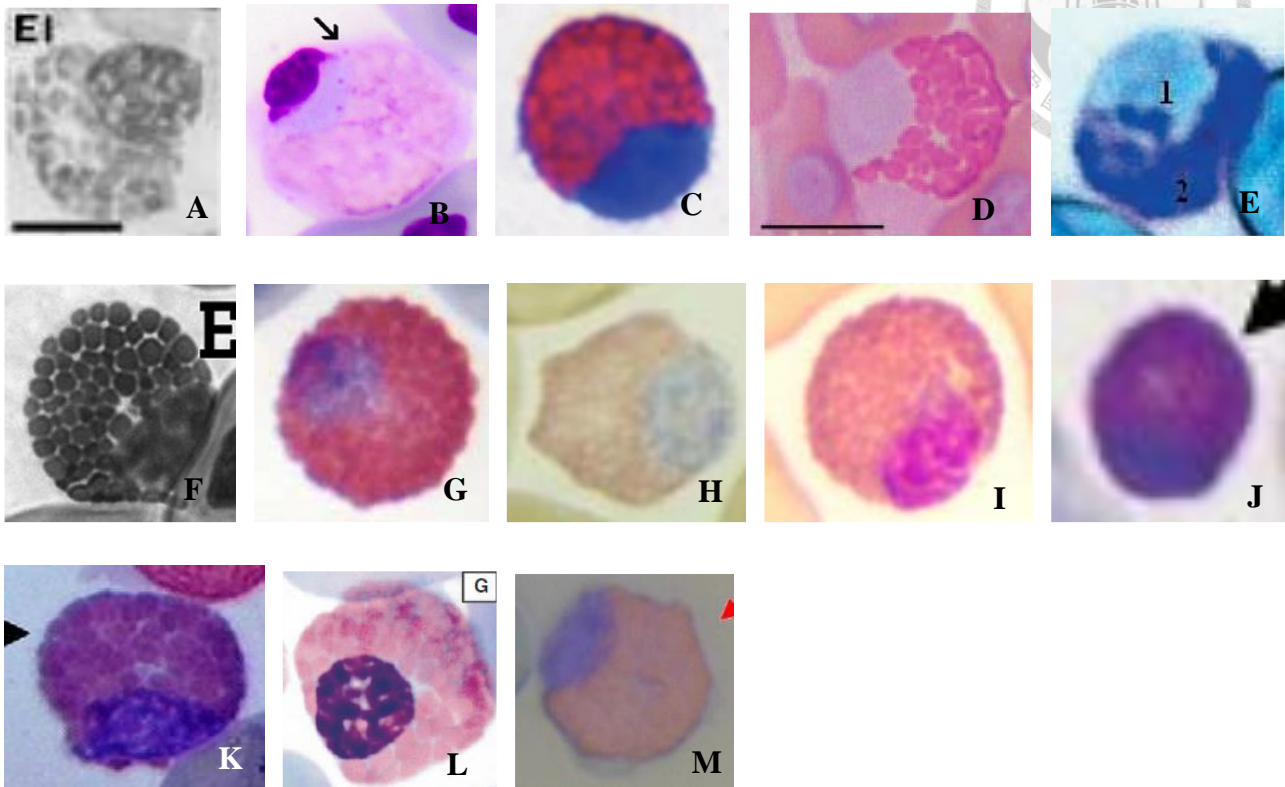
A: the D'Orbigny's sliders, Giemsa stain, scale bar=10.0μm (Azevedo & Lunardi, 2003); B: the yellow-bellied sliders, Diff-Quick stain (J. Hernández et al., 2017); C: the Sicilian pond turtle, May-Grünwald Giemsa stain (Arizza et al., 2014); D: the Chinese stripe-necked turtle, Wright–Giemsa stain, scale bar=10μm (Chung et al., 2009); E: the Hilaire's side-necked turtle, Leishmann stain (Pitol et al., 2007); F: the European pond turtles, Wright's stain (Metin et al., 2006); G: the Colombian slider, Wright's stain (Velásquez et al., 2014); H: the hatchlings of the Arrau turtles, May-Grünwald Giemsa stain (Oliveira et al., 2011); I: the Arrau turtles, May-Grünwald Giemsa stain (Oliveira-Júnior et al., 2009); J: the yellow-headed temple turtles, Wright–Giemsa stain (Chansue et al., 2011); K: the Geoffroy's side-necked turtle, Panoptic stain (Zago et al., 2010); L: Northern red bellied turtle (*Pseudemys rubriventris*), Wright–Giemsa stain (N. I. Stacy & Raskin, 2015); M: the common tortoises or the Caspian turtles or the European pond turtles, Giemsa stain (Javanbakht et al., 2013)

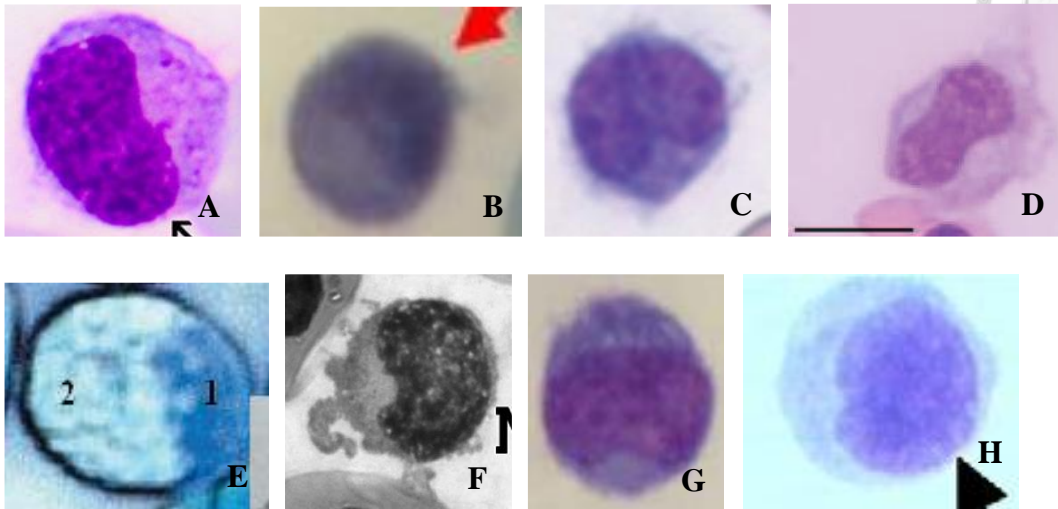# Appendix 22. Basophils of freshwater turtles
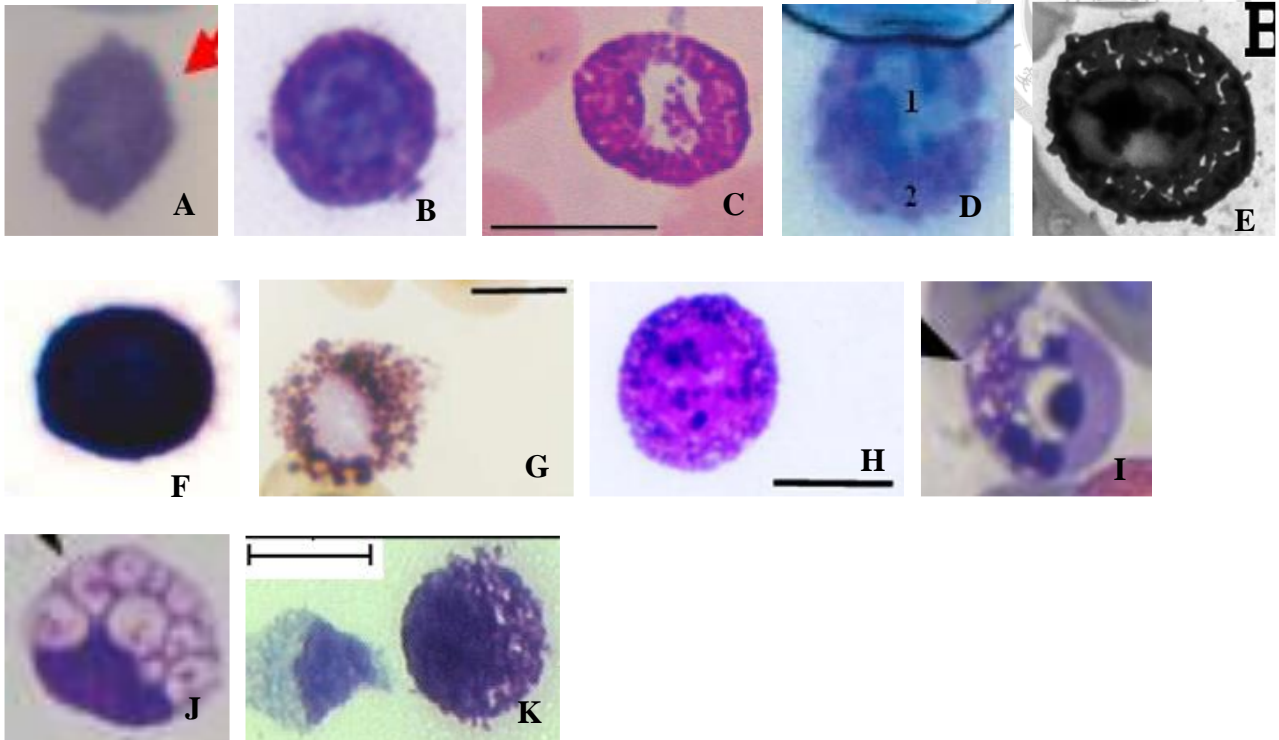
A: the common tortoises or the Caspian turtles or the European pond turtles, Giemsa stain (Javanbakht et al., 2013); B: the Sicilian pond turtle, May-Grünwald Giemsa stain (Arizza et al., 2014); C: the Chinese stripe-necked turtle, Wright–Giemsa stain, scale bar=10μm (Chung et al., 2009); D: the Hilaire's side-necked turtle, Leishmann stain (Pitol et al., 2007); E: the European pond turtles, Wright's stain (Metin et al., 2006); F: the Colombian slider, Wright's stain (Velásquez et al., 2014); G: the hatchlings of the Arrau turtles, May-Grünwald Giemsa stain, scale bar=10.0μm (Oliveira et al., 2011); H: the Arrau turtles, May-Grünwald Giemsa stain, scale bar=11μm (Oliveira-Júnior et al., 2009); I: the yellow-headed temple turtles, Wright stain (Chansue et al., 2011); J: the yellow-headed temple turtles, Wright–Giemsa stain (Chansue et al., 2011); K: the Geoffroy's side-necked turtle, Panoptic stain, scale bar=10μm (Zago et al., 2010)

# Appendix 23. Lymphocytes of freshwater turtles
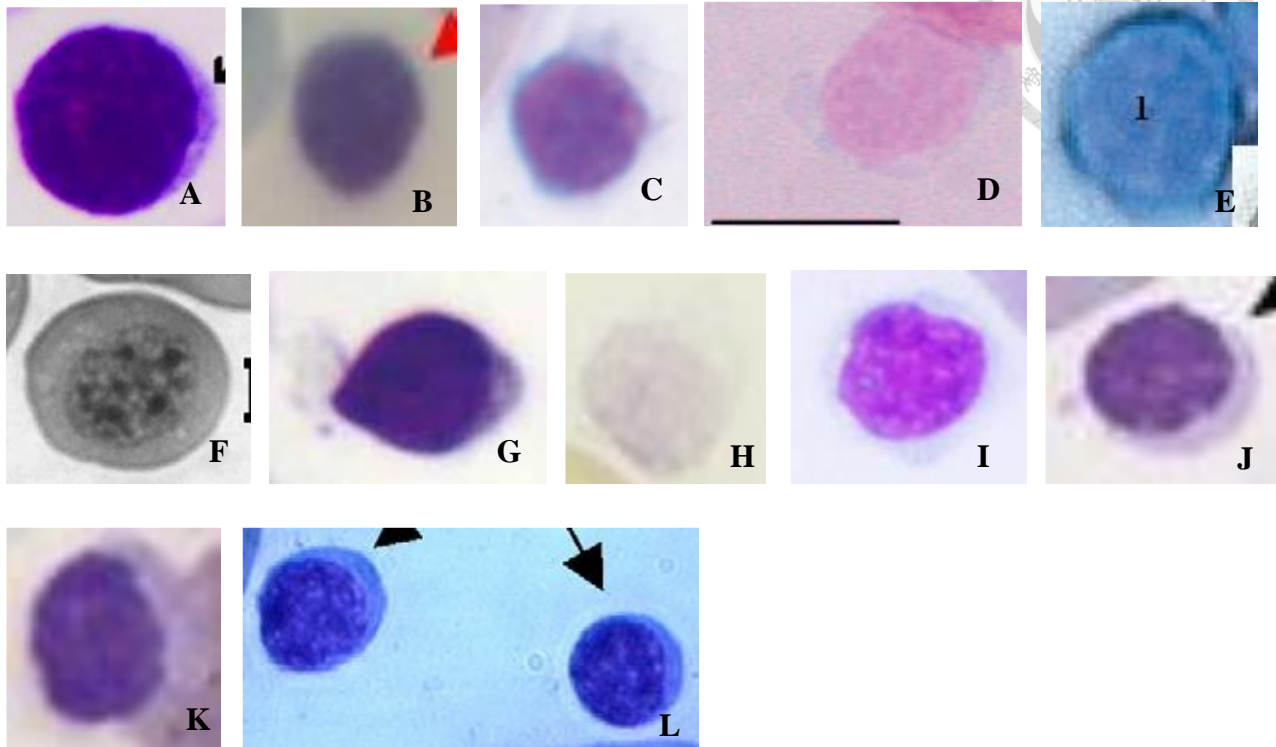
A: the yellow-bellied sliders, Diff-Quick stain (J. Hernández et al., 2017); B: the common tortoises or the Caspian turtles or the European pond turtles, Giemsa stain (Javanbakht et al., 2013); C: the Sicilian pond turtle, May-Grünwald Giemsa stain (Arizza et al., 2014); D: the Chinese stripe-necked turtle, Wright–Giemsa stain, scale bar=10μm (Chung et al., 2009); E: the Hilaire's side-necked turtle, Leishmann stain (Pitol et al., 2007); F: the European pond turtles, Wright's stain (Metin et al., 2006); G: the Colombian slider, Wright's stain (Velásquez et al., 2014); H: the hatchlings of the six-tubercled Amazon River turtles, May-Grünwald Giemsa stain (Oliveira et al., 2011); I: the Arrau turtles, May-Grünwald Giemsa stain (Oliveira-Júnior et al., 2009); J: the yellow-headed temple turtles, Wright–Giemsa stain (Chansue et al., 2011); K: the yellow-headed temple turtles, Wright–Giemsa stain (Chansue et al., 2011); L: the Geoffroy's side-necked turtle, Panoptic stain (Zago et al., 2010)

Appendix 24. Monocytes of freshwater turtles

A: the yellow-bellied sliders, Diff-Quick stain (J. Hernández et al., 2017); B: the common tortoises

or the Caspian turtles or the European pond turtles, Giemsa stain (Javanbakht et al., 2013); C: the

Sicilian pond turtle, May-Grünwald Giemsa stain (Arizza et al., 2014); D: the Chinese stripe-necked

turtle, Wright–Giemsa stain, scale bar=10μm (Chung et al., 2009); E: the Hilaire's side-necked

turtle, Leishmann stain (Pitol et al., 2007); F: the European pond turtles, Wright's stain (Metin et al.,

2006); G: the Colombian slider, Wright's stain (Velásquez et al., 2014); H: the Geoffroy's

side-necked turtle, Panoptic stain (Zago et al., 2010)

Appendix 25. Heterophil ultrastructure in freshwater turtles
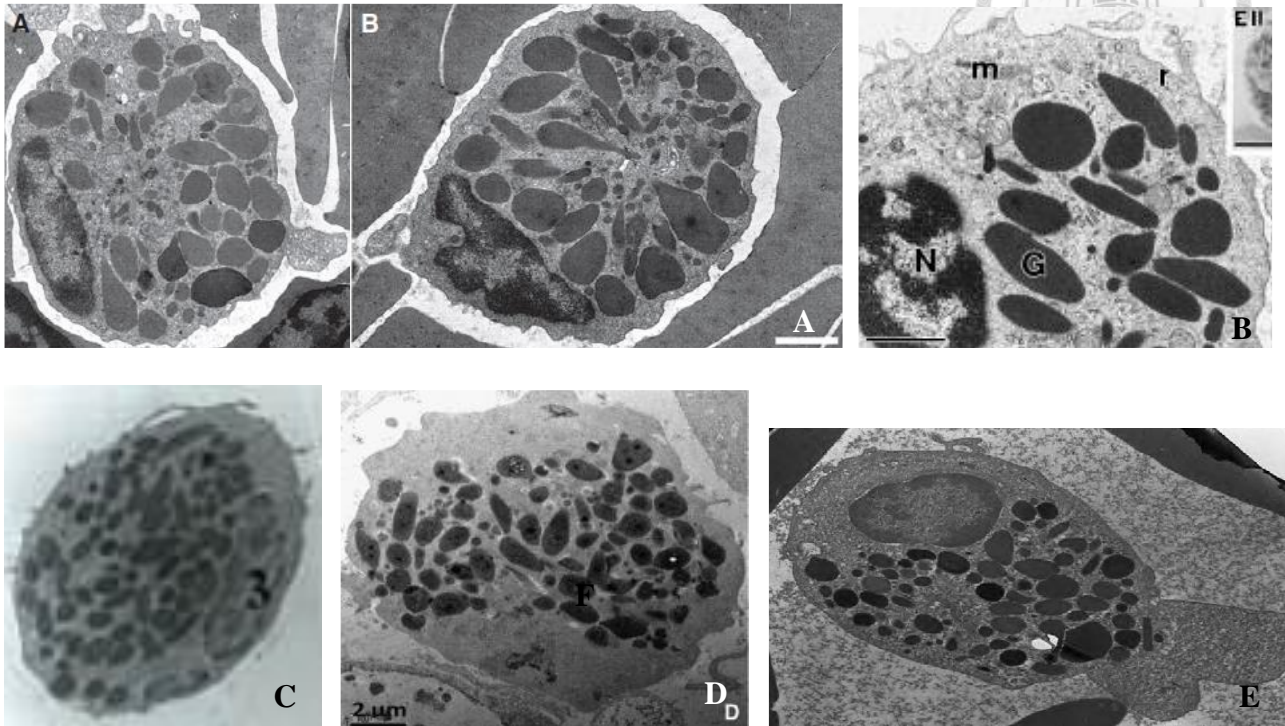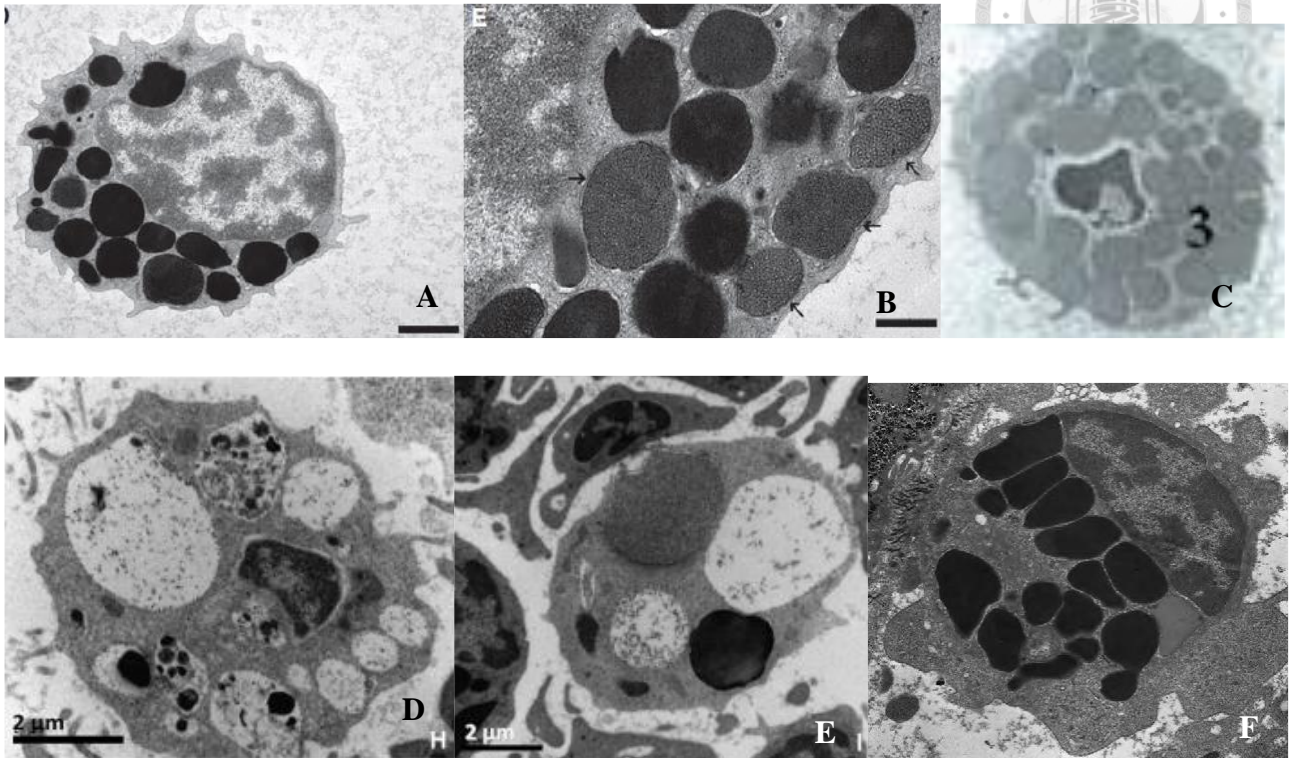

A: 2 heterophils of the yellow-bellied sliders, stained with uranyl acetate and lead citrate, scale bar=1.3μm (J. D. Hernández et al., 2016); B: a heterophil of a D'Orbigny's slider, stained with an alcoholic uranyl solution and lead citrate, scale bar=1.0μm (Azevedo & Lunardi, 2003); C: a heterophil of a Hilaire's side-necked turtles (Pitol et al., 2007); D a heterophil of a yellow-headed temple turtle, stained with uranyl acetate, scale bar=2μm (Chansue et al., 2011); E: a heterophil of a Geoffroy's side-necked turtle, stained with uranyl acetate and lead citrate (Zago et al., 2010)

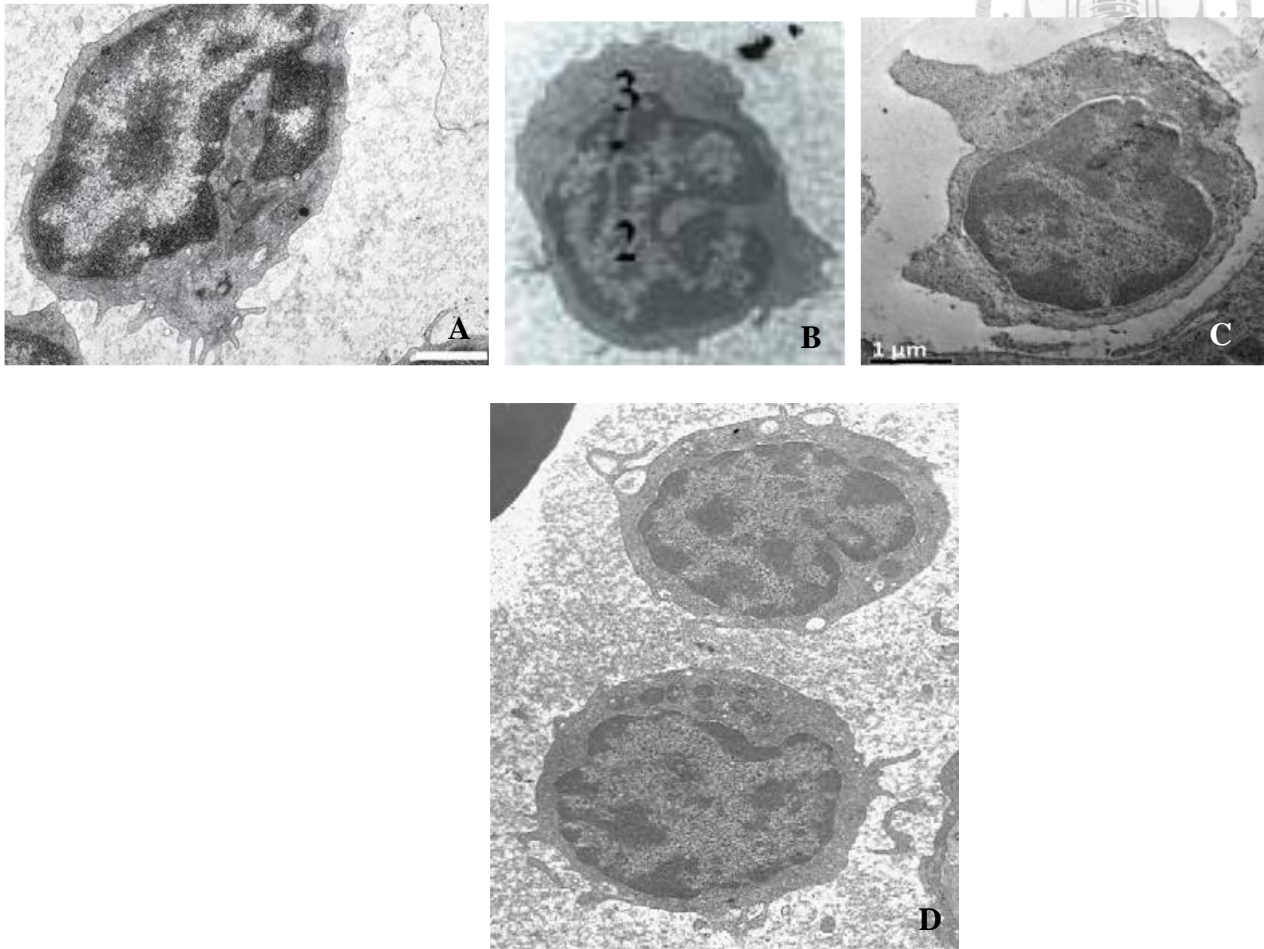# Appendix 26. Eosinophil ultrastructure in freshwater turtles
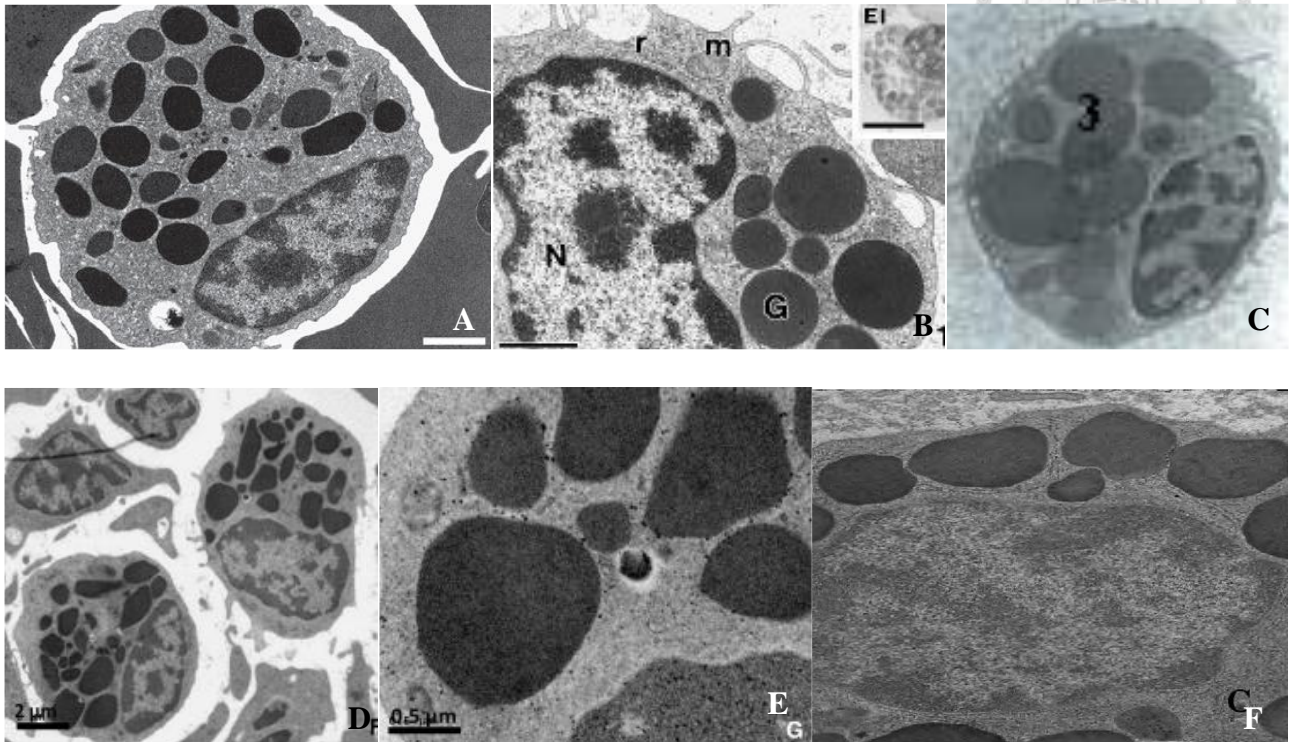
A: an eosinophil of a yellow-bellied slider, stained with uranyl acetate and lead citrate, scale bar=1.3μm (J. D. Hernández et al., 2016); B: cytoplasmic granules of an eosinophil of a D'Orbigny's slider, stained with an alcoholic uranyl solution and lead citrate, scale bar=1.0μm (Azevedo & Lunardi, 2003); C: an eosinophil of a Hilaire's side-necked turtles (Pitol et al., 2007); D: 2 eosinophils of a yellow-headed temple turtle, stained with uranyl acetate, scale bar=2μm (Chansue et al., 2011); E: cytoplasmic granules of an eosinophil from a yellow-headed temple turtle, stained with uranyl acetate, scale bar=0.5μm (Chansue et al., 2011); F: cytoplasmic granules of an eosinophil of a Geoffroy's side-necked turtle, stained with uranyl acetate and lead citrate (Zago et al., 2010)

Appendix 27. Basophil ultrastructure in freshwater turtles
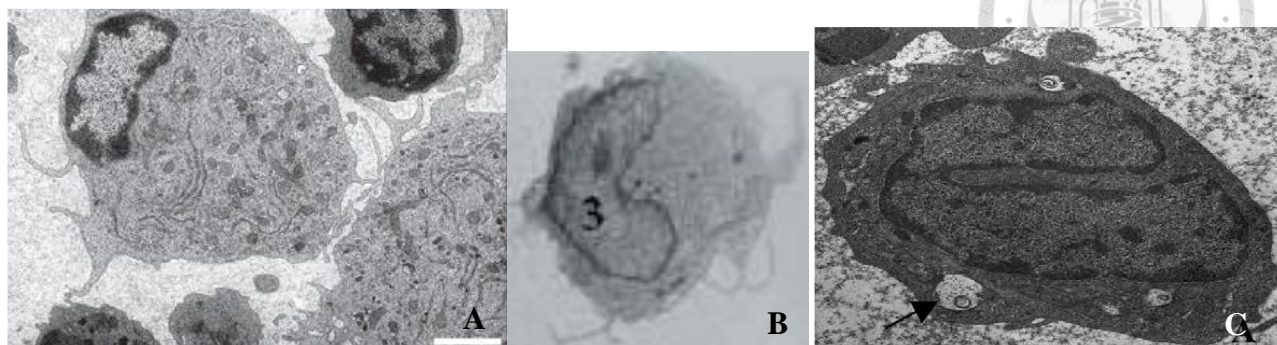

A: a basophil of a yellow-bellied slider, stained with uranyl acetate and lead citrate, scale

bar=1.3μm (J. D. Hernández et al., 2016); B: a yellow-bellied slider's basophil cytoplasmic granules

that were rich in microtubules, stained with uranyl acetate and lead citrate, scale bar=0.5μm (J. D.

Hernández et al., 2016); C: a basophil of a Hilaire's side-necked turtles (Pitol et al., 2007); D: a

basophil of a yellow-headed temple turtle, cytoplasmic vacuoles were filled with electron-dense

granules, stained with uranyl acetate, scale bar=2μm (Chansue et al., 2011); E: fine lamellar and

electron-dense cytoplasmic granules of a basophil from a yellow-headed temple turtle, stained with

uranyl acetate, scale bar=2μm (Chansue et al., 2011); F: a basophil of a Geoffroy's side-necked

turtle, stained with uranyl acetate and lead citrate (Zago et al., 2010)

Appendix 28. Lymphocyte ultrastructure in freshwater turtles

A: a lymphocyte of a yellow-bellied slider, stained with uranyl acetate and lead citrate, scale

bar=1μm (J. D. Hernández et al., 2016); B: a lymphocyte of a Hilaire's side-necked turtles (Pitol et

al., 2007); C: a lymphocyte of a yellow-headed temple turtle, stained with uranyl acetate, scale

bar=1μm (Chansue et al., 2011); D: a lymphocyte of a Geoffroy's side-necked turtle, stained with

uranyl acetate and lead citrate (Zago et al., 2010)

Appendix 29. Monocyte ultrastructure in freshwater turtles

A: a monocyte of a yellow-bellied slider, stained with uranyl acetate and lead citrate, scale

bar=1.6μm (J. D. Hernández et al., 2016); B: a monocyte of a Hilaire's side-necked turtles (Pitol et

al., 2007); C: a monocyte of a Geoffroy's side-necked turtle, stained with uranyl acetate and lead

citrate (Zago et al., 2010)

## Appendix 30. Avian heterophil toxic change grading system (T. Campbell, 2015)

Toxicity	Alternation in cellular morphology
1+	Increase in cytoplasmic basophilia
2+	Deeper cytoplasmic basophilia, partial degranulation
3+	Dark cytoplasmic basophilia, moderate degranulation, abnormal granules, cytoplasmic vacuolization
4+	Deep cytoplasmic basophilia, moderate to marked degranulation, presence of abnormal granules, cytoplasmic vacuolization, karyorrhexis or karyolysis

Appendix 31. Heterophil toxic change and/or left-shifting in sea turtles
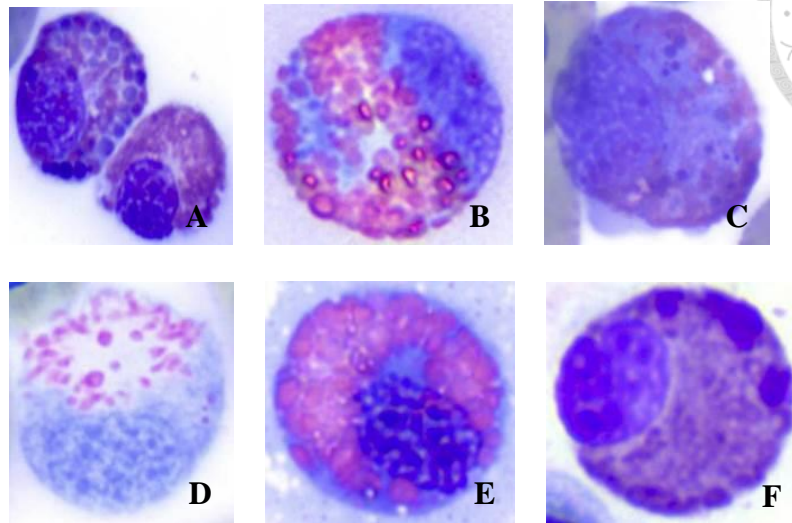

A: a left-shifted heterophil (upper left) next to a mature heterophil (lower right) in a green sea turtle,

Wright-Giemsa stain; B: a mildly toxic and left-shifted heterophil in a green sea turtle,

Wright-Giemsa stain; C: a moderately toxic and left-shifted heterophil in a green sea turtles,

Wright-Giemsa stain; D: a moderately toxic and left-shifted heterophil in a green sea turtles,

Wright-Giemsa stain; E: a mildly toxic heterophil in a loggerhead sea turtle, Wright-Giemsa stain; F:

a left-shifted heterophil in a Kemp's ridley sea turtle, Wright-Giemsa stain (Stacy Nicole I., 2014)
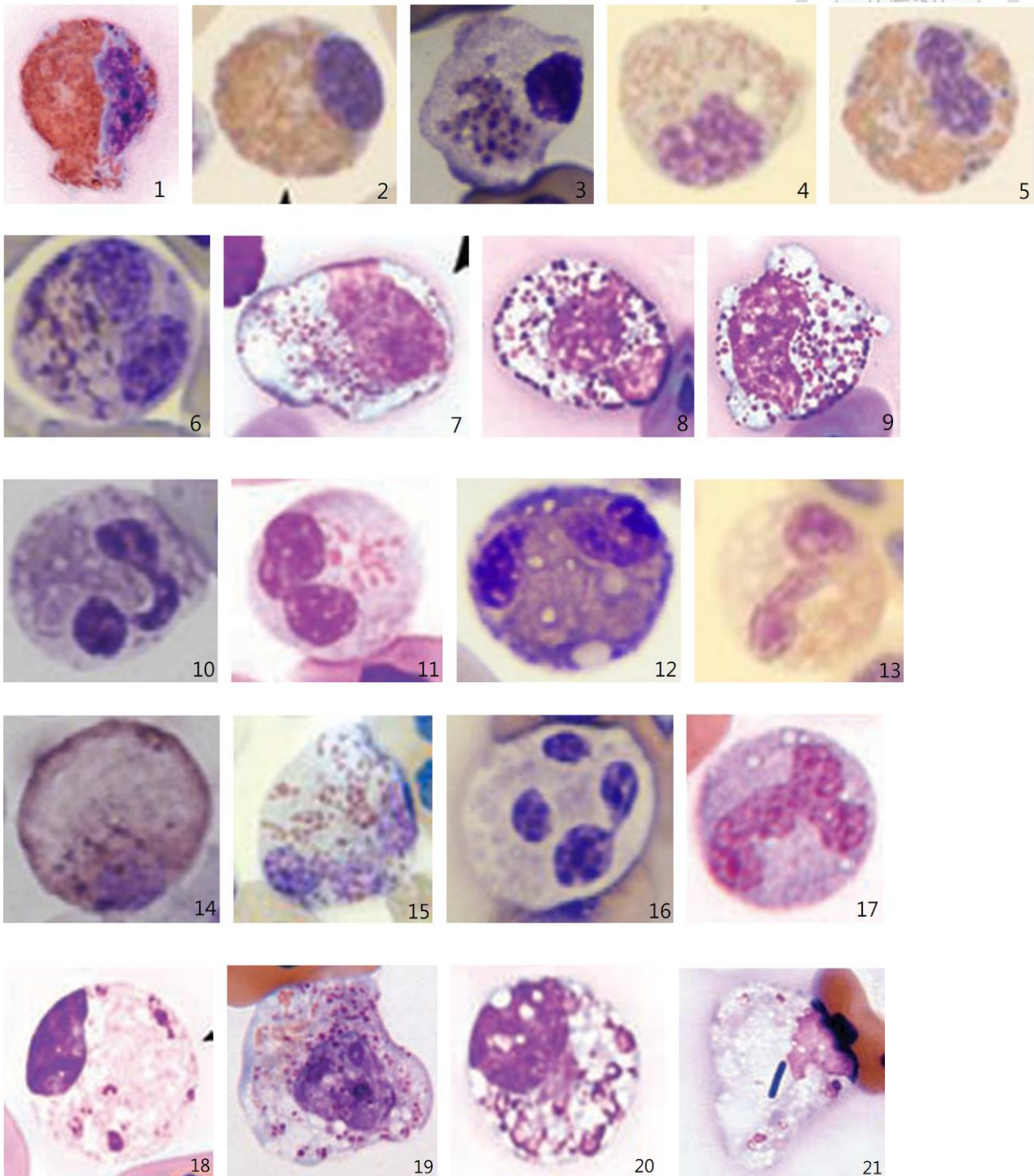
1-9: *Testudines*; 10-15: *Iguanidae & Agamidae*; 16-17: *Acrodonta*; 18-21: *Crocodilia*; each from

mild to severe on toxicity

1: a non-toxic, immature heterophil with band-shaped nucleus and a few primary, purple-staining

131
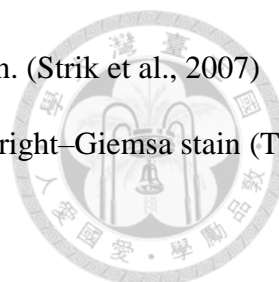
granules in a Gopher tortoise (*Gopherus polyphemus*). Wright-Giemsa stain. (Strik et al., 2007)

2: a 1 + toxic heterophil in a three-toed box turtle (*Terrapene carolina*), Wright–Giemsa stain (T. W. Campbell, 2015)

3: a heterophil with degranulation in a Hermann's tortoise, Hemacolor® rapid stain (Nardini et al., 2013)

4: a 2+ toxic heterophil in a Chinese pond turtle (*Chinemys reevesii*), Wright–Giemsa stain (T. W. Campbell, 2015)

5: a 3+ toxic heterophil with partial nuclear lobation in a three-toed box turtle (a species that does not lobe granulocyte nuclei), Wright–Giemsa stain (T. W. Campbell, 2015)

6: a heterophil with abnormal cytoplasmic granules in a Hermann's tortoise, Hemacolor® rapid stain (Nardini et al., 2013)

7: a severely toxic heterophil with cytoplasmic basophilia, degranulation, vacuolation, abnormal granulation, and pleomorphic nuclei in a common tortoise, Wright-Giemsa stain (Strik et al., 2007)

8: a severely toxic heterophil with bilobed nucleus in a common tortoise, Wright-Giemsa stain (Strik et al., 2007)

9: a severely toxic, immature heterophil in a common tortoise, Wright-Giemsa stain (Strik et al., 2007)

10: a heterophil with increased cytoplasmic basophilia in a green iguana, Diff-Quick stain (Nardini et al., 2013)

11: a moderately toxic heterophil with degranulation and cytoplasmic basophilia in a Chinese water dragon (*Physignathus cocincinus*), Wright-Giemsa stain (Strik et al., 2007)

12: a heterophil with vacuolation in a green iguana, Hemacolor® rapid stain (Nardini et al., 2013)

13: a 2+ toxic heterophil in a green iguana, Wright–Giemsa stain (T. W. Campbell, 2015)

14: a toxic heterophil with abnormal cytoplasmic granules in a green iguana, Diff-Quick stain

(Nardini et al., 2013)

15: a 3+ toxic heterophil in green iguana, Wright–Giemsa stain (T. W. Campbell, 2015)

16: a toxic heterophil with excessive nuclear lobation in a veiled chameleon (*Chamaeleo calyptratus*), Hemacolor® rapid stain (Nardini et al., 2013)

17: a severely toxic, left-shifted heterophil with cytoplasmic basophilia, degranulation, abnormal granulation, and excessive nuclear lobation in a Fischer's chameleon (*Chameleo fischeri*), Wright-Giemsa stain (Strik et al., 2007)

18: a toxic heterophil in an American crocodile (*Crocodylus acutus*), Wright-Giemsa stain (Strik et al., 2007)

19: a severely toxic, immature heterophil with degranulation, abnormal granulation, cytoplasmic basophilia, and cytoplasmic vacuolation in a Spectacled caiman (*Caiman crocodilus*), Wright-Giemsa stain (Strik et al., 2007)

20: a severely toxic heterophil with cytoplasmic basophilia, vacuolation, degranulation, and abnormal granulation in an American alligator (*Alligator mississippiensis*), Wright-Giemsa stain (Strik et al., 2007)

21: a severely toxic, heterophil with degranulation and intracytoplasmic, rod-shaped bacterium in an American alligator, Wright-Giemsa stain (Strik et al., 2007)

Appendix 33. Heterophil toxic change ultrastructure in chickens (Shini et al., 2008)
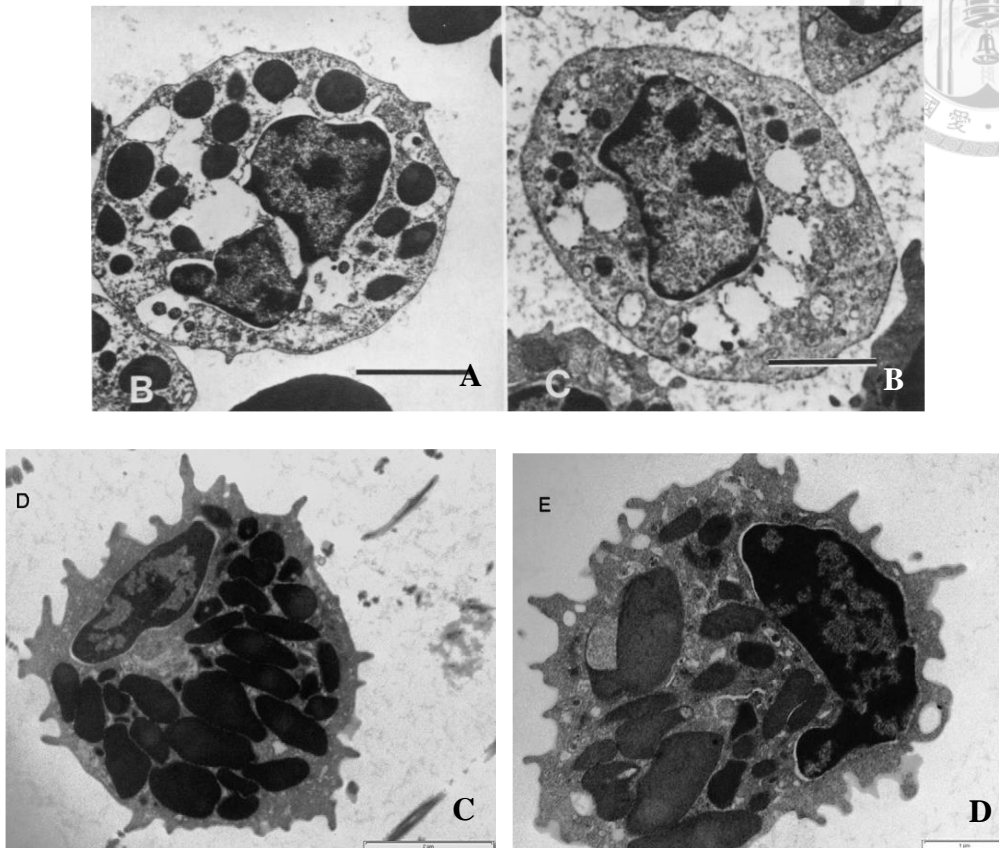

A: toxic heterophils from a turpentine-treated chicken, stained with uranyl acetate and lead citrate, scale bar=3μm; B: late toxic heterophils from a turpentine-treated chicken, stained with uranyl acetate and lead citrate, scale bar=1.5μm; C: toxic heterophils from a LPS-treated chicken, stained with uranyl acetate and lead citrate, scale bar=2μm; D: toxic heterophils from a LPS-treated chicken, stained with uranyl acetate and lead citrate, scale bar=1μm

Appendix 34. Uneven distribution of heterophil granules in Asian water monitors

(Salakij et al., 2014)
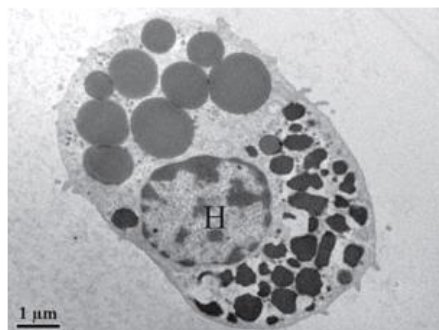
Appendix 35. Cell distribution within the buffy coat (Fontes Pinto et al., 2018)
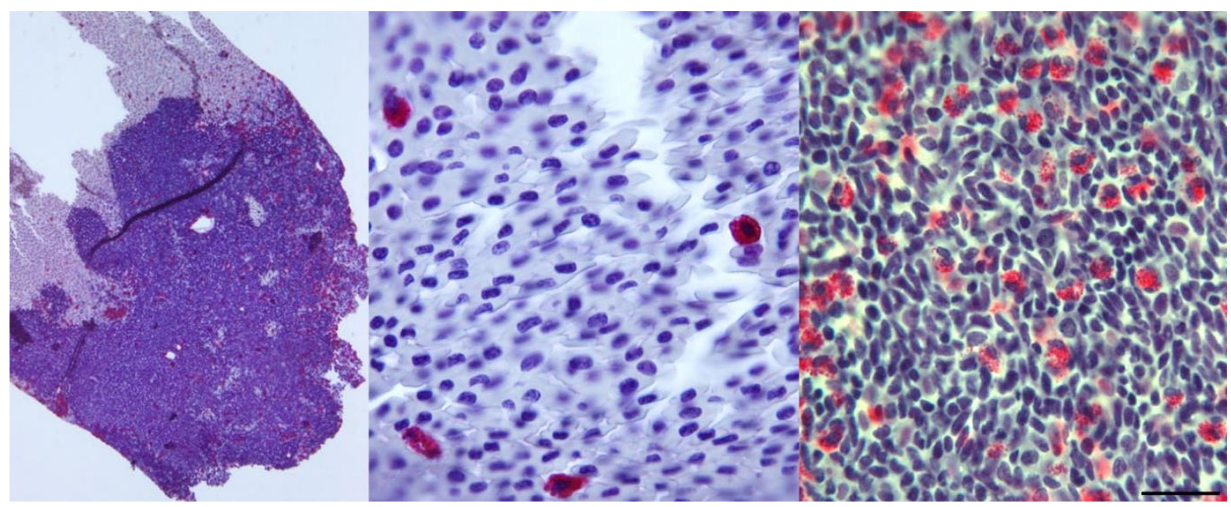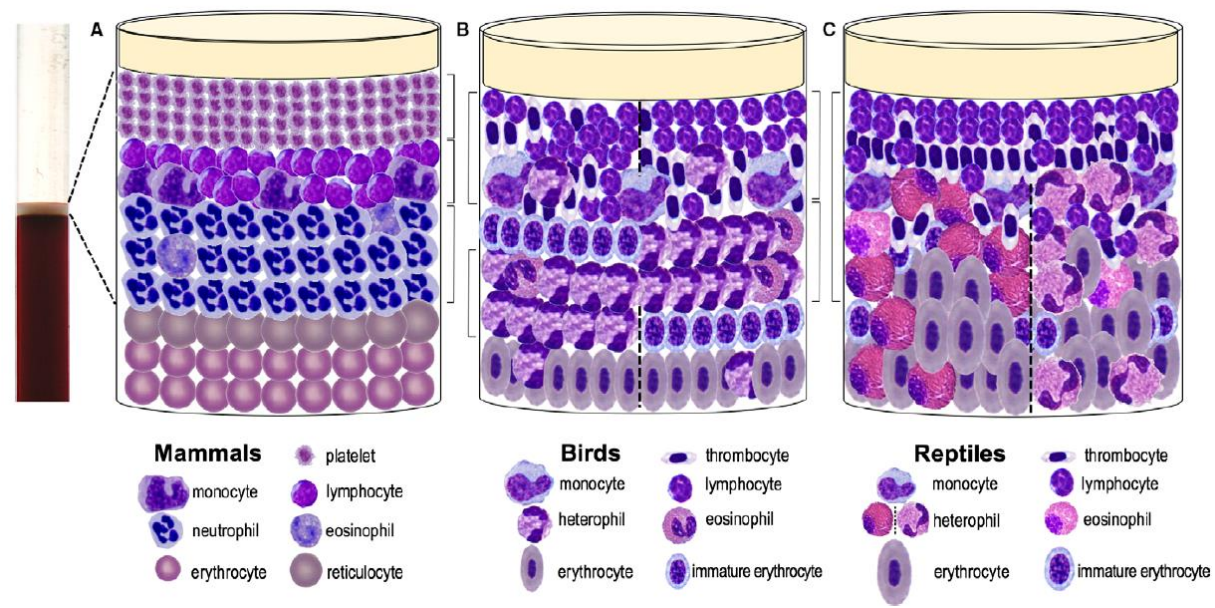
Heterophils were highlighted with Sirius red stain, seen admixed in erythrocytes (middle) or mononuclear cells (right)